Experimental verification of calculation methods for hollow core section fin-plate joints with varying strength grades

Application on joints used in practice

by

M.C.D. van Arragon

to obtain the degree of Master of Science
at the Delft University of Technology,
to be defended publicly on August 27 at 15:00 in 3Me Hall J.

Student number:	1515373	
Thesis committee:	Prof. dr. ir. M. Veljkovic	TU Delft
	Dr. ir. M.A.N. Hendriks	TU Delft
	Dr. M. Pavlović	TU Delft
	Ir. P. de Vries	TU Delft
	Ir. G. Pavlović	ASK Romein

An electronic version of this thesis is available at `http://repository.tudelft.nl/`.

Preface

You are reading the final writing in my time as a student, composed in the form of the master thesis. This paper is to fulfill the requirements for graduating as a Master of Science and Structural Engineer at the faculty of Civil Engineering at Delft University of Technology. The research conducted in the past year is dedicated to understanding and quantifying the parts that make up the resistance and the actions within the fin-plate joint with hollow core sections. The focus has been greatly on approaching this problem from an engineering perspective and on how to create more efficient joints in the design phase.

This project has been a collaboration between TUDelft and ASK Romein. The market is pushing for the use of high strength steels and more efficient weld designs thus the company is investing in increasing knowledge on their own products and ensuring safe designs. By experimentally validating new tools such as Component Based Finite Element Modelling and automatic welding procedures this can be achieved.

From the department of structural engineering there was a lot of support and discussions to get the most out of the experiments. I am very grateful to my supervisors Dr. M. Pavlovic, Ir. P. de Vries and Prof. M. Veljkovic whom all provided me with valuable guidance during different stages of the project.

In the office I would like to give my thanks to Alexander, Andy and my Supervisor Goran for giving me the opportunity for discussions and filling the gaps in knowledge. I also want to thank everyone at ASK Romein who put in so much effort to create the small and consistent welds that were needed to achieve successful and clear experimental results.

Performing the experiments would not have been possible without the help of the Stevinlab. I would like to thank Kevin, Fred and John for teaching me how to instrument the specimens and for spending many weeks performing the experiments with me.

Finally I would like to extend my thanks to Sebastian and Rui, who helped me to get started and to have many discussions over a cup of coffee.

M.C.D. van Arragon
Delft, July 2018

Abstract

This research studies the experimental and numerical behaviour of a simple beam to column joint using a fin-plate welded to an unstiffened rectangular hollow core section. The following aspects of the joint are investigated:

1. The resistance of the welded connection.
2. Defining the force distribution inside the joint.
3. Improvement of the design method for resistance of the fin plate connection.

Four series of controlled experiments are conducted to test the joints until failure. The series combine a S355 plate with S690/S355 column grade and matching (Class 46 on S355) and overmatching (Class 89 on S355) weld material. With the data from these experiments and coupon tests, a finite element model is created using DSS Abaqus. Results are validated to accurately follow the force-displacements obtained in the experiments.

Key findings from the experiment:

The resistance of the welds was found to be much greater than predicted using the nominal values from the Eurocode. The utilization of the *nominal design resistance* compared to the *failure load in experiments* was 19% following EN1993-1-8:2005 and 25% with EN1993-1-8:2020. The main reason for this was the high penetration depth and increased weld throat when welding a 3mm weld according to standard procedure, accounting for a 100% increase in resistance. The second reason was that the failure stress was 50% higher than nominal for both the matching and overmatching infused weld material.

Insights from the finite element models:

It was proven that for certain boundary conditions it is possible to only account for shear transfer through the weld. However it was found that when expanding the Abaqus model to a full building size the boundary conditions change such that also a moment needs to be transferred through the weld and the bolts. The ratio between the stiffness of the beam and the column face determines the magnitude of these moments. The addition to the stress in the start and end of the weld can result in a 75% lower design resistance when comparing to the same weld with only a shear load. The bolt group transfers the moment through horizontal forces, again depending on this ratio. The magnitude of this horizontal force component in the outer bolts can be equal to the vertical component.

The following calculation methods were proposed:

The moment transfer through the weld from bridging the bolts eccentricity can be reduced according to the stiffness ratio R between the beam and the column face. There are four stiffness factors which influence the force distribution; The column stiffness K_c, the column face stiffness K_cf, the plate bearing stiffness K_p and the beam rotation stiffness K_b. It was found that the governing influence comes from the face stiffness and the beam stiffness. The face stiffness can be calculated by integrating the resistance over the effective length of the column h_p.

To obtain proper model of the bending moment in the weld, the column face should be modelled as a rotational spring in global analysis, not as a hinged connection. This moment can then be transferred to the local analysis of the joint.

If there is no yielding in the beam cross-section then the problem can be simplified and welds should be calculated with taking into account the shear force V_{ed} and the bending moment M_{ed} which follows directly from the stiffness ratio R.

Contents

1 Introduction 1

2 Problem statement and research objectives 3
- 2.1 Research objectives on fillet welds . . . 5
- 2.2 Research objectives on the calculation model for an unstiffened column face. . . 5

3 Current calculation methods for fin-plate joints 7
- 3.1 Calculation methods for fillet welds . . . 7
  - 3.1.1 Directional method . . . 7
  - 3.1.2 Full strength method . . . 8
  - 3.1.3 Weld penetration in fillet welds. . . . 9
  - 3.1.4 Changes in design rules and overmatching welds . . . 10
  - 3.1.5 Effect on material usage . . . 11
- 3.2 Influence of calculation methods on the design load . . . 12
  - 3.2.1 Component method . . . 12

4 Literature on finite element modeling 15
- 4.1 Software . . . 16
- 4.2 Implicit/Explicit modeling . . . 16
- 4.3 Element type and size . . . 17
- 4.4 Material properties . . . 17
- 4.5 Stress state in Abaqus . . . 18

5 Experiment set-up 21
- 5.1 Full joint tests . . . 24
  - 5.1.1 Specimen design . . . 24
  - 5.1.2 Dimensions . . . 25
  - 5.1.3 Frame set-up . . . 26
  - 5.1.4 Instrumentation . . . 27
  - 5.1.5 Test results . . . 27
- 5.2 Plate material coupon tests . . . 28
- 5.3 Weld coupon tests . . . 29
- 5.4 Data analysis . . . 30
  - 5.4.1 Estimating frame friction from experiment data . . . 30
  - 5.4.2 Experiment results on shear resistance . . . 33
  - 5.4.3 Failure planes of specimens . . . 35
  - 5.4.4 Experiment results on fin-plate rotation . . . 37

6 Differences between nominal design and experiment 39
- 6.1 Margins on ultimate plate stress . . . 39
- 6.2 Margins on ultimate weld stress . . . 39
- 6.3 Margins due to the infused weld zone . . . 40
- 6.4 Margins on final joint resistance . . . 40

7 Material properties and model calibration 43
- 7.1 Calibrating true stress strain with Abaqus . . . 44
  - 7.1.1 Fin-plate S355 . . . 44
  - 7.1.2 RHS S690 . . . 44
  - 7.1.3 Welds and weld penetrated zones. . . . 44
  - 7.1.4 Calibration of the infused zone for experiment 2E1 . . . 46

7.2 Calibration of the infused zone for all experiments . . . 47
  7.2.1 Overview of true stress/strain curves . . . 48
  7.2.2 Abaqus results on fin-plate rotation . . . 48
7.3 Estimating failure strain for the infused weld zone . . . 49
7.4 Conclusions on model calibration . . . 50

8 Influence of column face stiffness **53**
8.1 Theory. . . . 53
8.2 Modeling . . . 55
8.3 Results for experiment sizings . . . 56
  8.3.1 Effective hinge location and weld stresses . . . 58
  8.3.2 Effective bolt forces. . . . 60
  8.3.3 IDEAstatica and a flexible face . . . 61

9 Expanding to full-size **63**
9.1 Modeling properties . . . 63
9.2 Finite element modelling technique . . . 65
9.3 Weld failure load . . . 65
9.4 Global deformation . . . 66
9.5 Local deformation . . . 67
9.6 Internal forces . . . 68
9.7 Rotation stiffness of the structure elements . . . 71
  9.7.1 Beam rotations . . . 72
  9.7.2 Column rotations . . . 72
  9.7.3 Column face rotations . . . 73
  9.7.4 Bearing in the bolt holes . . . 74
  9.7.5 Compatibility . . . 75
9.8 Validation of the proposed formula . . . 76
  9.8.1 Position of zero bending . . . 76
  9.8.2 Estimated failure load . . . 77
9.9 Possible simplifications of the calculation model . . . 79
9.10 Effect of cross-section yielding. . . . 80
9.11 Component based stiffness of the column face . . . 81
9.12 IDEAStatica modelling of full-size beams . . . 83
9.13 Conclusions on designing a weld for fin-plate joints . . . 85

10 Conclusions and recommendations **87**
10.1 On the design of the welds. . . . 87
10.2 On the use for fin-plate connections on SHS columns . . . 89
10.3 On the usage of IDEAStatica . . . 90
10.4 Recommendations for further research . . . 91
  10.4.1 Stress distribution in the weld . . . 91
  10.4.2 Single side welding . . . 91
  10.4.3 Effective column length. . . . 91
  10.4.4 The effect of the bolt thread and bearing . . . 92

A New specimens **93**

B Welding procedures **97**
B.1 S355 weld material . . . 100
B.2 S690 weld material . . . 101

C Estimation of joint resistance **103**
C.1 Nominal eurocode calculation procedure . . . 103
  C.1.1 Joint geometry . . . 103
  C.1.2 fin-plate resistance . . . 104
  C.1.3 weld resistance . . . 105
  C.1.4 Bolt resistance . . . 105

C.2 Set 1 - C690-W355-F355-B355-3mm 106
  C.2.1 Estimated joint resistance 1E1 1E2 106
C.3 Set 2 - C690-W355-F355-B355-3mm-single 107
C.4 Set 3 - C690-W690-F355-B355-3mm-single 108
C.5 Set 4 - C355-W690-F355-B355-3mm-single 108

Bibliography **109**

1

Introduction

There is a growing interest in the use of high strength steel in structural applications. In recent years the manufacturing costs for higher grades are going down. The commonly used S235 is phasing out while S355 is becoming the standard. The structural benefit from such a change is that less material can be used, which would result in lighter structures and a slight environmental bonus. The design rules, however, are yet to catch up with the new development. The current Eurocode design rules and internal knowledge within steel companies are mostly solid for standard connections up to S460; but beyond that there are hesitations in the application.

Complementary to a higher member grade is that connections are also designed with higher grades. This introduces changes that can affect the behaviour in joints and importantly in brittle welded connections, as increasing the grade can reduce the ductility in the material. Design philosophies are commonly based on this ductility, meaning a structure can redistribute forces in the plastic stage. The new uncertainties can result in the creation of over dimensioned joints and thus the over-usage of material and labor hours in construction.

The research is performed in cooperation with the design bureau and manufacturer ASK Romein. With five factory locations in the Netherlands and Belgium the company is pioneering in research as preparation of using up to S690 steels in future column-beam joints. Also for their current products, the planning and execution of welded connections with stiffeners, extension plates, stubs and so on is a big factor in the cost and time of a project. A practical contribution of this research is providing guidance for more efficient joint creation and to add knowledge in realistic plastic behaviour.

This report presents the results from the experimental verification of a simple (non moment resisting) column-beam joint consisting of an unstiffened hollow section column with a welded fin plate which is bolted to an I profile beam. The results will be presented in two ways: The first being the resistance side showing measured strength of the joint elements. The second is an extensive study on determining the influence of the overall structure geometry and profile choices on the force distribution within the joint. A calculation method and a component stiffness parameter will be presented.

In order to have the results as reliable as possible, the scope will be limited to profiles similar to the experiment. This limits to using square hollow sections in S355 and S690 with a width of 200mm and a thickness ranging from 8-32mm, the length being either 1m or continuous with a 3m building storey height. The weld geometry is limited to a single pass (3mm) on *one side* with S355 or S690 welding wire. The fin-plate is S355 with 2 columns of bolts. The beam is varied between IPE330, 400 and 550 with lengths of 1.2, 6 or 8 m.

The outline of this thesis is as follows:

- The problem statement and research objectives are outlined with relevant background information in chapter 2.

- A study is conducted for creating an accurate physical representation using a finite element model, this is done in chapter 4.
- For a specific beam-column joint a series of experiments is performed to determine its properties and real behaviour, this set-up is explained in chapter 5. The methods used to create data useful for FEM calibration are shown in chapter 5.1.2.
- The calculations according to the 2005 and proposed 2020 version of EN1993-1-8 for this joint are done in chapter 6. The utilization of the design values for strength and geometry aspects, in percentage of the experimental values, are calculated and illustrated to give insight on what points where over-strength is likely to occur.
- For the experiment joints a finite element material and geometry model is made in Abaqus. The aim of this model is to create accurate displacement behaviour and failure criteria for the experiments. later on these models will be used to expand to different geometry. The calibration is done with coupon tests and experiment results, the procedure and results are shown in chapter 7.
- It was found that the force distribution, most importantly the position of zero bending moment, greatly depends on the stiffness of the beam and column elements. In chapter 8 the sensitivity of the thickness of the column face on these stresses is reviewed with FEM models based on limitedly calibrated material models.
- Since the experiment is performed with a down scaled size, the real length of the beam/column elements is at least 3 times greater. Due to different rotations, this has a big influence on the failure load of the joint. The range of failure loads and influential factors are examined with fully calibrated Abaqus models. With this data an analytical model is set up to describe the stiffness problem in such a way that it can be applied in the global bending/shear model of a simple fin-plate joint. Concisely it describes where you should take the point of zero bending when calculating stresses in the weld, bolts, column face and fin-plate. Secondly it provides a stiffness model for the column can be used with the component method. This is all reviewed in chapter 9.

2

Problem statement and research objectives

In this chapter the problem statement and the research objects are presented. This is done by dividing them into two sections. One section focuses specifically on the usage of welds and presents its research questions. The other on the force distribution within the examined joint and its research questions.

The joint focused on in this research is a square hollow section column, with a fin plate welded on its face and on which a beam is bolted. This is a type of joint that is becoming increasingly popular, the reason being the economical assembly in both the factory and on the job site. Figure 2.1 shows the usage of such a joint in an office building carrying a floor beam.

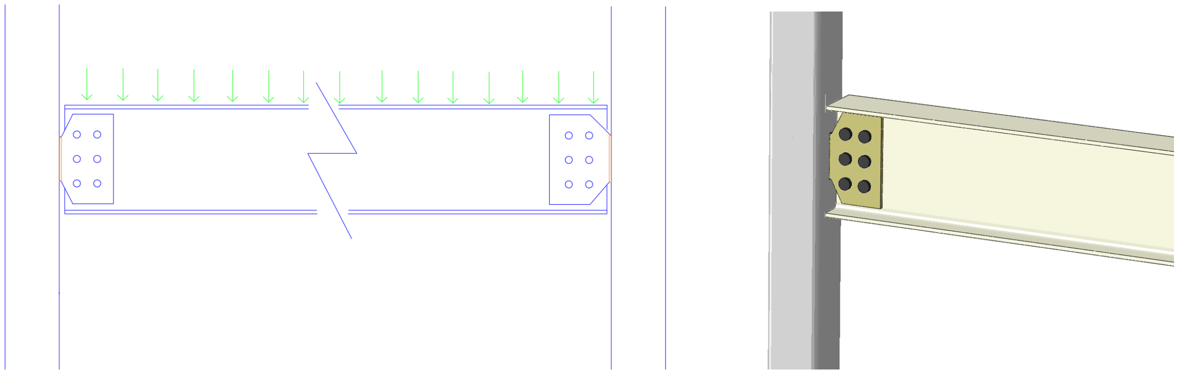

Figure 2.1: Fin-plate joint examined in this thesis

The fin plate can rotate when mounted on the face of a hollow core section, this has a big influence on the force distribution inside the joint and creates a behaviour that is not fully quantified. There is no complete set of rules in EN1993-1-8:2005 to efficiently design for this type of joint. From the following two sources the current calculation procedure is derived:

- The recommendations for the design of simple steel joints [5] based on EN1993-1-8:2005.
- On inquiries to collect information that were performed during a workshop on the ease of use of EN1993-1-8 with engineers from Dutch steel manufacturers and engineering companies, and at the company ASK Romein.

The common answer during the inquiries corresponds to what was stated in the recommendations. The first step is to check the beam as a simple beam (figure 2.2a), there will be a span and a loading which results in a simple $M = \frac{1qL^2}{8}$ check, this is then checked against the resistance and a profile is chosen. The rest of the joint is then checked with eurocode rules for:

Known

- Fin-plate in bearing
- Fin-plate in shear: net section
- Fin-plate in shear: gross section
- Fin-plate in shear: block tearing
- Beam web in bearing
- Beam web in shear: net section
- Beam web in shear: gross section
- Beam web in shear: block tearing
- Edge distance requirements

Unknowns

- Bolt shear resistance
- Avoid (premature) failure of welds
- Elastic bending resistance of fin-plate

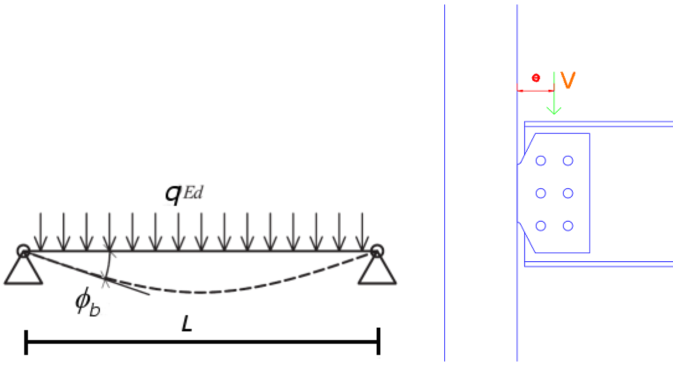

(a) simply supported beam

(b) fin-plate connection

Figure 2.2: Beam and column elements

A key finding is that there are unknowns originating from the last three listed steps. For the welds there was the possibility to use the directional method and calculate a bending and shear contribution, or a full strength weld was applied. For the addition of the moment, and the moment used for checking the bending resistance of the fin-plate $M_{e,d} = V_{e,d} \cdot e$ was used. For e the distance to the center of the bolt group was generally taken, however with two columns of bolts some suggested to take the distance to first bolts, stating that it takes most of the shear force. For the forces in the bolts the opposite is taken, here the distance e is taken as 0, which results in the largest forces. The two extremes that are taken here are shown in 2.3. In reality there will be only one force distribution acting in this connection. Predicting the correct model will have a big effect on the efficient design of the joint and is the key elements of this thesis. A more in depth review is presented in chapters 2.1 and 2.2 in which the research questions will be presented.

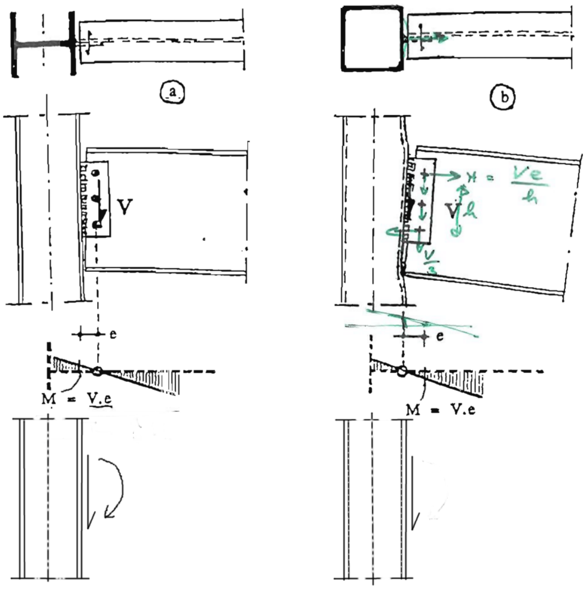

Shear + bending through weld

Shear only through weld

Figure 2.3: Two extremes in force distribution[9, ch. 2]

2.1. Research objectives on fillet welds

In order to motivate the usage of the different calculation methods for welds the following questions should be answered:

- What is the resistance of a single pass weld and what factors influence this resistance?

- What is the resistance of an overmatched single pass weld and what factors influence this resistance? *The scope will be limited to applying S690 weld material with an S355 fin-plate*

- Can the influence ratio of 25% base material and 75% filler material on the nominal design value, as proposed in the new eurocode 1993-1-8, be justified from experiment data?

- What is the design load acting on the weld and what factors influence this load? *The scope will be limited to square hollow core sections*

In chapter 3.1 background information on the terms mentioned here will be given.

2.2. Research objectives on the calculation model for an unstiffened column face.

These questions will be answered by means of the following research goals:

- Determine the column face stiffness influence
- Determine the influence of the bolts
- Determine the influence of the beam stiffness
- Set up an engineering approach to calculate such flexible joints

In chapter 3.2 background information on the terms mentioned here will be given.

3

Current calculation methods for fin-plate joints

This chapter reviews the current calculation methods used to calculate welds and the force distribution within the joint. For the welds the directional method and full-strength method will be reviewed. Secondly the impact of the assumed force distribution and the component method for dealing with stiffness problems is reviewed.

3.1. Calculation methods for fillet welds

3.1.1. Directional method

For calculating the stress state in fillet welds the current Eurocode recommends using the directional method [13, ch. 4.5.3.1]. This method works by taking all the stresses working on the 45° throat plane, see figure 3.1, and checking them against the Von-Mises stress criteria for the critical part the weld.

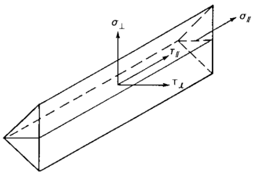

Figure 6.8 — Stresses on the throat section of a fillet weld

$$\sqrt{\sigma_\perp^2 + 3(\tau_\perp^2 + \tau_\parallel^2)} \leq \frac{f_u}{\beta_w \gamma_{M2}} \quad \text{and} \quad \sigma_\perp \leq \frac{0{,}9 f_u}{\gamma_{M2}}$$

Figure 3.1: Directional method from EN 1993-1-8

For the fin-plate connection, which is loaded in shear and bending, the stresses resulting from a combination of shear and bending can be super positioned from two separate formulas. The equations from figure 3.2 provide the peak stress in the critical sections of the welds (A and C). This peak stress is based on a linear stress increase along the length of the weld.

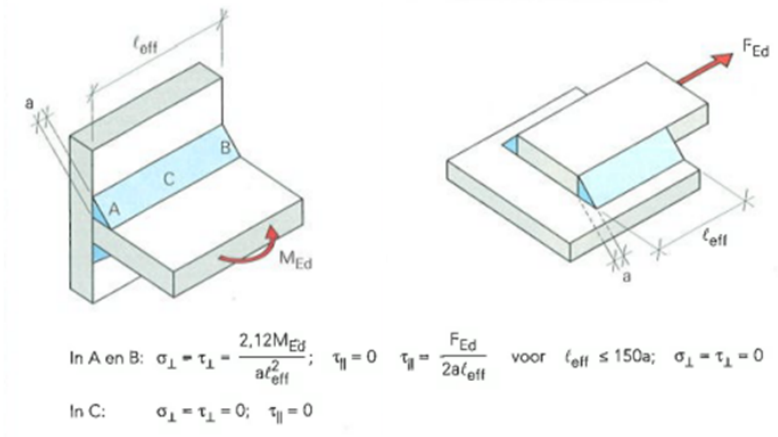

ℓ_{eff}
a
A
B
C
M_{Ed}
F_{Ed}
ℓ_{eff}
a
In A en B: $\sigma_{\perp} = \tau_{\perp} = \frac{2,12 M_{Ed}}{a\ell_{eff}^2}$; $\tau_{\parallel} = 0$ $\tau_{\parallel} = \frac{F_{Ed}}{2a\ell_{eff}}$ voor $\ell_{eff} \leq 150a$; $\sigma_{\perp} = \tau_{\perp} = 0$
In C: $\sigma_{\perp} = \tau_{\perp} = 0$; $\tau_{\parallel} = 0$

Figure 3.2: Deriving stresses from forces

The main forces that theoretically act on the weld are shear and bending in one direction. In reality there could be additional forces acting on it. These could be due to eccentric loading, tolerances in construction, uneven loading in different floor spaces or asymmetric welding. These are just a few examples where the contribution is not always known and is often *avoided*.

3.1.2. Full strength method

To avoid these forces the concept of full strength welding is introduced, in this philosophy the weld throat size is chosen such that it will out perform its plate under any magnitude and direction of loading. The method is based on the yield strength of the plate and the design ultimate strength of the weld. Figure 3.3 and the corresponding formulae show that the plate should be yielding before the ultimate stress is reached in the weld, this way there will be some deformation before the weld fails.

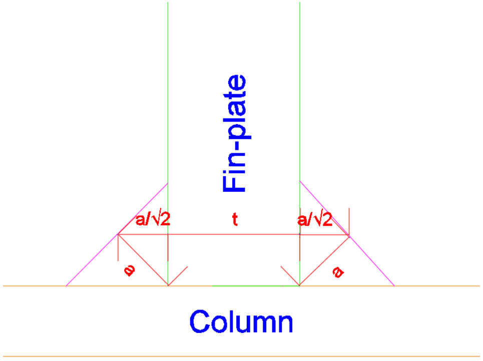

Fin-plate
a/√2
t
a/√2
a
a
Column

$$Q_{r,d,plate} = \frac{f_y \cdot t_p}{y_{m0}} \quad (3.1)$$

$$Q_{r,d,weld,\perp} = \frac{f_u \cdot 2 \cdot a}{\beta \cdot y_{m2} \cdot \sqrt{2}} \quad (3.2)$$

$$Q_{r,d,weld,\perp} > Q_{r,d,plate} \quad (3.3)$$

$$a > \frac{f_y \cdot t_p \cdot \beta \cdot y_{m2}}{\sqrt{2} \cdot f_u \cdot y_{m0}} \quad (3.4)$$

Figure 3.3: Schematic for full strength design

For different base materials there will be different ratio's of the desired throat thickness. In the eurocode it is prescribed that the weld material should be the same strength as the base material, or stronger. For calculations the values for f_y and f_u should be taken as matching with the base material. There are proposed changes to this matching clause, which will shortly be discussed in chapter 3.1.4. For higher grades of steel the ratio between the ultimate and yield strength is smaller, and the correlation factor B_w is increased with decreased ductility. For different grades the resulting thicknesses are shown in table 3.4. [7]. Aside from these ratios, there is a requirement for fillet welds in structural applications that the minimum thickness is 4mm.

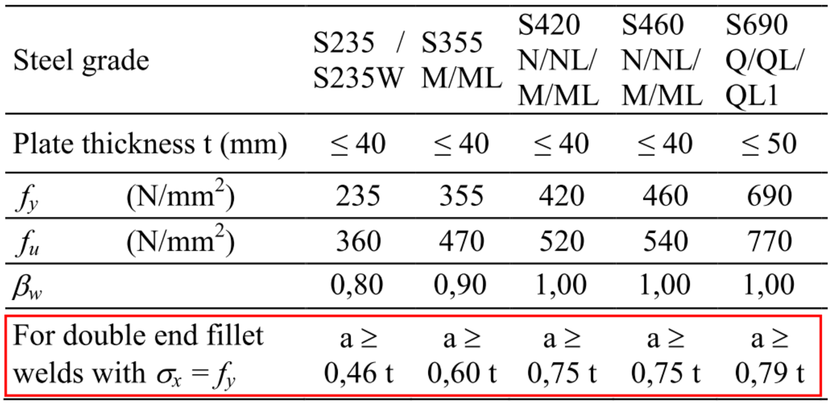

Steel grade	S235 / S235W	S355 M/ML	S420 N/NL/ M/ML	S460 N/NL/ M/ML	S690 Q/QL/ QL1
Plate thickness t (mm)	≤ 40	≤ 40	≤ 40	≤ 40	≤ 50
f_y (N/mm^2)	235	355	420	460	690
f_u (N/mm^2)	360	470	520	540	770
β_w	0,80	0,90	1,00	1,00	1,00
For double end fillet welds with $\sigma_x = f_y$	a $\geq$ 0,46 t	a $\geq$ 0,60 t	a $\geq$ 0,75 t	a $\geq$ 0,75 t	a $\geq$ 0,79 t

Figure 3.4: Full strength weld size based on material strength [7]

Not every code gives the same design recommendations for fillet welds, the American AISC specification recommends a different calculation method resulting in smaller throat sizes compared to EC3 [7, Table 3]. The difference is 0.38t compared to 0.46t for S235 and 0.49t compared to 0.6t for S355. The Swedish code recommends values in between the two [7, Ch 4].

To illustrate the importance of efficient weld design, the throat thicknesses should be expressed in the amount of times a welder has to pass over a weld to achieve this thickness. Via conversations with the welders at ASK Romein the following patterns for fillet welds were found:

- In a single pass a thickness of 3-5mm can be achieved depending on the speed and heat input.

- For a 6mm weld 3 passes are needed.

- Going up to 10mm requires 7 or 8 passes.

These numbers all depend on the experience and preference of the welder, but it is clear that the amount of work for them could be described by a non linear relationship with the throat thickness.

3.1.3. Weld penetration in fillet welds

In chapter 4.5.2 of EN1993-1-8 [13] it is permitted to take into account the penetrated zone, see figure 3.5. This is under the condition that the extra penetration can consistently be achieved. This penetrated zone can be achieved in two ways:

- The first is by grinding the edge of the plate material to create a combination of a butt and fillet weld. Since both welding and grinding are labor intensive this is only interesting when the required weld size is $a > 12mm$. [16] More specifically the benefit here comes from decreasing the volume of the weld triangle, which depends on $V = f(a_{outer}^2)$.

- The second method is by consistently providing enough heat input in the weld procedure to infuse the base material together, this can be quantified by measuring the depth of penetration in a cut-out of the weld. Even without changing any weld procedure this infused zone can already be present and could be measured.

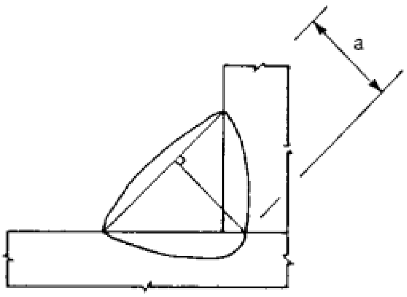

Figure 3.5: Increased a due to penetrated zone

3.1.4. Changes in design rules and overmatching welds

Relevant to the connections examined in this thesis, and similar joints, are new proposed changes in the design rules. These changes have an impact on allowable stresses and the theoretical force distribution within a joint. For simplification there might be references to the 2005 and 2018 eurocodes throughout this document, these refer to the following 2 documents:

Eurocode 3: design of steel structures - part-1-8 Design of joints - 2005 [13].

Eurocode 3: design of steel structures - part-1-8 Design of joints - Draft v4.0 2018 [14].

A change in the design resistance of the weld material is proposed. The original philosophy was that the material strength of the welds should always be equal or stronger than the base material. For calculations the ultimate strength of the base material should be taken. The formulas required to calculate the resistance of the welds are shown below:

$$\sigma_{vm} < \frac{f_u}{\beta_w y_{m2}}$$
$$\sigma_{\perp} < \frac{0.9 f_u}{y_{m2}}$$

Where:
σ_{vm} = Acting Von Mises stress acting on the throat section.
$\sigma_{\perp}$ = Normal stress acting perpendicular on the throat section.
β_w = Correlation factor between weld and base materials.
y_{m2} = Material factor related with brittle failure.
f_u = Characteristic ultimate stress in the weakest part joined.

In the 2018 code the filler material is allowed to be taken in the calculation. The motivation is largely based on the research findings from Rasche (2010) [17]. On a large number of tests a relationship was found between increasing the filler material strength and the resistance of the welded connection. The resistance should be based on 25% base material and 75% filler material. Because not all combinations have been sufficiently researched, the change is applicable only for S460 and up. The change is shown in the following formulas:

$$\begin{aligned} \sigma_{vm} &< \frac{f_u}{\beta_{w,mod} y_{m2}} \\ \sigma_{\perp} &< \frac{0.9 f_u}{y_{m2}} \\ f_u &= 0.25 f_{u,PM} + 0.75 f_{u,FM} \end{aligned}$$

Where:
$\beta_{w,mod}$ = Correlation factor between weld and base materials.
f_u = Characteristic ultimate stress of the welded zone.
$f_{u,PM}$ = f_u from weakest part joined.
$f_{u,FM}$ = f_u from filler material, as shown in table 3.6.

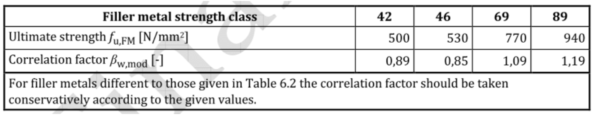

Filler metal strength class	42	46	69	89
Ultimate strength $f_{u,FM}$ [N/mm^2]	500	530	770	940
Correlation factor $\beta_{w,mod}$ [-]	0,89	0,85	1,09	1,19
For filler metals different to those given in Table 6.2 the correlation factor should be taken conservatively according to the given values.				

Figure 3.6: Classes of weld materials [14]

Because weld materials generally have less ductility than the base materials they are defined by classes related to their ultimate strength. This class (Figure 3.6) is what defines them as being matching, over-matching or under-matching to the parent materials. The procedures and weld material used for the experiment are listed in Appendix B.1. The default material procedure used in the company for matching S355 is Outershield MC715-H, with a typical ultimate strength of 580 MPa (class 46). For matching S690 is Megafil 742M, with a typical ultimate strength of 960 MPa (class 89).

This code change allows the use of over-matching and under-matching welds for S460 and stronger base materials. This could allow using a 6mm class 46 weld or a 5mm class 89 weld for a certain design situation, reducing the amount of weld passes. It also allows the use of a thicker undermatching weld with cheaper filler material. The rules are not applicable for all strength classes, for this thesis it will be applied to S355 material to verify its applicability.

Lastly the minimum nominal design throat thickness is proposed $a > 3mm$ compared to $a > 4mm$ before. The load carrying capacity of such small welds will be investigated.

3.1.5. Effect on material usage

The difference between a full strength weld and one that is calculated by the directional method can be significant. This means that the designer has to make a well informed decision to either go for the full strength weld and deliver an expensive product, or to reduce the weld size and save costs. For the joint that will be used in experiments later on, this problem is shown in figure 3.7. Since a full strength weld depends on the plate thickness, for scenarios where this thickness has been increased to cope with bending or for practical purposes, the difference in full and partial can be very large.

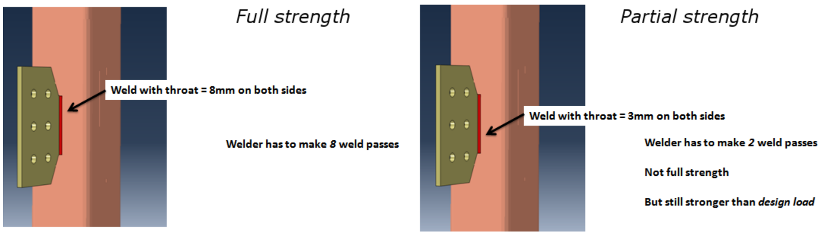
Full strength
Weld with throat = 8mm on both sides
Welder has to make 8 weld passes
Partial strength
Weld with throat = 3mm on both sides
Welder has to make 2 weld passes
Not full strength
But still stronger than design load

Figure 3.7: Choice of full strength vs partial strength for a 15mm S355 fin-plate loaded with a 200 kN shear force

3.2. Influence of calculation methods on the design load

Coming back to the calculation example from chapter 3. The second unknown originated from the check of the fin-plate for Bending in its strong axis, and the weld for shear and bending. When a stiff column is used, for example an HEB profile where the welded plate is the extension of the web, there will not be a lot of movement from the column and generally one can calculate the connection with a vertical force applied at a certain distance e, generally taken somewhere in the center of the bolt group. Knowing where to place the force exactly could be very beneficial to the the stresses caused by that bending moment, an illustration for the design resistance of a certain weld (length = 300mm, a = 3mm), based on the eccentricity of the load is given in figure 3.8. It can be seen that the weld design resistance against the applied vertical force drops rapidly to around 50% at the center of the bolt group. For the joint used in experiments (length = 160mm, a = 3mm) the difference is more pronounced with only 31% design resistance remaining compared to taking $e = 0$.

The moment that follows from $M_{e,d} = V_{e,d} \cdot 100[mm]$ could be provided by the column if it was an H profile with a stiff web. However for configurations with the flexible face of a hollow core section, and a weld length of only 160mm, it is very unlikely that this face can provide this moment, the fin-plate will simply rotate along with the beam end rotation. Designing the weld for this moment would then also be an inefficient design. The real position of e could then be somewhere in between 0 and the bolt group, increasing the design resistance.

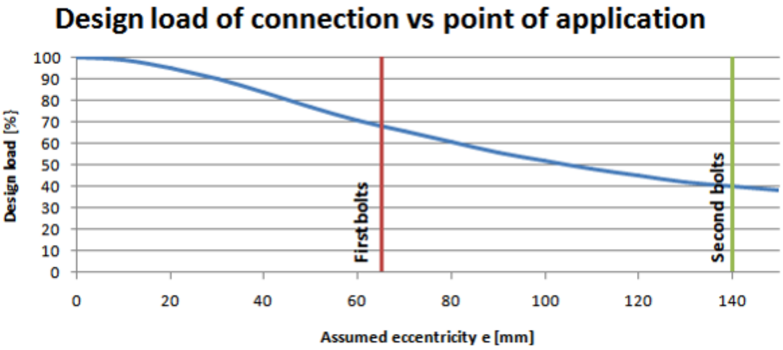

Figure 3.8: Influence of application point on design resistance of the weld for a 300mm weld

3.2.1. Component method

The current eurocode gives guidelines how to start with this problem. In short this is a stiffness problem, where the main point is that a stiffer joint will take up more forces. The **Component method** classifies a joint into three categories:

- Pinned joints. These joints should transfer the forces without generating significant bending moments. The rotation capacity required for the connecting member should be satisfied.

- Full strength joints. These are stiff joints, which require to have a higher moment resistance than both the beam and column it connects. A moment resisting joint would fall into this category.

- Partial strength joints. If a joint does not fall into the other categories it should classified as a non-full-strength joint.

These classifications are shown in figure 3.9a. The stiffness of the joint S_j will be judged against the stiffness of the beam K_b and column K_c. The stiffness of the joint is calculated by taking the addition of each individual 'Basic' element, Figure 3.9b illustrates how much individual components a joint can consist of. [19]. This research will only focus on pinned joints.

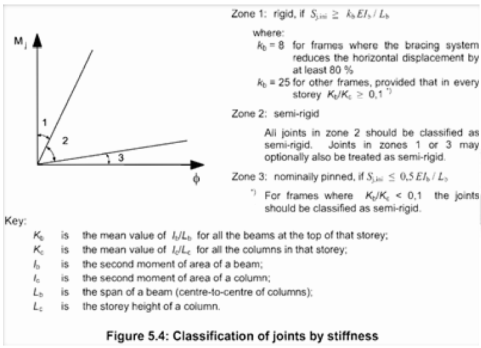

Zone 1: rigid, if $S_{j,ini} \geq k_b EI_b / L_b$

where:
$k_b = 8$ for frames where the bracing system reduces the horizontal displacement by at least 80 %
$k_b = 25$ for other frames, provided that in every storey $K_b/K_c \geq 0,1$ *)

Zone 2: semi-rigid

All joints in zone 2 should be classified as semi-rigid. Joints in zones 1 or 3 may optionally also be treated as semi-rigid.

Zone 3: nominally pinned, if $S_{j,ini} \leq 0,5 EI_b / L_b$

*) For frames where $K_b/K_c < 0,1$ the joints should be classified as semi-rigid.

Key:

K_b	is	the mean value of I_b/L_b for all the beams at the top of that storey;
K_c	is	the mean value of I_c/L_c for all the columns in that storey;
I_b	is	the second moment of area of a beam;
I_c	is	the second moment of area of a column;
L_b	is	the span of a beam (centre-to-centre of columns);
L_c	is	the storey height of a column.

Figure 5.4: Classification of joints by stiffness

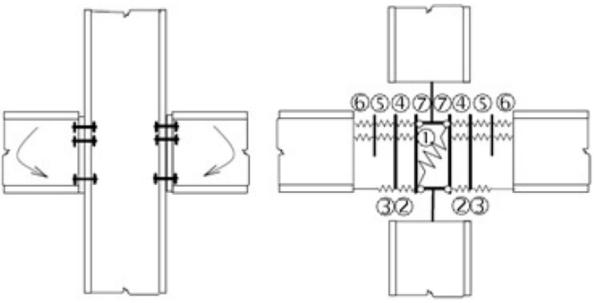

(a) Classification based on stiffness of beam and column

(b) Illustration of all the elements used in the component method [19]

Figure 3.9: Eurocode classification

Most of the basic components for this method have been designed for H or L profiles. The list presented in table 6.1 of EN1993-1-8 is extensive, but it is by no means complete. Some concerns about the validation of certain components, such as the interaction factor B for two beams attached to one column, have been raised. [12, ch 2.5] But most importantly, for the joint researched there are no formulas describing bending stiffness of the column face, which is the key element in efficient weld design.

4

Literature on finite element modeling

In order to obtain reliable results to answer the research questions a computer model will be created. There are several levels of accuracy and simplicity when running computer aided calculations for steel joints. Traditionally there are empirically or analytically validated design formulas used to check every element (plates, welds, bolts etc.) of the joint, this can be used for the component method or in a frame calculation. These are valid for any geometric configuration of a joint as long as the engineer is able to relate them to the basic element cases listed in the code [12, ch. 2.2]. Because each element is examined separately, and the code provides a safe lower bound solution, the interaction between the basic cases is limited. This can be overcome by applying a finite element model. There are more motivations for using such a model, this become very relevant when predicting the experiment behaviour:

- A realistic force and stiffness interaction between elements.

- Plastic redistribution of peak stresses.

- Non linear behaviour.

- A solution for an element that can not easily be reduced to a basic case.

In this Thesis, two methods are examined: The first one is 'regular' finite element modeling (FEM). This method refers to slicing up the complex geometry of an entire joint into small elements with geometry that can be managed and calculated in a reliable manner. The second method is Component based finite element modeling (CBFEM). This method uses regular FEM and the component method in synergy. This allows for a more accurate stiffness interaction and some plastic redistribution in steel plates, at the same time elements that do not benefit from this like bolts and welds are modeled as nonlinear springs and can be calculated by the component rules. It should be noted that the written comparison here is limited for illustration purposes and is not the complete picture.

What is important here is that even though computers are getting faster all the time, the computation time and the time to create a model can still take many hours when using FEM. Also the engineer needs to have an understanding of the model inputs and results in order to fully evaluate a joint. The CBFEM method tries to be more accessible for engineering purposes by using component based joint generation, and by reducing the calculation time to mere minutes using component rules.

The rest of this chapter will focus mainly on the choices made for the finite element models which are expected to show accurate results corresponding to the experiment results. The behaviour should match in:

- The slip phase of the joint.

- The linear-elastic phase of the joint.

- The plastic stage of the joint.

- The failure/fracture load of the joint.

The starting points for this modeling are based on the research done in the master thesis by S. Navarro [12] and G. Maheninggalih [11]. This chapter is subdivided into the sections:

- Software

- Implicit/Explicit modeling

- Element types and size

- Material properties

4.1. Software

The finite element software used for verification of IDEAStatica, and to be validated with the experiment, is Abaqus by DSS Simula. While other software could be used for steel joints (such as Diana), it is important that there is enough knowledge and experience to get suitable results. Thus the primary reason for starting with this software is that it has been used and validated for similar purposes by Dr. M. Pavlovic and others at Delft University of Technology. [12] [15] [6]

4.2. Implicit/Explicit modeling

There are two types of solvers in Abaqus to be used in non-linear analysis, implicit solver and explicit solver.

An *Explicit* solver does an incremental displacement or force step, where at the end of an increment a new stiffness matrix is generated based on the new geometry and material properties. The solution for each timestep depends as an increment on the previous timestep solution. There is no equilibrium of internal forces in this method. This means the solution can deviate from the real solution at each timestep if the time increment is not small enough.

The *Implicit* solver works in the same way as Explicit, with the addition of a force equilibrium at each step. This force equilibrium is numerically calculated each step, if a converging solution is found then this method is more accurate. The problem with this solver, is that for contact surfaces and bolt-slip convergence problems can occur. [20]

For this last reason the Explicit solver is used, with a small enough stable time increment. The settings used for all analysis are shown in figure: 4.1.

Combined with a total step time of 1000-10000 seconds, these settings proved suitable for a quasi-static analysis using this dynamic solver. [12, ch. 3.5.4] This was done by verifying:

- The resulting input force should roughly match the reaction forces. This is to check if static equilibrium is present.

- The amount of kinematic energy should not be too large compared to the internal energy in the system.

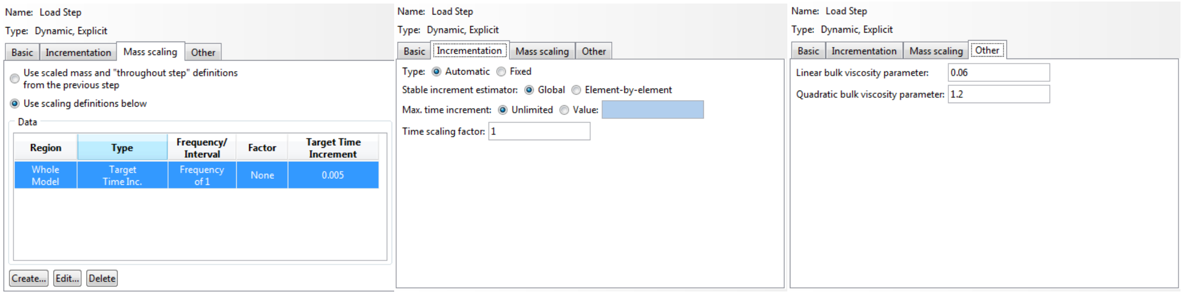

Name: Load Step
Type: Dynamic, Explicit

○ Use scaled mass and "throughout step" definitions from the previous step
● Use scaling definitions below

Data

Region	Type	Frequency/ Interval	Factor	Target Time Increment
Whole Model	Target Time Inc.	Frequency of 1	None	0.005

Name: Load Step
Type: Dynamic, Explicit

Type: ● Automatic ○ Fixed
Stable increment estimator: ● Global ○ Element-by-element
Max. time increment: ● Unlimited ○ Value:
Time scaling factor: 1

Name: Load Step
Type: Dynamic, Explicit

Linear bulk viscosity parameter: 0.06
Quadratic bulk viscosity parameter: 1.2

Figure 4.1: Timestep settings in Abaqus [12]

4.3. Element type and size

In a sensitivity analysis done by (Navarro [12]) it was found that using solid elements was suitable for modeling all elements, including the bolts and weld. Elements made from C3D8R or C3D8I both showed suitable results [12, p. 28], Since C3D8I elements have 4 integration points (compared to 1 in the reduced element) it is better at prediction bending behavior. The drawback from using the full integration elements is the computation time, since the models already take 10 hours to run on available hardware the reduced integration elements are used. The condition for this to work is to make the mesh small enough on area's with stress concentrations; the welds, the bolt holes. Accurate results were found with the element sizes as in table 4.1. In chapter 7.2.2 it was found that the bolt threads still require additional parameters. Transition zones are made by Tetrahedron elements. An image of the final experiment model is included in figure 7.1.

Table 4.1: Element sizes

Position	Element type	Element size [mm x mm x mm]
Column	C3D8R	10x10x2
Column face around weld	C3D8R	2.5x5x2
Column face against weld	C3D8R	2.5x1x2
Weld	C3D8R	1x1x1
Fin-plate against Weld	C3D8R	1x1x1
Fin-plate near Weld	C3D8R	2.5x2.5x2.5
Fin-plate near bolts	C3D8R	2.5x2.5x2.5
Fin-plate outer rim	C3D8R	10x10x2.5
Beam	C3D8R	10x10x2.5
Beam near bolts	C3D8R	2.5x2.5x2.5

4.4. Material properties

For the material properties there will be two models used:

1. Strain hardening

The eurocode (EN1993-1-5 Annex C) allows four different methods for modeling of material behaviour, these are listed in figure 4.2. There is a big reserve in strength after reaching the yield stress. Since the models are going to be validated by experiments, it would not make sense to not take this in to account. For modeling of the design strength for a model the hardening model with nominal values will be used. This is still a lower bound for the actual failure load and stiffness, thus the model should always reach its failure load earlier compared to the experiments.

2. True stress strain

For the more accurate behaviour and failure of the load, true stress strain is used. This behaviour has to be calibrated with coupon tests. Parameters in this calibration are also the element size and element type. a calibrated material model used with different elements can result in an over/under estimation of the results. Thus this model can only be used with validated accuracy on a joint with similar geometry as the experiment joint. This model will however allow for extraction and analysis of the stresses and strains present along each position in the joint.

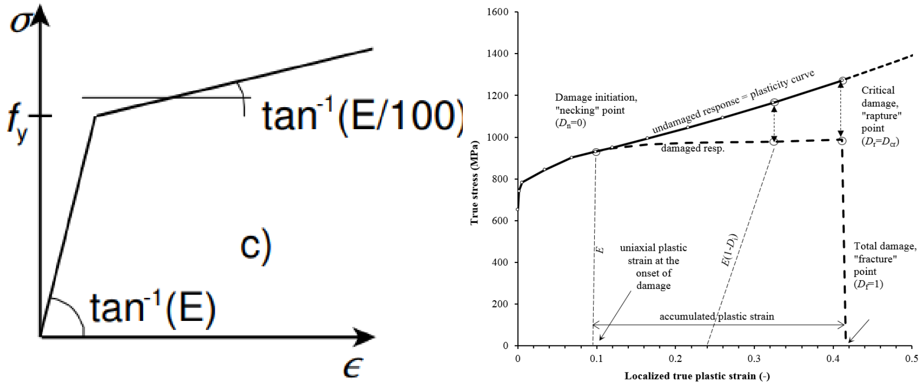

(a) Nominal hardening (b) True stress strain and damage modeling

Figure 4.2: Difference in material modelling

4.5. Stress state in Abaqus

The method used for modeling plastic material is by using the Von-Mises stress state and equivalent strain. This assumes that yielding of the metal is independent of the equivalent pressure stress. This is confirmed experimentally for most metals under positive pressure stress but may be inaccurate for metals under conditions of high triaxial tension when voids may nucleate and grow in the material. [18, ch 23.2.1] The tips of welded part of the joint is exactly this part with a high triaxial (combination of shear with a distinction of compression or tension) state, this effect needs to be taken into account to accurately predict post yielding behaviour.

The following terms are important in this context:

- **The von-Mises equivalent stress** is defined by the principle stresses in x,y and z direction in an integration point.

$$\sigma_{eq} = \frac{1}{\sqrt{2}}\sqrt{(\sigma_1-\sigma_2)^2+(\sigma_1-\sigma_3)^2+(\sigma_3-\sigma_2)^2}$$

- **The equivalent strain** is defined by the principle strain in x,y and z direction in an integration point.

$$\epsilon_{eq} = \frac{\sqrt{2}}{3}\sqrt{(\epsilon_1-\epsilon_2)^2+(\epsilon_1-\epsilon_3)^2+(\epsilon_3-\epsilon_2)^2}$$

- **The stress triaxiality** is defined as the ratio of the hydrostatic stress and the von Mises equivalent stress.

$$t = \frac{\sigma_H}{\sigma_{eq}} = \frac{(\sigma_1+\sigma_2+\sigma_3)/3}{\frac{1}{\sqrt{2}}\sqrt{(\sigma_1-\sigma_2)^2+(\sigma_1-\sigma_3)^2+(\sigma_3-\sigma_2)^2}}$$

In research done by Changsik et al (2011, [3]) the effect of triaxility on the fracture strain for their mild steel specimens is clearly displayed with the help of figure 4.3. There is an exponential relationship between fracture strain and triaxiality, this means that increasing the tension on an element will decrease the strain it is expected to fail at.

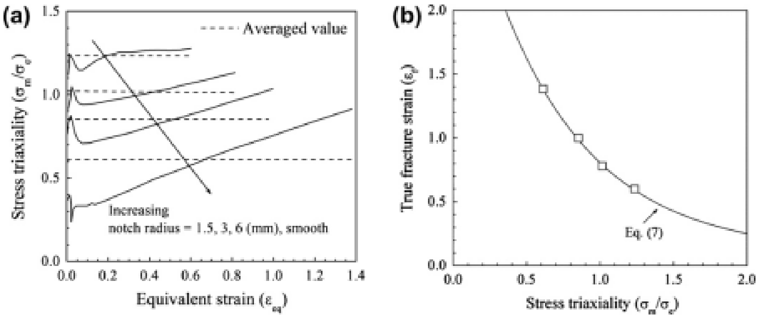

Fig. 11. (a) Variations of the stress triaxiality with the equivalent strain for smooth and notched bar tensile tests, and (b) fracture strain as a function of the stress triaxiality.

Figure 4.3: Effect of tri-axial state on true fracture strain [3]

In order to cope with this phenomena the recent approach is to use shear and ductile damage modelling in abaqus. The input for this method is the damage initiation and the damage progression. Again this method has to be calibrated in a similar way as the true stress/strain method. [15] In figure 4.2 the difference in the effective true stress/strain is shown.

5

Experiment set-up

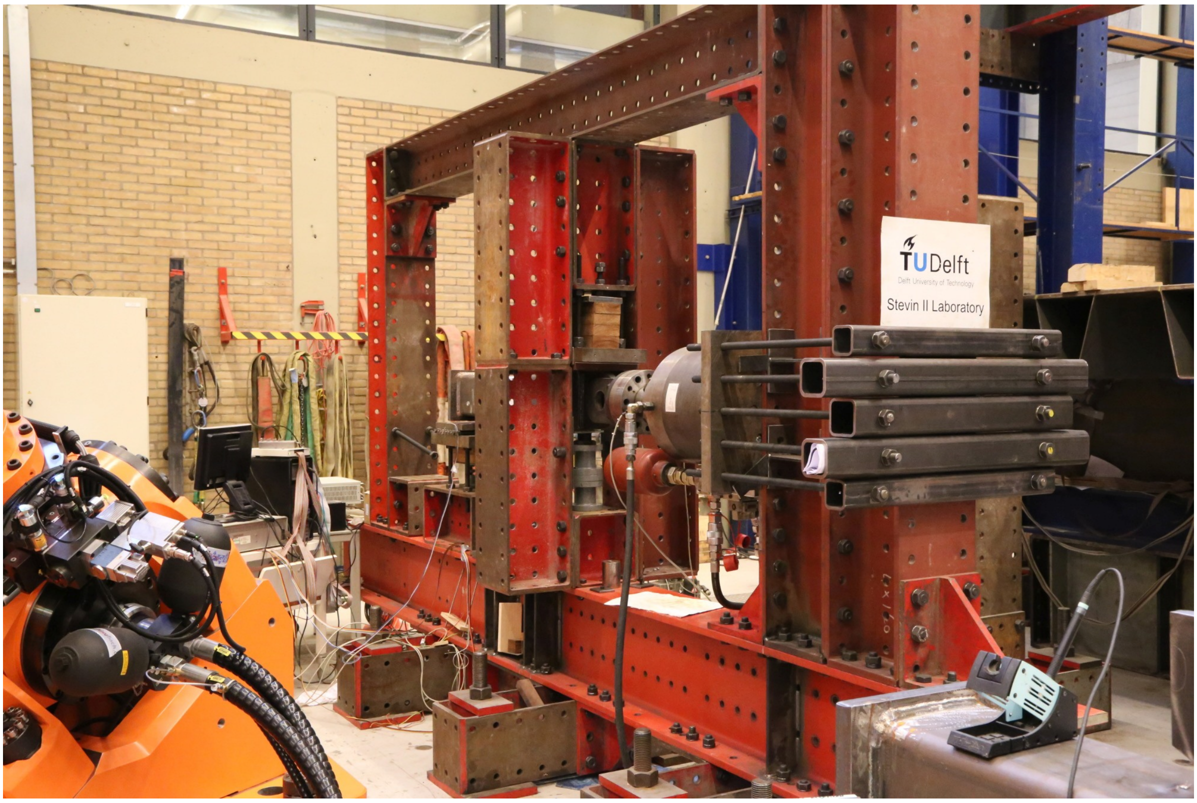

Figure 5.1: Specimen 2E1 in test set-up

A series of experiments have been conducted in the Stevinlab at TUDelft as shown in figure 5.1. In this chapter the motivation for setting the experiment parameters, the specimen set-up and the frame set-up will be presented.

Data collected from experiments could validate and correct input parameters for calculation methods and models. In general, a joint is designed according to a set of rules stated in a national code. With a non standard joint, however, the margins and applicability might not be fully known to the engineer. This generate uncertainties for the design.

There are three types of experiments performed:

1. A series of full scale joints are tested for strength and stiffness.

2. Tensile coupon tests for each plate material.

3. Tensile and shear tests on the welds.

The set-up of the full scale experiment joints includes a few key considerations :

- *Why a square hollow section as a column?*
The column face is flexible, which can reduce the stresses in a welded connection on it. See chapter 8 for a complete explanation.

- *Why single side and double side fin-plate welds?*
Welding is expensive, if it can be done on a single side with the minimum throat thickness then unnecessary man hours can be avoided. The asymmetric behaviour should be examined in order to find a range of applicability.

- *Why use overmatching weld strength?*
Historically the stress used for the calculation of the weld resistance is limited to that of the base material, and the weld material has to have a higher failure stress. In the new eurocode rules this has been adjusted to include a 75% weld material and 25% base material composition. This allows for the possibility of using a thinner weld with a higher stress allowance. Again less welding means more efficient manufacturing. This research will found out whether this holds or not.

Ultimately the experiment has three main goals:

1. The first is to validate the ultimate strength with the questions listed above.

2. To verify a FEM model technique such that it behaves accurately with reality, even after reaching the plastic deformation stage. This can then be extended to other geometry.

3. To validate the outcome of the commercial software for this type of joint.

The experiment set-up is summarized in the flowchart in figure 5.2.

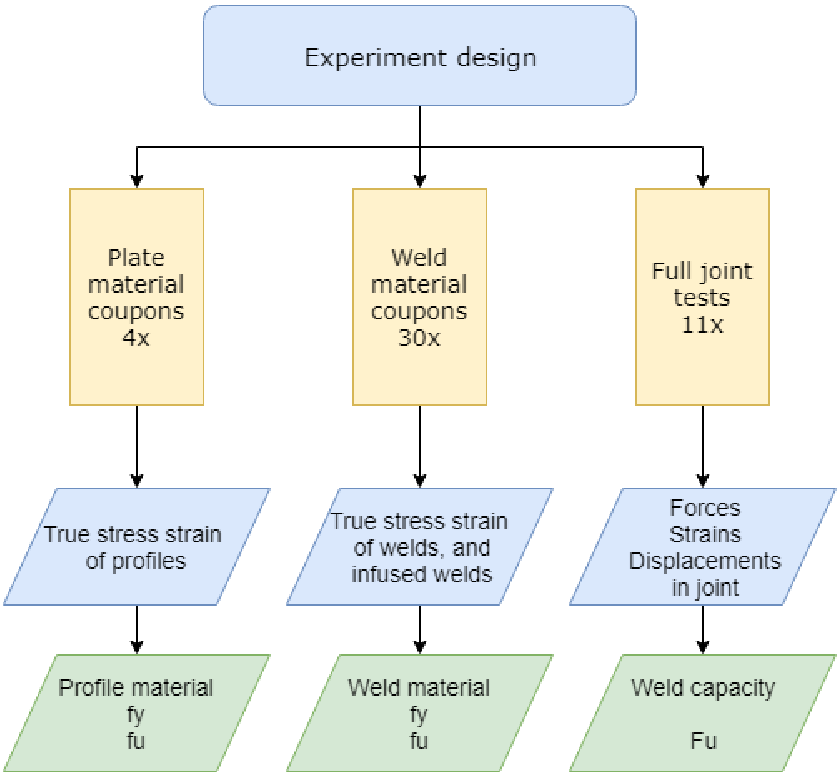
Experiment design
Plate material coupons 4x
Weld material coupons 30x
Full joint tests 11x
True stress strain of profiles
True stress strain of welds, and infused welds
Forces Strains Displacements in joint
Profile material fy fu
Weld material fy fu
Weld capacity Fu

Figure 5.2: Experiment flowchart

5.1. Full joint tests

5.1.1. Specimen design

The experiment consists of 11 specimens, the parameters for this have been designed in a such way that they behave like a joint that will be used in practice. This means that:

- The connection has not been scaled down, the dimensions are such that they comply with the **design** load for the beam section.

- The welds are in accordance to the certified welding procedure from ASK Romein and Hillebrand BV, see appendix B for procedures. This means that the welds are done by hand by an experienced welder. A 3mm weld is handled as a weld where the throat size is bigger or equal to 3mm. This is not counting the heat affected zone in the base material, no pre-treatment is done but there is also no effort made in trying to avoid making this zone. In the end results the throat size of the failure planes turned out to be >5mm. Since according to current Eurocode rules the weld material has to match or overmatch the base material strength, by default a weld material with a yield stress of 480 MPa is used complementary for S355 base materials in the company.

There are four sets of specimens. The original calculation for the specimens followed nominal values. In the first set the welding was done on both sides of the plate. The weld resistance turned out to be much higher than expected and the failure mode was unwanted shear failure and net section yielding of the fin-plate. Therefore the decision was made to first reduce the length of the weld by creating a cut for specimen 1E3. When this turned out to be not enough the whole plan was re-evaluated. In the new sets the welds reduced to 160mm on a single side of the fin-plate, a 70% reduction in weld length.

In table 5.1 an overview of the final sets is shown. The difference in the fin-plates and welds for set 1 compared to the rest is displayed in figures 5.3 and 5.4. A full overview of the production drawings is provided in appendix A.

Table 5.1: Specimen overview - Nominal values

Identity	Column	Fin-plate	Beam	Weld yield [N/mm^2]	Weld throat [mm]	Weld length [mm]
1E1	S690	S355	S355	>355	3	2x300
1E2	S690	S355	S355	>355	3	2x300
1E3	S690	S355	S355	>355	3	2x220
2E1	S690	S355	S355	>355	3	160
2E2	S690	S355	S355	>355	3	160
3E1	S690	S355	S355	>690	3	160
3E2	S690	S355	S355	>690	3	160
3E2	S690	S355	S355	>690	3	160
4E1	S355	S355	S355	>690	3	160
4E2	S355	S355	S355	>690	3	160
4E2	S355	S355	S355	>690	3	160

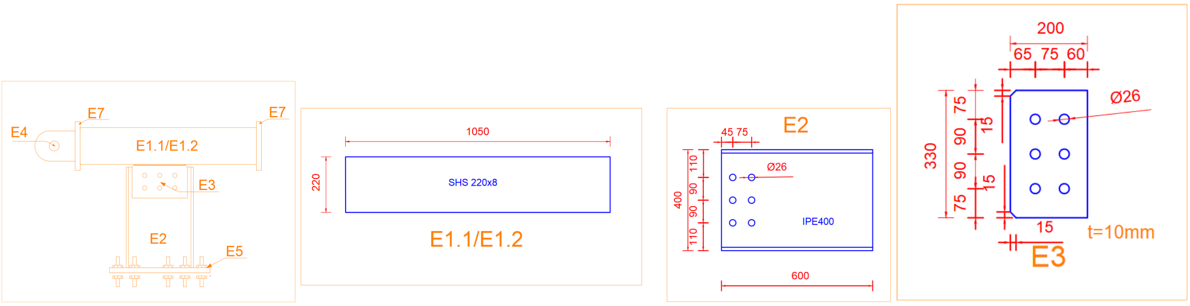
E4
E7
E7
E1.1/E1.2
E3
E2
E5
1050
220
SHS 220x8
E1.1/E1.2
45 75
E2
Ø26
110
90
90
110
400
IPE400
600
200
65 75 60
Ø26
330
75
90
90
75
15
15
15
t=10mm
E3

Figure 5.3: 1E* specimen set

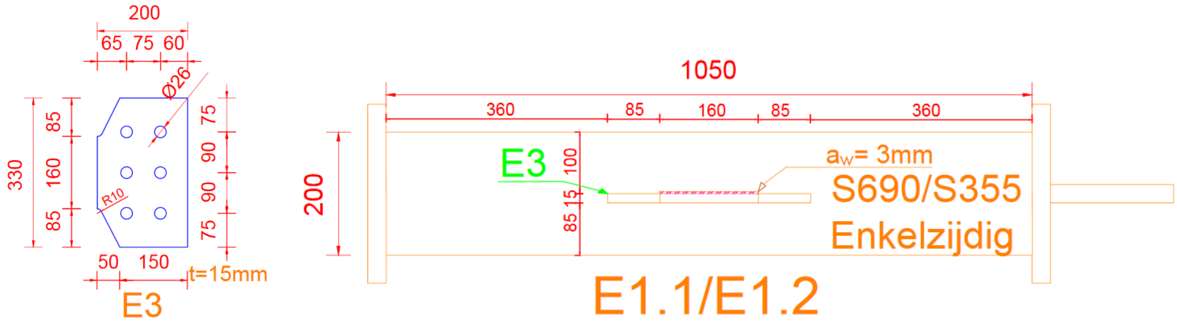
200
65 75 60
Ø26
330
85
160
85
75
90
90
75
R10
50 150
t=15mm
E3
1050
360
85
160
85
360
200
E3
100
85 15
a$_w$= 3mm
S690/S355
Enkelzijdig
E1.1/E1.2

Figure 5.4: 2E*, 3E*, 4E* specimen set

5.1.2. Dimensions

The specimens are produced with tolerances in their geometry and minimum requirements for their material properties. In order to create any model to match this, these elements should be implemented. The thickness of each plate element is measured and the yield/ultimate stresses are measured from coupon tests (table 5.2), more details about these coupon tests can be found in the chapter on material calibration (chapter 7).

* 3.6mm outer throat + 1.8mm burned into base material, see figure 7.4

Table 5.2: Specimen materials - real values

Identity	Nominal thickness / throat [mm]	Measured thickness / throat [mm]	Nominal yield [N/mm^2]	Measured yield [N/mm^2]	Nominal ultimate [N/mm^2]	Measured ultimate [N/mm^2]
Column S690	8	8.13	690	714	770	836
Column S355	8	7.5				
Beam web	8.6	8.53	355	435	470	532
Fin Plate 1E	10	10.18	355	375	470	553
Fin Plate 2E,3E,4E	15	15.02	355	375 (est)	470	553 (est)
Weld	3	5.4-6*	480	-	590	-

5.1.3. Frame set-up

The frame is used for the experiment is specifically designed for a beam-column joint. For an expected specimen failure load of 700 kN, to ensure that it remains in elastic stage the design load was set to 1400 kN. Since the available material was limited, it was not realistic to reach this load. In the end the limit of the bolts in the specimen clamp (Brittle failure) reduced the frame design load to 1000 kN. In figure 5.5 the side and 3d view of the frame is shown. The hydraulic jack provides a pushing force onto the specimen, which is clamped onto the frame (figure 5.7), two stiffeners ensure that there is no deformation of the frame beam flanges. The boundary conditions used for modelling later on have to follow the actual structure, the roller/slider supports are shown in figure 5.6.

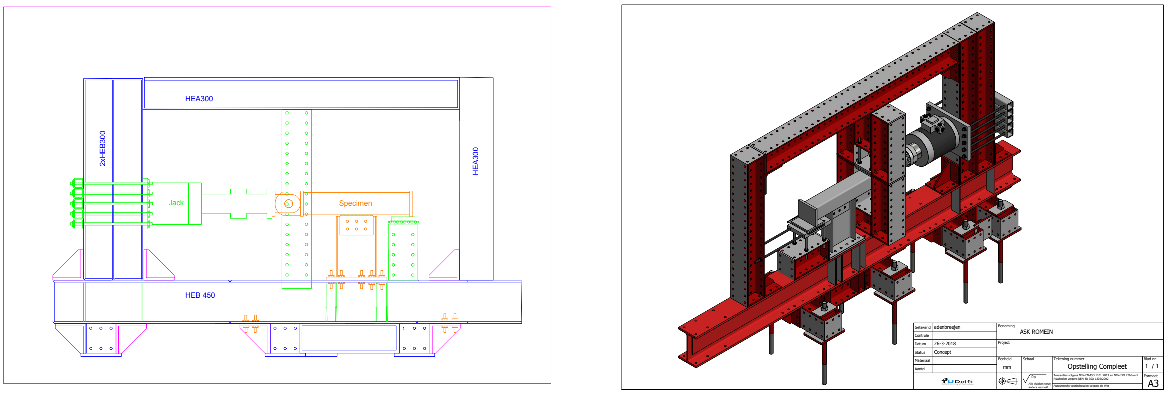
HEA300
2xHEB300
HEA300
Jack
Specimen
HEB 450
ASK ROMEIN
26-3-2018
Concept
Opstelling Compleet
A3

Figure 5.5: Frame sketch

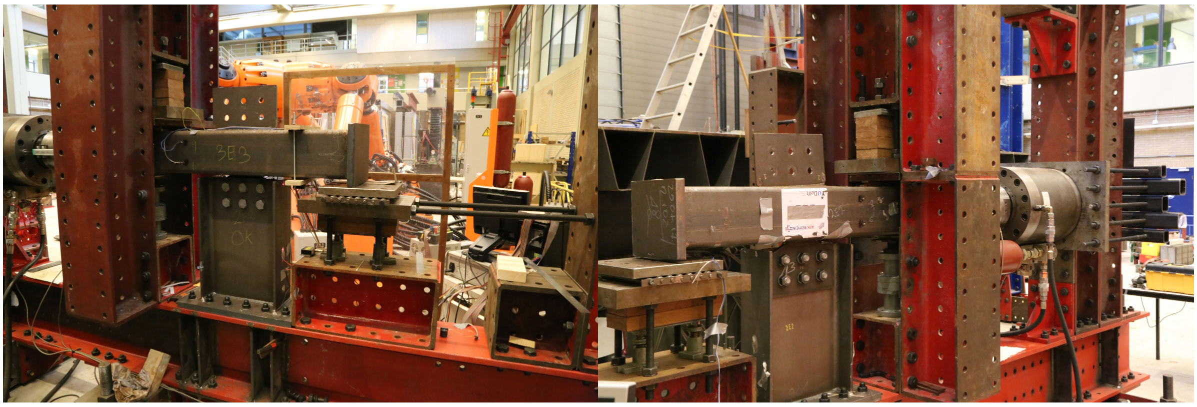

Figure 5.6: Roller supports

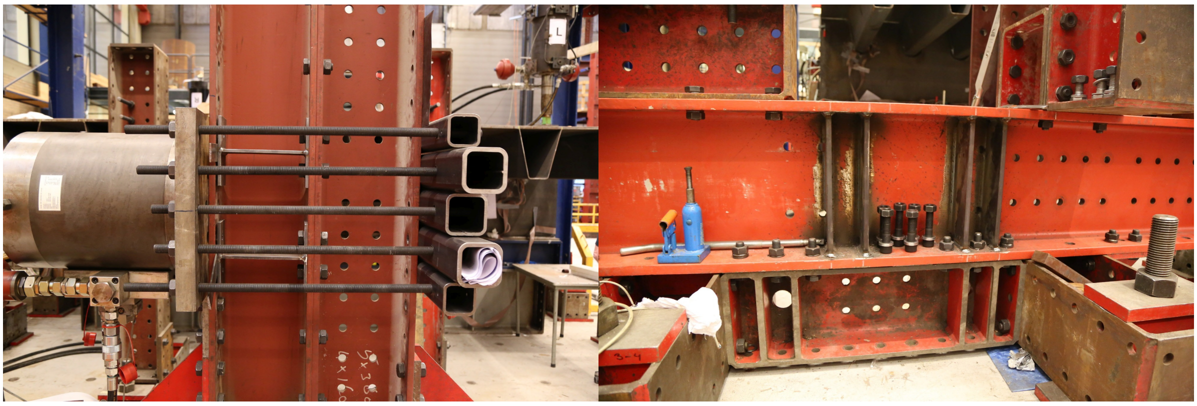

Figure 5.7: Specimen clamp and jack mount

5.1.4. Instrumentation

The specimen is set up to measure strains, rotations and displacements. The strains are measured with 12 strain gauges as shown in figure 5.8, the purpose of these is to validate the strains occurring in the abaqus models. The rotation of the fin-plate is measured by two LVDT's and the relative displacement between beam and column is measured by a laser. Lastly the slip of the complete specimen is monitored with another LVDT.

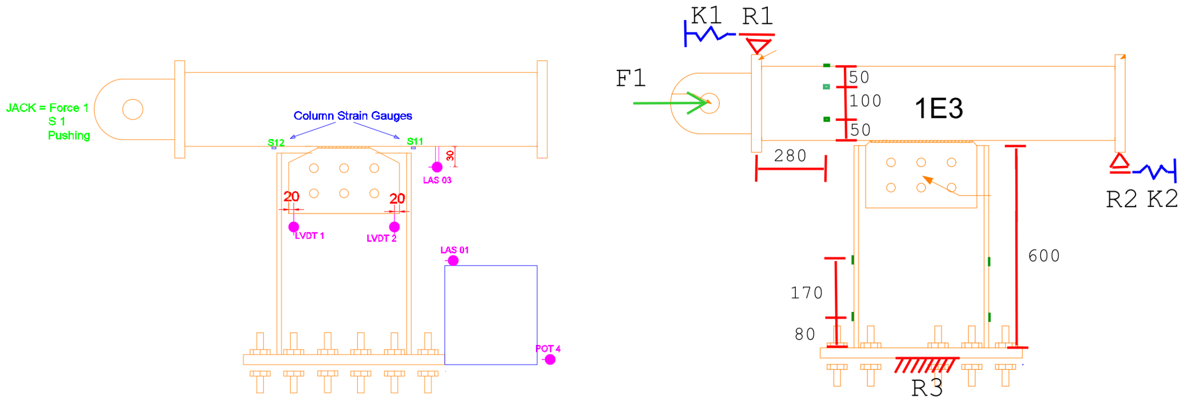

(a) Measurements used for rotation (b) Supports and strain gauges in 1E3

Figure 5.8: Instrumentation for rotation and strain measurements

5.1.5. Test results

The failure loads and mechanisms of the main experiments will be presented in this chapter. Table 5.3 categorizes each specimen into a failure mode and provides the failure load. There are three important modes that were observed;

- Fin-plate yielding: Here the fin-plate deforms plastically near the weld, but no fracture is observed. The experiment is performed with controlled hydraulic displacement with a maximum jack displacement of 50 mm. When the fin-plate reaches a certain plastic strain the deformation increases without adding any significant force increment, when the maximum displacement is reached the experiment is stopped.

- Buckling of the IPE beam: The maximum force the beam could take up with its bending resistance, without causing too much jack displacement, was around 700 kN. After reaching this force level an extra block of wood was added to support the beam and to decrease the lever arm from 600 mm to 300mm. When further increasing the force the beam web buckled near this added support.

- Shear failure in the infused weld zone (IWZ): In this failure mode the weld zone failed in a brittle/sudden manner. Producing a loud bang and a clear fracture plane in the fin-plate.

Table 5.3: Specimen failure overview

Identity	Column	Weld [N/mm^2]	Fin-plate t [mm]	Weld length [mm]	Failure load [kN]	Failure mechanism
1E1	S690	>355	10	2x300	690	Fin-plate yield*
1E2	S690	>355	10	2x300	860	Beam buckle
1E3	S690	>355	10	2x220	820	Fin-plate yield
2E1	S690	>355	15	160	539	IWZ shear
2E2	S690	>355	15	160	550	IWZ shear
3E1	S690	>690	15	160	660	IWZ shear
3E2	S690	>690	15	160	659	IWZ shear
3E2	S690	>690	15	160	630	IWZ shear
4E1	S355	>690	15	160	623	IWZ shear
4E2	S355	>690	15	160	654	IWZ shear
4E2	S355	>690	15	160	644	IWZ shear

* This test had frame failure of the moment clamp and was loaded four times. It is not possible to determine the force distribution in this joint.

5.2. Plate material coupon tests

For each element a coupon has been cut out and tested in a tensile pulling test. Each material only has been tested once. The manufacturing drawings are presented in figure 5.9. The results for the yield and ultimate (engineering) stress are displayed in table 5.4. It should be noted that for the fin-plate only a coupon with 10mm thickness is made, the material model from this will also be used for the 15mm thick plate.

Table 5.4: Coupon yield and ultimate stress

coupon	grade	width [mm]	thickness [mm]	f_y [N/mm^2]	f_u [N/mm^2]
RHS	S355	19.95	7.50	-*	526
RHS	S690	20.00	8.13	-*	836
Fin plate	S355	19.99	10.18	375	553
IPE400 web	S355	19.92	8.53	435	532

* Coupons of RHS sections were initially bended (relief of residual stresses in faces of the RHS section). This caused problems with the extensiometer, resulting in unreliable strain recordings. Yield ($R_{p,0.2}$) strength can not be determined from the test results. Reference length extensiometer: 62 mm

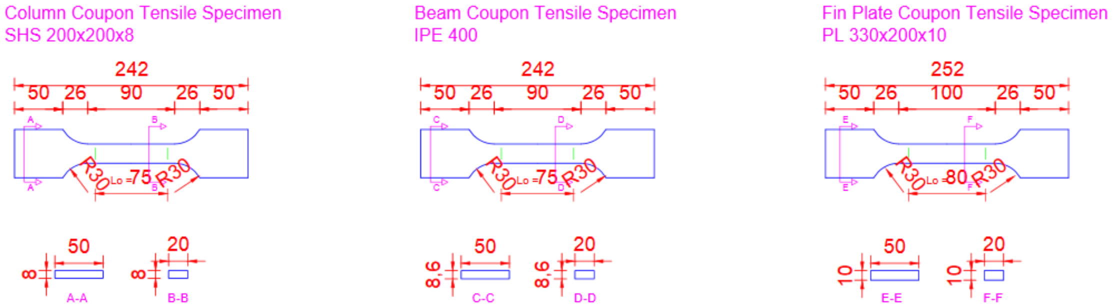
Column Coupon Tensile Specimen
SHS 200x200x8
242
50 26 90 26 50
R30 Lo =75 R30
50
20
8
8
A-A
B-B
Beam Coupon Tensile Specimen
IPE 400
242
50 26 90 26 50
R30 Lo =75 R30
50
20
8.6
8.6
C-C
D-D
Fin Plate Coupon Tensile Specimen
PL 330x200x10
252
50 26 100 26 50
R30 Lo =80 R30
50
20
10
10
E-E
F-F

Figure 5.9: Manufacturing drawings of coupons

5.3. Weld coupon tests

The main experiment gives a good result on the shear resistance of the welded connection. It is however not possible to estimate failure strains and the progression of the true stress/strain curve of the weld material and the infused weld zone. A series of tensile and shear tests have been performed. In this thesis only a single tensile and a single shear specimen is used, the results will be used to estimate the failure strain for only the S355 weld material. The geometry of these specimens is shown in figure 5.10, the dimensions in table 5.5. In this table the throat size of the weld, and the effective throat size are given. This effective size is including the infused weld zone. In chapter 7.3 the results are processed.

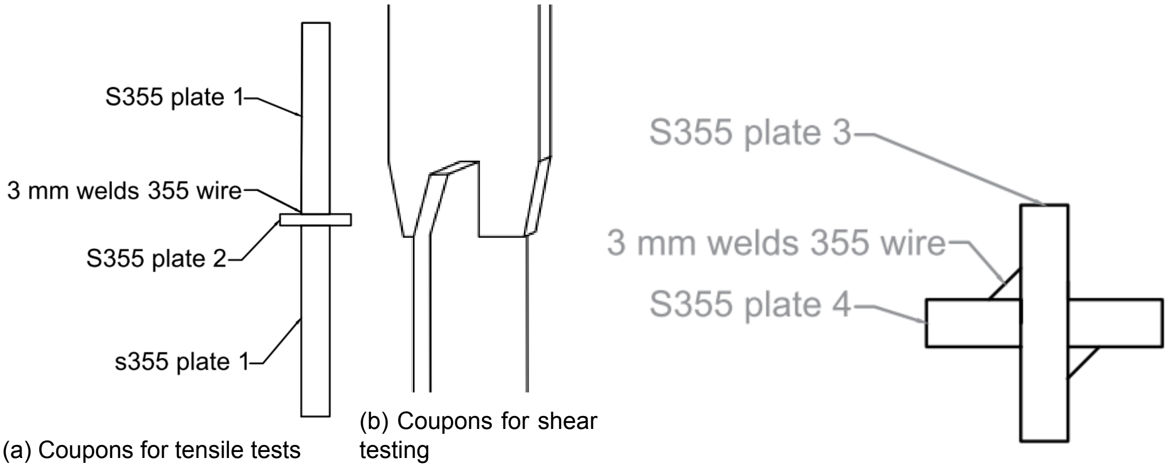
S355 plate 1
3 mm welds 355 wire
S355 plate 2
s355 plate 1
S355 plate 3
3 mm welds 355 wire
S355 plate 4

(a) Coupons for tensile tests

(b) Coupons for shear testing

Figure 5.10: Coupons for welds

Table 5.5: Measured geometry weld coupon

coupon	plate 1 [t x b x l]	plate 2 [t x b x l]	plate 3 [t x b x l]	plate 4 [t x b x l]	weld a, a_{eff} [mm,mm]	weld l [mm]
T-specimen	20x50x350	20x50x100			3.2, 5.2	50
S-specimen			20x150x400	20x150x400	3.1, 5.1	50

5.4. Data analysis

The raw results will be processed to determine the load transfer through the specimen. The force applied from the jack is not equal to the force transferred through the joint. The two supports that keep the SHS column level provide a resistance in horizontal direction which needs to be calculated. The location and size of the failure planes with their failure stresses are then determined. The rotations of the fin-plate are then calculated.

5.4.1. Estimating frame friction from experiment data

Often the friction force in an experiment frame is neglected. The goal of this chapter is to determine if this force is indeed negligible or if there really is an influence. The practical limits of the used measurement equipment allow only for a good estimate to be made. The free body diagram used in this chapter is displayed in figure 5.11.

The method used for determining this friction is as follows:

- Convert strain gauge data on column to a normal force and bending moment. For this a linear strain distribution and a linear stress/strain relation is assumed. See figure 5.11.
- Convert strain gauge data on beam to a normal force and bending moment. Because of local disturbances only the strain gauge data at 80mm from the end-plate is used, for this a linear strain distribution and a linear stress/strain relation is assumed. The strain gauges at 250mm from the end-plate show more disturbances from the force introduction by bolts, using a linear strain distribution here will not be accurate. The vertical reaction force R3 is equal to the normal force.
- From the bending moment in the column a shear force is determined, which corresponds to the vertical reaction force R1.
- The strain gauges on the beam could not be used to obtain a bending moment and normal force with the linear assumptions used for the column element. The distance to the bolts and to the moment clamp is too short. To obtain the reaction force R3 the model from Abaqus has been used. In figure 5.12b the strains measured in the experiment are compared to those found in the model, the correlation is accurate enough for this purpose.
- The difference between R1 and R3 is R2.
- The horizontal reaction force in R1 and R2 is assumed to be a function of the vertical force. From literature a friction coefficient of 0.04 is used (Teflon on Teflon). $R1_{Horizontal} = K1 * R1_{Vertical}$
- The ratio between the total horizontal friction force and the applied force is determined. This ratio is determined for three force levels, and will be used to determine an equivalent 'Applied jack force' from the FEM analysis.

Table 5.6: Properties of elements

Element	SHS 200x8	IPE400	unit
Height	200	400	[mm]
A	6166	8381	[mm^2]
I	$3.628 \cdot 10^7$	$2.3131 \cdot 10^8$	[mm^4]
E	210000	210000	[N/mm^2]

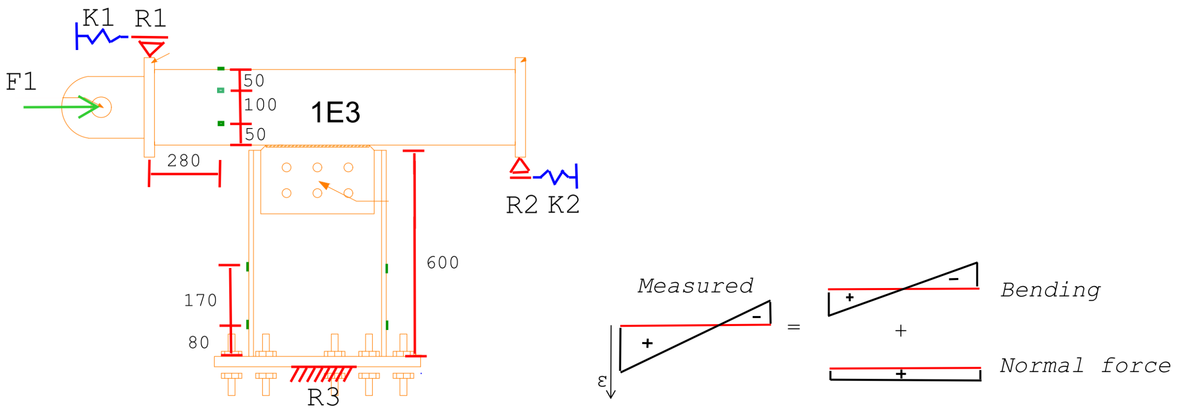

(a) Supports and strain gauges in 1E3

(b) Estimated strain distribution

Figure 5.11: Elements used for determining friction

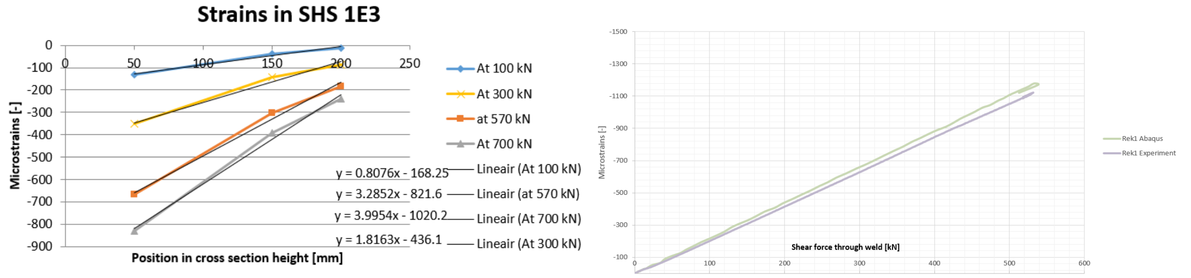

(a) 1E3 SHS strain gauges

(b) 2E1 strain gauge verification

Figure 5.12: Strain gauge measurements

Table 5.7 shows the strains and resulting moment/normal force SHS column for 4 different force levels. From this table it is clear that the measured normal forces are 13% higher than the applied jack force. This is physically not possible, it means the assumptions in the cross sectional area and/or the strain distribution is at least 13% off. This is compensated by adding an additional 10% to the friction force. The friction loss table also shows that the second support would provide a downward force onto the specimen at 100 kN load level, this is not possible so this data point will also be ignored.

Table 5.7: Bending moment and normal force in the SHS column

Jack Force	Avg Normal microstrain	Bending microstrain	Normal force	Bending moment	Shear Force
[kN]	[-]	[-]	[kN]	[kNm]	[kNm]
1E3					
100	-87	-80	-113	-6	-22
300	-254	-181	-329	-13	-49
570	-493	-328	-638	-25	-89
700	-620	-399	-803	-30	-108

Table 5.8: Friction loss in the set-up

Jack Force [kN]	$R1_{vertical}$ [kN]	$R2_{vertical}$ [kN]	$R3_{vertical}$ [kN]	$(R1+R2)_{horizontal}$ [kN]	Estimated friction loss [%]
1E3					
300	49.4	-13.3	-36.1	2.8	0.9
2E1					
300	53.0	-44.7	-8.3	3.9	1.3

This procedure has been repeated for the other experiment sets, the results are shown in table 5.9. Also included in this table are the results of experiment 1E1, this value has to be interpreted with consideration of the following notes:

- This experiment had load cells at the supports, meaning the values of the vertical support reactions are measured directly. They have then been multiplied by 0.04 to estimate the horizontal reaction. The measurements exceeded the 100 kN rating of the units, so they have not been used in next experiments.
- The experiment frame was different from the one used for the other tests, it showed deformation and was dismantled after use. These displacements are the reason why this measurement will be not be used.

The conclusion is that 1.5% friction loss should be taken when taking the force transfer through the weld compared to the force transfer in the jack.

Table 5.9: Average friction loss for all sets

Specimen	min [%]	max [%]	average friction loss [%]
1E1	1.40	1.70	1.50
1E3	0.70	1.40	0.90
2E*	1.30	1.73	1.44
3E*	1.04	1.37	1.17
4E*	1.19	2.07	1.53

5.4.2. Experiment results on shear resistance

Eight of the specimens showed shear failure of the weld. A hand calculation to determine the ultimate stress has been made. This is done by measuring the shear plane at failure and determining the force transfer in the weld. Furthermore the trajectory of the failure plane is determined.

In the first table in figure 5.14 the position and location of failure plane is shown (green = fin plate HAZ, yellow = column HAZ, red = weld), position 0 is the compression zone and 160 the tension zone. The total length of the shear plane also takes into account the extra weld material around the ends of the fin-plates, this results in 160+12+12 = 184mm for most specimens.

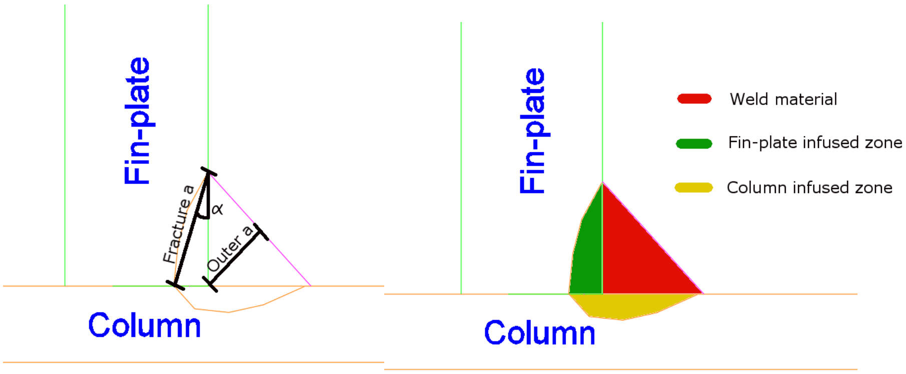

(a) Dimensions measured before and after testing

(b) Zones through which the fracture progresses

Figure 5.13: Dimensions for showing fracture progression

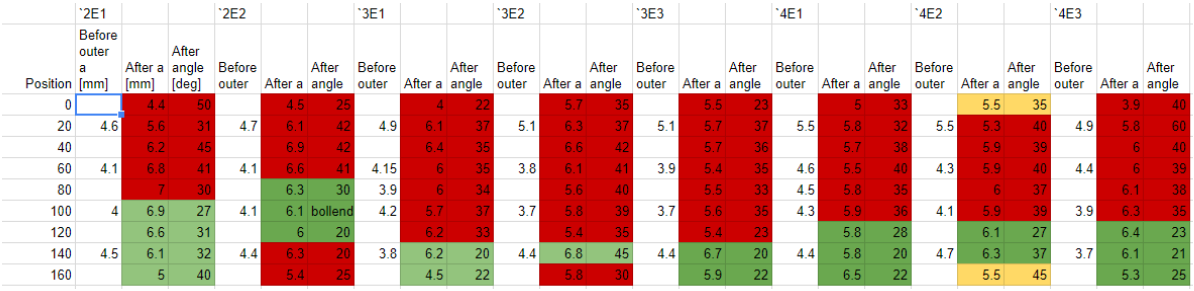

	`2E1			`2E2			`3E1			`3E2			`3E3			`4E1			`4E2			`4E3		
Position	Before outer a [mm]	After a [mm]	After angle [deg]	Before outer	After a	After angle	Before outer	After a	After angle	Before outer	After a	After angle	Before outer	After a	After angle	Before outer	After a	After angle	Before outer	After a	After angle	Before outer	After a	After angle
0		4.4	50		4.5	25		4	22		5.7	35		5.5	23		5	33		5.5	35		3.9	40
20	4.6	5.6	31	4.7	6.1	42	4.9	6.1	37	5.1	6.3	37	5.1	5.7	37	5.5	5.8	32	5.5	5.3	40	4.9	5.8	60
40		6.2	45		6.9	42		6.4	35		6.6	42		5.7	36		5.7	38		5.9	39		6	40
60	4.1	6.8	41	4.1	6.6	41	4.15	6	35	3.8	6.1	41	3.9	5.4	35	4.6	5.5	40	4.3	5.9	40	4.4	6	39
80		7	30		6.3	30	3.9	6	34		5.6	40		5.5	33	4.5	5.8	35		6	37		6.1	38
100	4	6.9	27	4.1	6.1	bollend	4.2	5.7	37	3.7	5.8	39	3.7	5.6	35	4.3	5.9	36	4.1	5.9	39	3.9	6.3	35
120		6.6	31		6	20		6.2	33		5.4	35		5.4	23		5.8	28		6.1	27		6.4	23
140	4.5	6.1	32	4.4	6.3	20	3.8	6.2	20	4.4	6.8	45	4.4	6.7	20	4.4	5.8	20	4.7	6.3	37	3.7	6.1	21
160		5	40		5.4	25		4.5	22		5.8	30		5.9	22		6.5	22		5.5	45		5.3	25

Figure 5.14: Data table

In the table of figure 5.15 the failure shear stress is determined. With the assumption of "No other stresses are present" an equivalent Von Mises stress is calculated. The results are presented in this table. There are other stresses present due to bending and normal force transfer, these will be neglected in this chapter. This assumption is justified by the chapters researching the column thickness and size influence, these found the influence to be within 0-3%.

In chapter 5.4.3 the failure planes for each specimen are shown with photographs.

Results:

For the S355 welds: Average Von Mises of 867 MPa at failure

For the S690 welds: Average Von Mises of 1037 MPa at failure

The difference in ultimate stress between (column S690 + weld S690) and (column S355 + weld S690) is negligible. The failure mode is however different, with a longer path through the fin-plate base material for the S355 column.

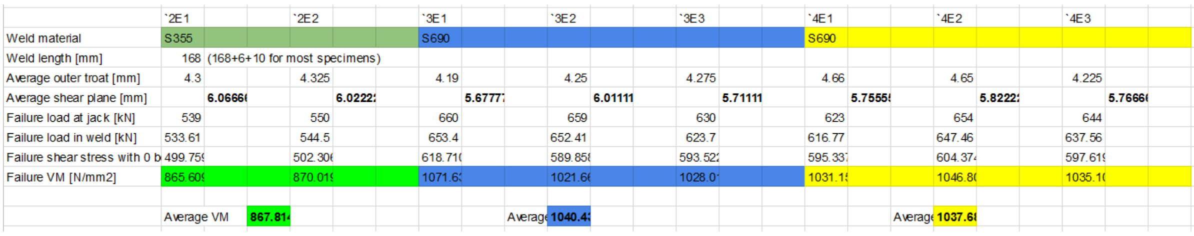

	`2E1			`2E2			`3E1			`3E2			`3E3			`4E1			`4E2			`4E3		
Weld material	S355						S690									S690								
Weld length [mm]	168	(168+6+10 for most specimens)																						
Average outer troat [mm]	4.3			4.325			4.19			4.25			4.275			4.66			4.65			4.225		
Average shear plane [mm]		**6.0666**			**6.0222**			**5.6777**			**6.01111**			**5.71111**			**5.7555**			**5.8222**			**5.7666**	
Failure load at jack [kN]	539			550			660			659			630			623			654			644		
Failure load in weld [kN]	533.61			544.5			653.4			652.41			623.7			616.77			647.46			637.56		
Failure shear stress with 0 b	499.75			502.30			618.71			589.85			593.52			595.33			604.37			597.61		
Failure VM [N/mm2]	865.60			870.01			1071.6			1021.6			1028.0			1031.1			1046.8			1035.1		
	Average VM		**867.81**						Averag	**1040.4**								Averag	**1037.6**					

Figure 5.15: result table

5.4.3. Failure planes of specimens

The specimens failed in brittle shear, this means that there was very little deformation until there was a sudden ’bang’. This makes it impossible to obtain the point of initial fracture by visual inspection during the experiment, there was no fracture at the ends of the welds before failure. From the fracture planes from the failed fin-plates a good estimation of the size of the infused weld zone can be made, the measurements from these planes are used in the previous chapter. To illustrate the method of failure, figure 5.16b is added. This figure looks at the failed weld in the set-up, the column is horizontal and pushed to the right, the beam is vertical and is clamped after 600mm, the fracture is between the fin plate and the column face. In this picture the column is pushed such that a small tension force is on the right side perpendicular to the column face, compression on the left, in the other figures this tension side is at ’160mm’ and the compression at ’0mm’. Figures 5.17, 5.18 and 5.19 show the detached plates with the fracture pattern visible. Figures 5.16a, 5.17, 5.18 and 5.19 show a sketch of the cross section with the fracture plane.

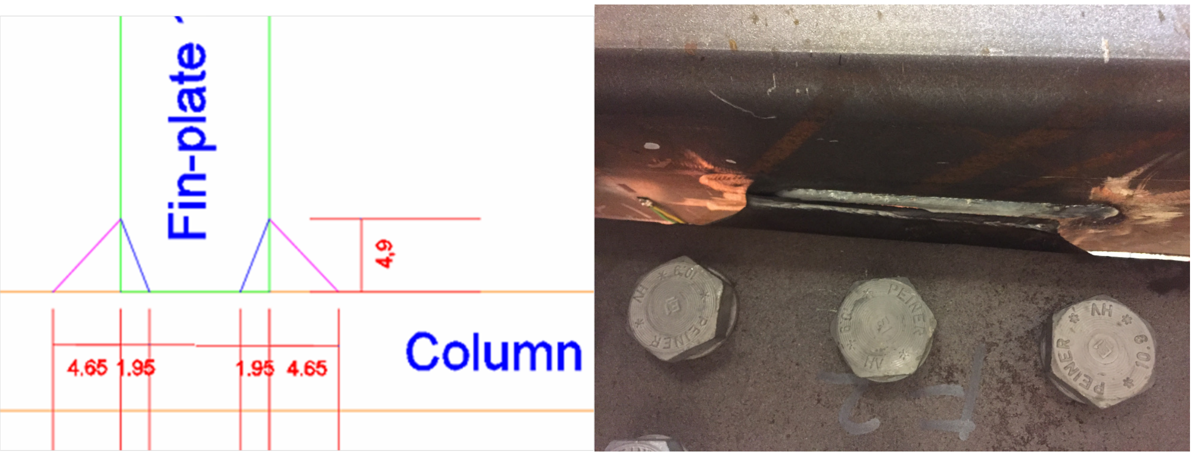

(a) 1Ex HAZ Size

(b) General weld failure of 2Ex 3Ex 4Ex

Figure 5.16: Weld shear in experiment frame

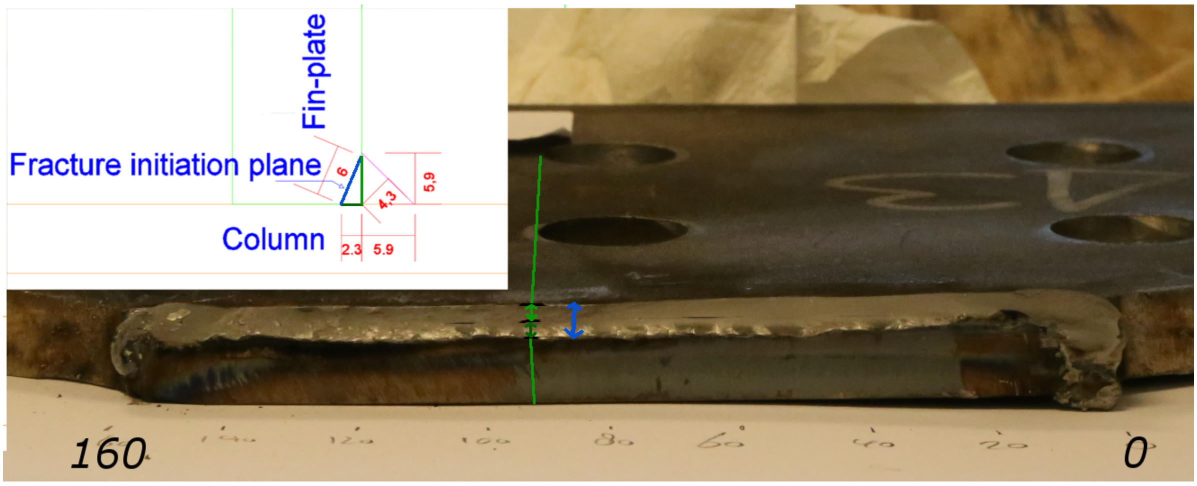

Figure 5.17: 2E1 infused zone and failure plane after testing

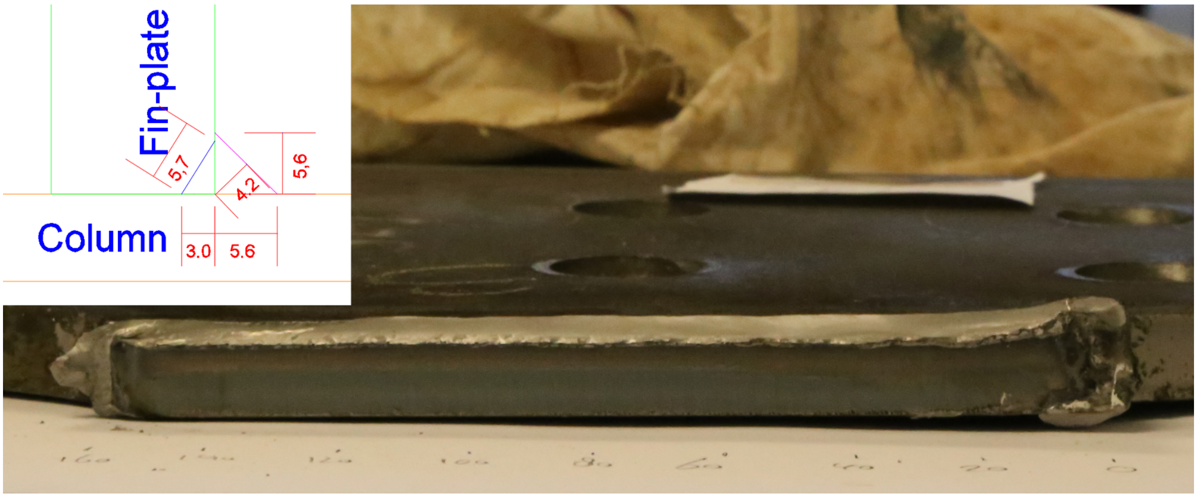
Fin-plate
5,7
4,2
5,6
Column
3.0
5.6

Figure 5.18: 3E1 failure plane after testing

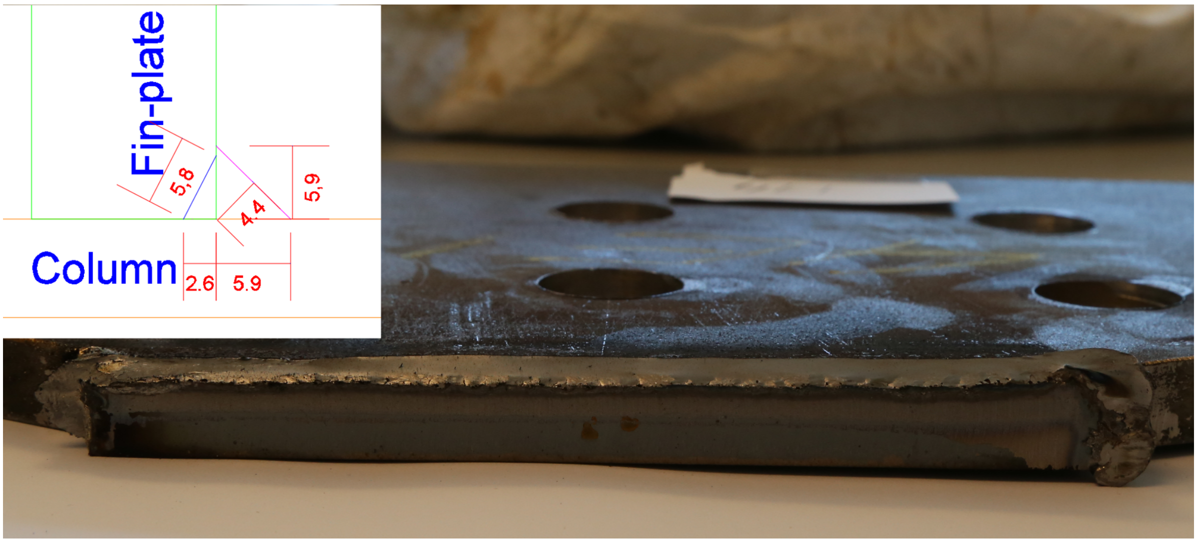
Fin-plate
5,8
4,4
5,9
Column
2.6
5.9

Figure 5.19: 4E1 failure plane after testing

5.4.4. Experiment results on fin-plate rotation

The column face is not a stiff element, the fin-plate is therefore allowed to rotate. Three instruments are used to determine the rotation for each specimen; Strain gauge 11 is located on the column face in transverse direction, it measures the extension of the face in the part where the fin-plate pulls the material outward. Gauge 12 is located in a similar position, but the presence of the compression force disturbs the strain measurement too much. The gauges are only used to validate the Linear displacement measurements (LVDT 1 and 2). These are used to generate a reliable rotation from two measurement points. In 5.8a the position of these instruments are shown.

The results are shown in figure 5.20. The graphs are distinguished into two sets; on the left are the experiments with the S355 column, on the right the S690 column. The results show a big spread in measured data. With visual data during the experiments and a short study on varying several parameters in abaqus the spread can be explained.

- The initial differences in rotation and stiffness can be contributed to the spacing and slip in the bolt holes. The bolts have 1mm spacing all around (on average).

- The vertical supports have been observed to move at least 1 mm during the tests, this has been reproduced in Abaqus. The result is that there was a $0.002[rad](\approx 5\%)$ influence on the rotation.

- The bolts have not been tightened equally in all tests, in test 3E3 some were loose which explains the varying curve.

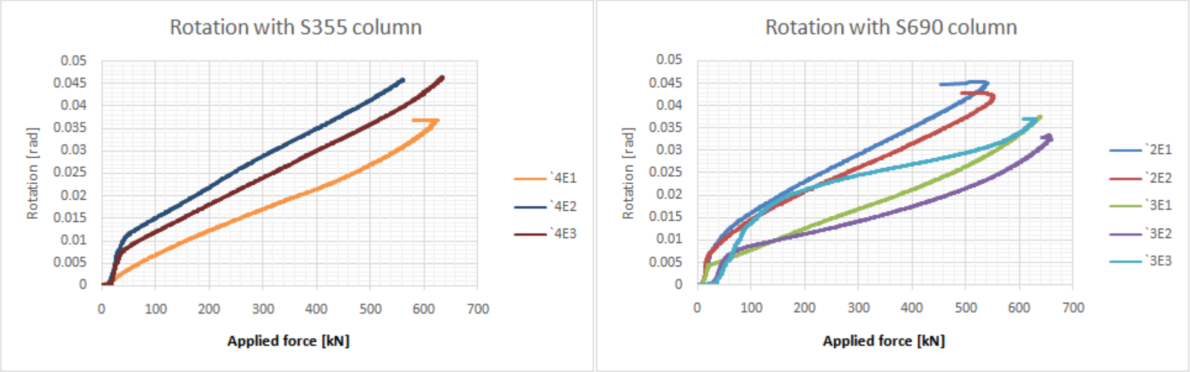

Figure 5.20: strains and rotations from measurements

6

Differences between nominal design and experiment

This chapter is dedicated to give the reader a clear and concise overview on the margins between nominal and realistic loads. The goal is to give insight on possibilities to make more efficient joint designs. The calculations are made according to EC 1993-1-8 version 2005 and the proposed revision. It should be noted that calculations are done with a shear-only force transfer through the weld, meaning $M_{e,d} = 0$, using $M_{e,d} = V_{e,d} \cdot e$ would decrease the design load even more. See appendix C for calculation procedure.

6.1. Margins on ultimate plate stress

The margins for the base material are listed in table 6.1. The values are given as a percentage of the nominal yield and ultimate and their lowest measured counterpart.

Table 6.1: Real base material properties and margin

Material	Yield		Ultimate	
	$[\frac{N/mm^2_{nom}}{N/mm^2_{real}}]$	[%]	$[\frac{N/mm^2_{nom}}{N/mm^2_{real}}]$	[%]
S355	$\frac{355}{375}$	95%	$\frac{470}{532}$	88 %
S690	$\frac{690}{710}$	97%	$\frac{770}{836}$	92 %

6.2. Margins on ultimate weld stress

The margins for the base material are listed in table 6.2. The values are given as a percentage of the nominal ultimate and their lowest measured counterpart. The comparison between the proposed new Eurocode and the current code has been made, in both comparisons the material factor y_m is not taken into account, correlation factors β_w have been taken into account. The material factor will be taken into account when comparing the design loads for this joint.

Table 6.2: Real weld material properties and margin

Material	Ultimate EC 2005 $[\frac{N/mm^2_{nom}}{N/mm^2_{real}}]$	[%]	Ultimate EC 2020 $[\frac{N/mm^2_{nom}}{N/mm^2_{real}}]$	[%]
MC-715H on S355 base	$\frac{522}{865}$	60%	$\frac{572}{865}$	66%
742M on S355 base	$\frac{522}{1040}$	50%	$\frac{691}{1040}$	66%

6.3. Margins due to the infused weld zone

The effective depth of the infused weld zone zone, which can transfer a significant force, is listed in table 6.4. This value depends on the amount of heat input used during welding, and is not proportional with the nominal weld throat size. In the table it will be displayed as a percentage of the 3mm weld. In figure 6.1 the position of these planes are shown for the 2E1 experiment.

Table 6.3: Real weld size

Material	HAZ size $[mm]$	fracture planes $[\frac{mm_{nom}}{mm_{real}}]$	utility [%]
MC-715H on S355 base	2	$\frac{3}{6.0}$	50%
742M on S355 base	2.5	$\frac{3}{5.6}$	54%

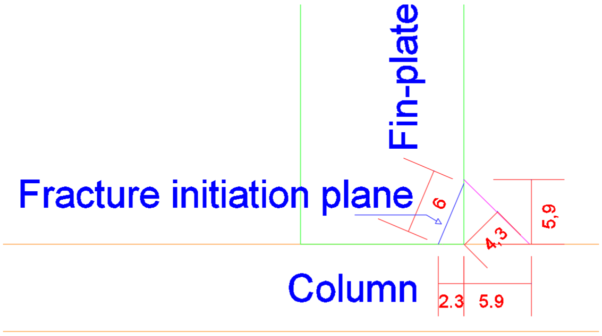

Figure 6.1: Cross-section illustration of the real weld size and the real fracture plane

6.4. Margins on final joint resistance

The weld resistance is the governing failure mechanism of the joint, the values of the experiment will be compared to the design values according to Eurocode 1993-1-8 version 2005 and the proposed revision for 2020. In Appendix C the hand calculation is included. Table 6.4 shows how much the design resistances utilize compared to the failure load. The proposed revision results in 25% utilization for all specimens, this means that the margin is the same and the calculated proportions of base and filler material are correct.

Table 6.4: Joint margins, design and experiment

Material	Ultimate EC 2005 $[\frac{kN}{kN}]$	utility [%]	Ultimate EC 2020 $[\frac{kN}{kN}]$	utility [%]	IDEAStatica real $[\frac{kN}{kN}]$	utility [%]
MC-715H on S355/s690 base	$\frac{115}{530}$	22%	$\frac{135}{530}$	25%	$\frac{455}{530}$	86%
742M on S355/s690 base	$\frac{115}{620}$	19%	$\frac{153}{620}$	25%	$\frac{520}{620}$	84%
742M on S355/s355 base	$\frac{115}{610}$	19%	$\frac{153}{610}$	25%	$\frac{520}{620}$	84%

In the same table the weld failure loads from IDEAStatica are presented. These are based on the same boundary conditions as in the experiment and the ultimate strength and dimensions of the weld material f_u is as measured from the experiments. The utility of 84% shows that the software can provide a close estimate to experiments. Because the software uses a lower amount of plastic redistribution (5%) and no hardening than reality the outcome is on the safe side. Again nominal values will result in a much lower utility.

7

Material properties and model calibration

In this chapter a model using Abaqus will be calibrated to predict the real behaviour of the joint as close as possible. This is done by creating accurate material models and segmenting all geometry into their appropriate materials. For calibration the leading deformation points of the entire joint are those relative between the column and the beam, the influence of the experiment frame is the least for this measurement point and thus best for calibration. See figure 7.1 for this point.

The chapter starts with the coupon tests for each plate material, followed by the weld and heat affected zones and ending with the results for the whole models.

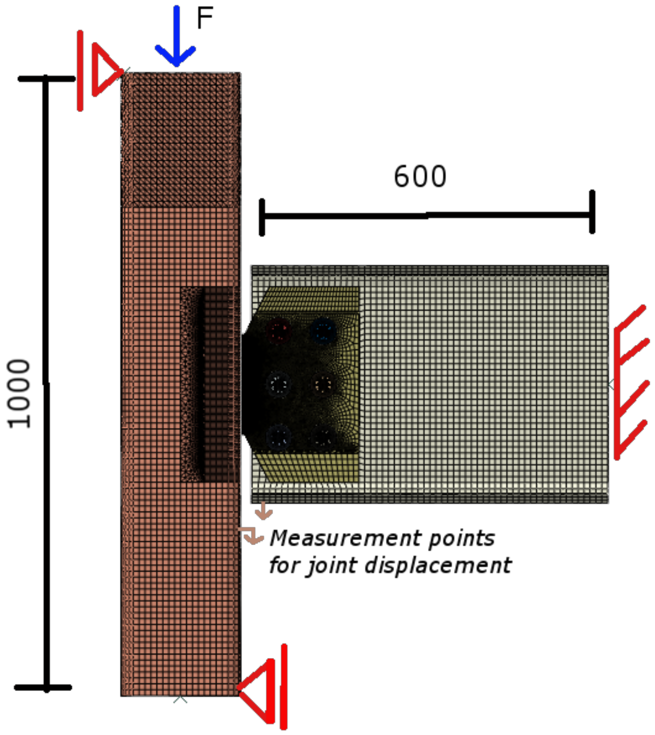

Figure 7.1: Experiment and model measuring point

7.1. Calibrating true stress strain with Abaqus

In an iterative process the true stress strain curves are calibrated from the coupon tests with Abaqus. First the curves up to the ultimate stress are determined, after this point necking will occur. This means that the engineering stress will show softening until fracture, the local cross-section of the specimen will however reduce and the true stress will continue to harden until fracture. The calibration is done with 2.5mm and 1mm C3D8r elements(Where applicable).

7.1.1. Fin-plate S355

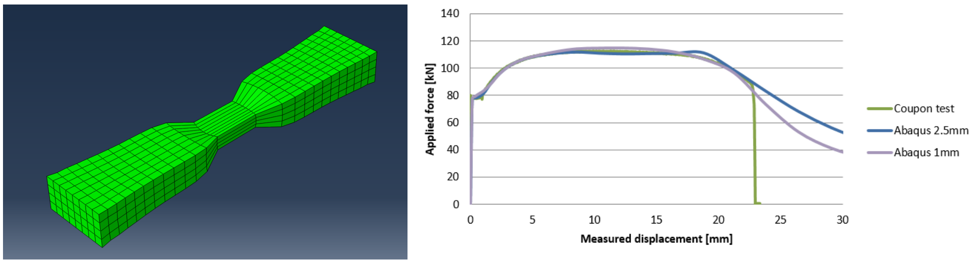

(a) Failure mode of coupon in Abaqus (b) Engineering stress/strain from coupon and FEM

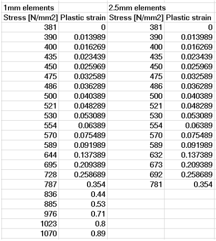

1mm elements		2.5mm elements	
Stress [N/mm2]	Plastic strain	Stress [N/mm2]	Plastic strain
381	0	381	0
390	0.013989	390	0.013989
400	0.016269	400	0.016269
435	0.023439	435	0.023439
450	0.025969	450	0.025969
475	0.032589	475	0.032589
486	0.036289	486	0.036289
500	0.040389	500	0.040389
521	0.048289	521	0.048289
530	0.053089	530	0.053089
554	0.06389	554	0.06389
570	0.075489	570	0.075489
589	0.091989	589	0.091989
644	0.137389	632	0.137389
695	0.209389	673	0.209389
728	0.258689	692	0.258689
787	0.354	781	0.354
836	0.44		
885	0.53		
976	0.71		
1023	0.8		
1070	0.89		

(c) Plastic strains

Figure 7.2: Calibration of Fin-plate S355 for 1mm and 2.5mm C3D8R elements

7.1.2. RHS S690

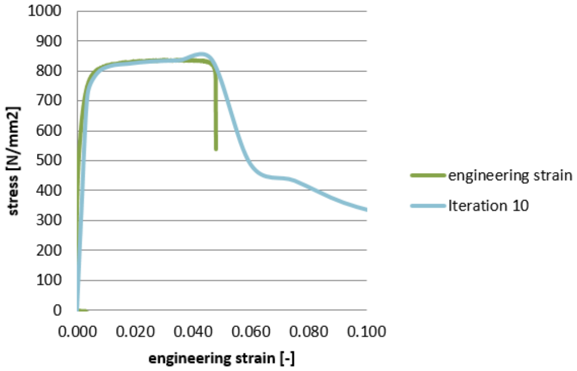

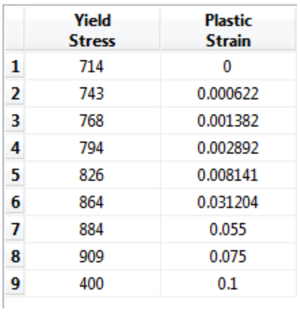

	Yield Stress	Plastic Strain
1	714	0
2	743	0.000622
3	768	0.001382
4	794	0.002892
5	826	0.008141
6	864	0.031204
7	884	0.055
8	909	0.075
9	400	0.1

(a) Engineering stress/strain from coupon and FEM (b) Plastic stress/strains in Abaqus

Figure 7.3: Calibration of SHS S690 for 2.5mm C3D8R elements

7.1.3. Welds and weld penetrated zones

In order to model the welds in abaqus it is important to note that they consist of two different parts:

1. The weld material, in light blue in figure 7.4.

2. The penetrated zone into the base materials, also referred to as the burn-in, diluted heat affected zone, or infused zone. Shown in green in figure 7.4.

The infused zone of only the fin-plate will be modeled, this is because this part is found to be in the fracture plane after testing and this allows for estimating the failure stress. Since the research done from a structural engineering perspective the parameters to be determined for these zones are the:
1. Yield stress.
2. Yield plateau and strain.
3. Slope of the true stress/strain after yielding.

4. Strain of maximum engineering stress.
5. Slope and fracture strain until failure.

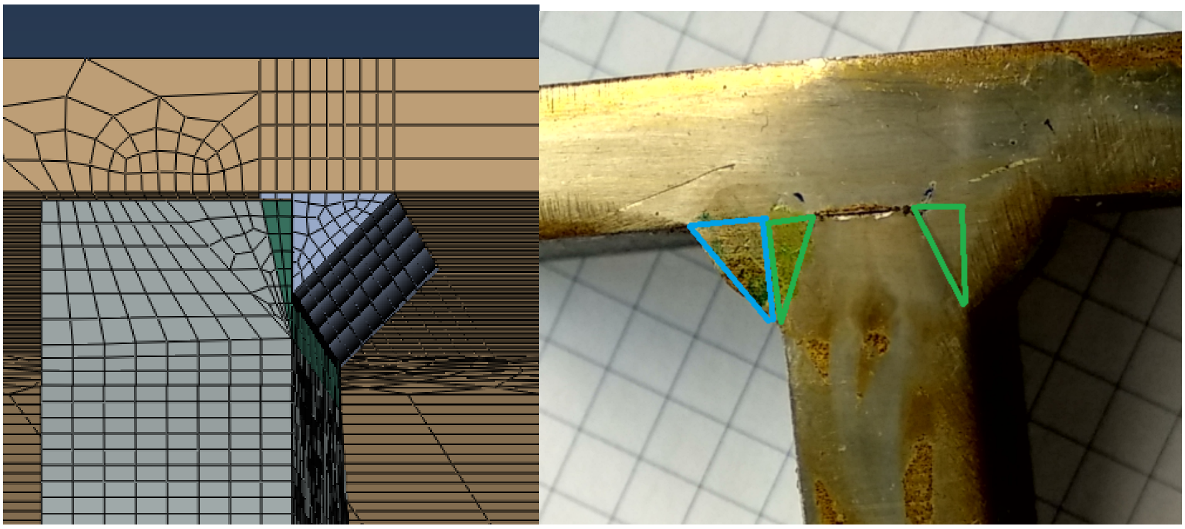

Figure 7.4: Location of the HAZ and mesh size

The properties of the infused zone will be estimated from the full-scale experiment data. The original plan was to obtain this data from T-specimen tensile tests, however, the welds were too strong compared to the base plates and the failure modes obtained were either on the edge of the HAZ or in the base material. The data from these tests does provide comparison material for the maximum engineering stress of the combined HAZ and weld material. Since there are four variables (stresses and strains in the HAZ, and in the weld material) that need to be solved, some research has been done to couple these parameters and reduce the amount of unknowns.

From research done by J. Carrier et al. [4] and D. Kozak [10] the properties of the infused zone resemble the weld material much closer than the base material. Figure 7.8b illustrates the outcome of their research. The indication is that influence of the base material should be around 15%. Thus for this research the assumption is that the HAZ has properties relative to that of the weld material, at first the ratio of 75% weld material and 25% base material was used, as proposed in the new eurocode. however after a few iterations it became clear that this would not hold up for the strains, as the HAZ did not provide the correct stiffness.

Further research done by T. Bjork et al. [2, Chapter 3.4] also suggests that using such a percentage based ratio could be applied to consider the dilution of HAZ. It also shows that the value of the ultimate strength of welds without penetration, based on the eurocode ultimate strength, varies between 140 230% for their UHSS welds. For a penetration which can be found in the experiments $\frac{a_{eff}-a}{a} = \frac{5.7-4}{4} \approx 0.4$ the variance is still between 110-190% based on the eurocode ultimate strength. This spread is very large and greatly dependent on the weld material used. Therefor a best estimate will be made and iterated with experiment data.

In chapter 7.1.4 the HAZ has been calibrated with the experiment data, the reason this is possible without knowing the ratio of weld/HAZ is that the start of the failure plane runs on the boundary of the HAZ and the base material and not through the weld. The influence of changing the ratio is illustrated in figure 7.5. Since the properties of the HAZ have been fixed the weld material is the only thing varying. For example with an $f_u = 891MPa$ for the HAZ and $f_u = 554MPa$ for the base material;

- The 5% influence weld material has $f_u = \frac{891-554\cdot 0.05}{1-0.05} = 909MPa$.

- The 15% influence weld material has $f_u = \frac{891-554\cdot 0.15}{1-0.15} = 950MPa$.

- The 25% influence weld material has $f_u = \frac{891-554\cdot 0.25}{1-0.25} = 1004MPa$.

The only influence of changing the ratio seems to be on the stiffness of the joint, the 5% model leans towards being too soft, while the difference in increasing above 15% seems to have no effect. Therefore the ratio of 15% is used for modelling.

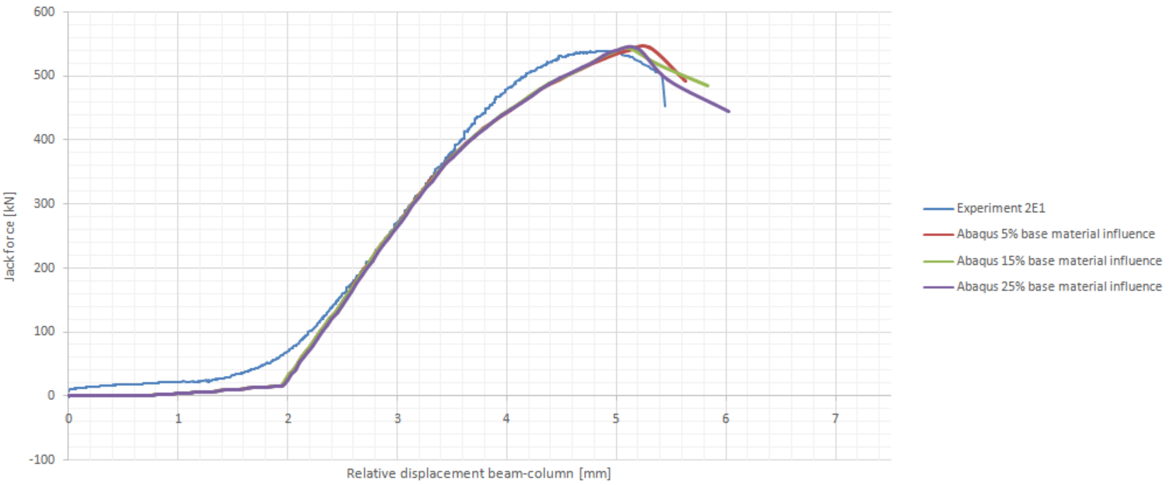

Figure 7.5: Influence of the strength of the weld over the HAZ

7.1.4. Calibration of the infused zone for experiment 2E1

The procedure will be explained with the four models displayed in table 7.1 and figure 7.8a.

- First the dimensions of the heat affected zone are measured from the 3mm S355 welds from the first series, which have been cut out and photographed in figure 7.4. The assumption is made that it will be the same in this series.

- The stress curves will have three points; f_y,$f_{90\%}$ and f_u. It is assumed there is no yield plateau for the weld and HAZ. for the HAZ the following values are assumed: f_y = 566 [N/mm^2], f_u = 891 [N/mm^2]. The value for f_y is estimated from the manufacturer's data listed in Appendix B. The value for f_u is taken the shear resistance from chapter 5.4.2 with 3% added as was estimated from the bending influence in chapter 8.

- A model without any HAZ is run and compared to experiment data of the joint stiffness in shear. Figure 7.7 shows this and the other models.
- A model with a fully elastic weld, f_u = 1000 [N/mm2] and E=210000 [N/mm2], is then run to estimate the maximum stiffness possible without a heat affected zone. This is referred to as the superweld model.

- From the weld model a rough yield stress and strain are estimated and with this data a new model is created where the bottom part of the fin-plate is fully elastic, f_u = 1000 [N/mm2] and E=210000 [N/mm2]. This is referred to as the superfp model.

- With the results from these models the curves are tweaked in 5 iterations to match experiment data.

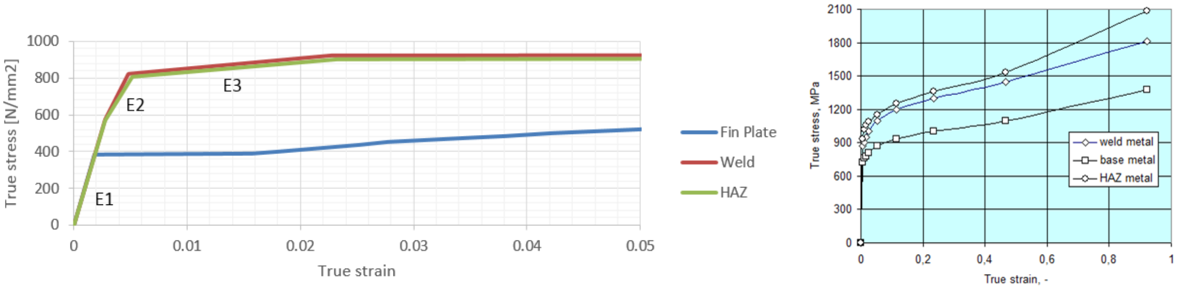

(a) Curves for calibrating modeling

(b) Curves from literature [10]

Figure 7.6: Material Stress Strain curves

Table 7.1: Slopes in the stress strain curves for calibration

	Weld				HAZ		
Identity	E1 [N/mm^2]	E2 [N/mm^2]	E3 [N/mm^2]	Burn-in [mm]	E1 [N/mm^2]	E2 [N/mm^2]	E3 [N/mm^2]
22-02-2018	$2.1 \cdot 10^5$	$2.1 \cdot 10^3$	$2.1 \cdot 10^3$	-	-	-	-
26-02-2018 / superweld	$2.1 \cdot 10^5$	$2.1 \cdot 10^5$	$2.1 \cdot 10^5$	-	-	-	-
28-02-2018 / superfp	$2.1 \cdot 10^5$	$1.1 \cdot 10^4$	$7.0 \cdot 10^3$	∞	$2.1 \cdot 10^5$	$2.1 \cdot 10^5$	$2.1 \cdot 10^5$
12-03-2018 / HAZ	$2.05 \cdot 10^5$	$1.24 \cdot 10^5$	$5.3 \cdot 10^3$	2.3	$2.05 \cdot 10^5$	$1.0 \cdot 10^5$	$5.2 \cdot 10^3$

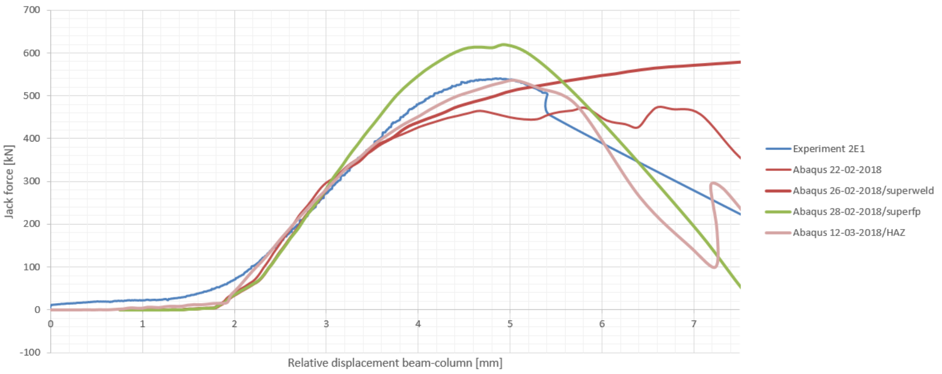

Figure 7.7: Iterations for the diluted weld zone

7.2. Calibration of the infused zone for all experiments

The following plastic strains are used for the final Abaqus modelling, figure 7.8. There is no distinction made between the 3E series and 4E series since the failure stress of the weld/haz material is virtually the same when using the s690 weld material in an S355 base material.

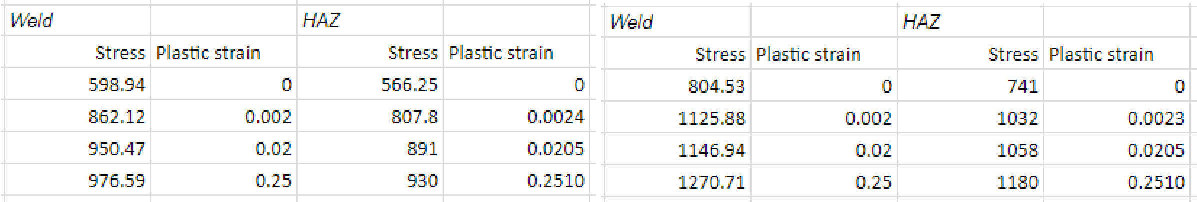

Weld		*HAZ*	
Stress	Plastic strain	Stress	Plastic strain
598.94	0	566.25	0
862.12	0.002	807.8	0.0024
950.47	0.02	891	0.0205
976.59	0.25	930	0.2510

(a) Plastic strains for S355 weld

Weld		*HAZ*	
Stress	Plastic strain	Stress	Plastic strain
804.53	0	741	0
1125.88	0.002	1032	0.0023
1146.94	0.02	1058	0.0205
1270.71	0.25	1180	0.2510

(b) Plastic strains for s690 weld

Figure 7.8: Material Stress Strain data

7.2.1. Overview of true stress/strain curves

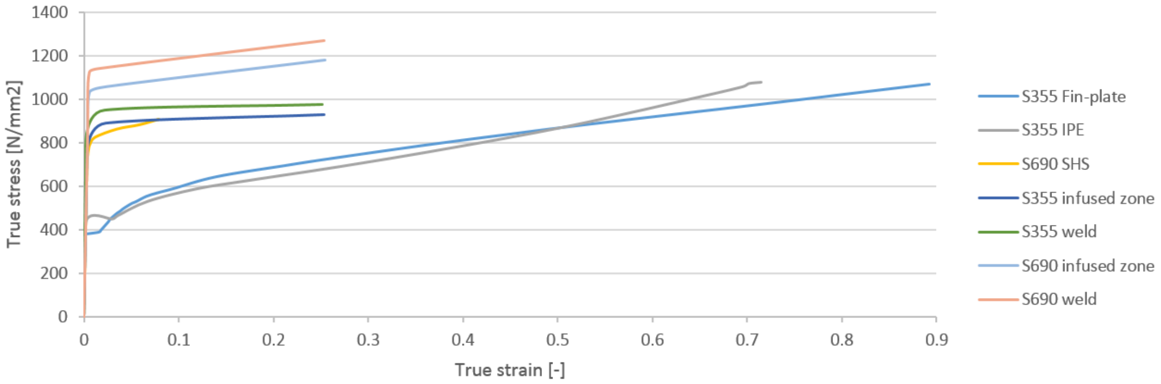

Figure 7.9: Calibration stress curves

7.2.2. Abaqus results on fin-plate rotation

The rotation of the fin-plate in abaqus should resemble the findings from the experiment. In figure 7.10a the first 100 kN of loading has been removed and only the remainder will be examined. An important difference has been found:

- The bolt thread cuts into beam and fin-plate material with 1mm depth, see figure 7.10b. Since this happens on the top and bottom bolt, and in both the plate and beam, the actual contribution can be described by equation 7.1. Since this is not modeled in abaqus, the abaqus model for 2E1 does not match in figure 7.10a. The model is too stiff around the bolt holes, however this attributes mostly to the deformation of the holes in the direction perpendicular to the column face. The deformation in the joint in the direction aligned with the column length is still matching up with experiment data, see chapter 7, because it is sufficiently accurate the bolt threads will not be modelled for further abaqus comparison models.

$$R = \frac{2 \cdot (1+1)[mm]}{180[mm]} = 0.022[rad] \approx 50\% \tag{7.1}$$

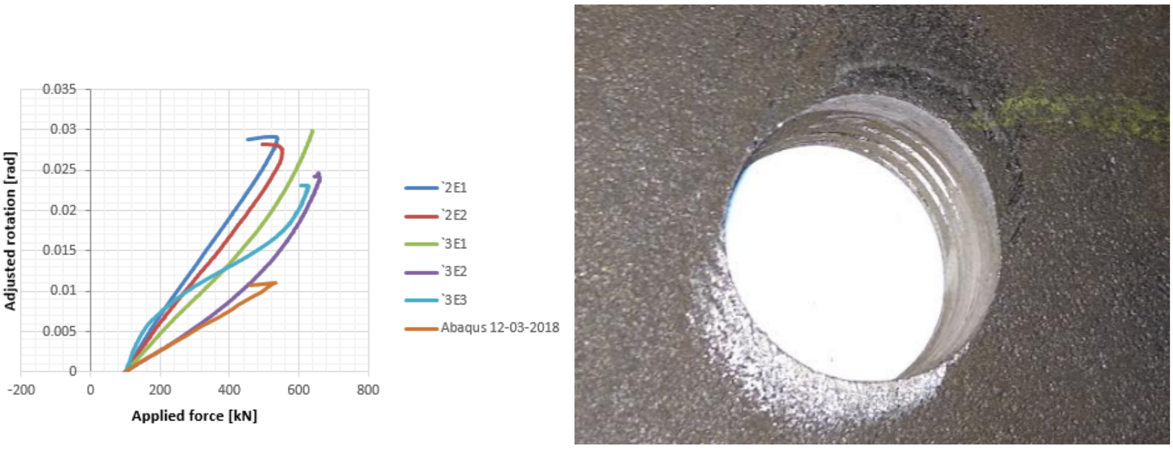

(a) Adjusted strains and rotations from measurements (b) Bolt thread in base material

Figure 7.10: Abaqus and real rotations

7.3. Estimating failure strain for the infused weld zone

The failure criteria used for the weld material is not accurate. In figure 7.9 the graphs for the infused weld material and weld material were shown, these graphs are an estimation based only on the main experiment data. The failure criteria in this model is based an equivalent strain of 25%, which seemed realistic for the shear failure that occurred. In reality there are more factors that influence failure, these factors include the combination of shear and tension/compression (Tri-axial state) on damage progression within the material. Damage modelling for steel has proven to be an accurate method to predict failure, There was however not enough data to model this based on the main experiment.

All the models have been run with the stress curves that have this problem. To prevent re-running the models the following steps are taken:

- The geometry of the shear/tension coupon specimens is measured and modelled in abaqus.

- The material properties from figure 7.9 are used as input.

- The resulting force/displacement graphs are compared with the tests.

- At the displacements at failure the equivalent plastic strains are measured in abaqus. This is done at the position of the expected failure initiation in the heat affected zone.

- At these points the Tri-axial stress is calculated and the strains are fitted against the curve from literature. Resulting in a curve that will predict the failure strain based on the stress state.

- For the other models, the stress state is then locally measured and their failure load is reached when the failure strain is reached.

The graphs in figure 7.11 show how accurate the original material model performs with the test data. From these graphs two points are defined at which the material stops redistributing forces, from these points the failure criteria is defined. The data extracted at these points are listed in table 7.2.

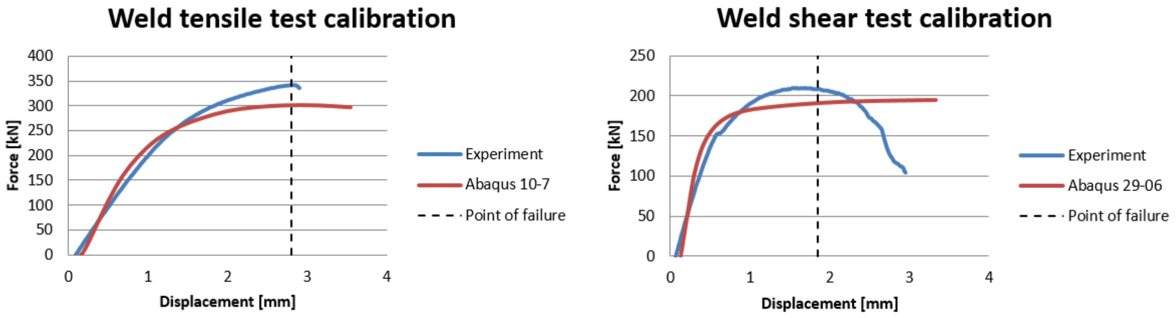

(a) Performance on the tensile test

(b) Performance on the shear test

Figure 7.11: Accuracy of material model on test data

Table 7.2: Resulting failure criteria

coupon	Pressure [MPa]	Von-Mises [MPa]	Tri-axiality [-]	fracture strain [-]
T-specimen	366	908	0.40	0.13
S-specimen	31	925	0.03	>0.23

The data from table 7.2 is not sufficient for interpolation between the two stress states. Changsik et al. [3, eq 7] suggests that the relationship is exponential for their mild steel, see equation 7.2.

$$\epsilon_f = 3.29e^{-1.54\sigma_m/\sigma_e} + 0.1 \tag{7.2}$$

To fit this expression to the two data points, it will be curve-fit to estimate the weld material. Formula 7.3 will be used to estimate the failure for the abaqus models.

$$\epsilon_f = 0.25e^{-1.54\sigma_m/\sigma_e} \tag{7.3}$$

7.4. Conclusions on model calibration

The results for the models are compared to the experiment results. The relative displacement column/beam is used as the comparison value. Also the results from IDEAStatica are included, these results are based on the real yield and ultimate stresses for the base materials and the welds (from weld coupons). It should be noted that IDEAstatica does not take into account the extra weld material at the start and end of the fin-plate. Material factors are 1.0.

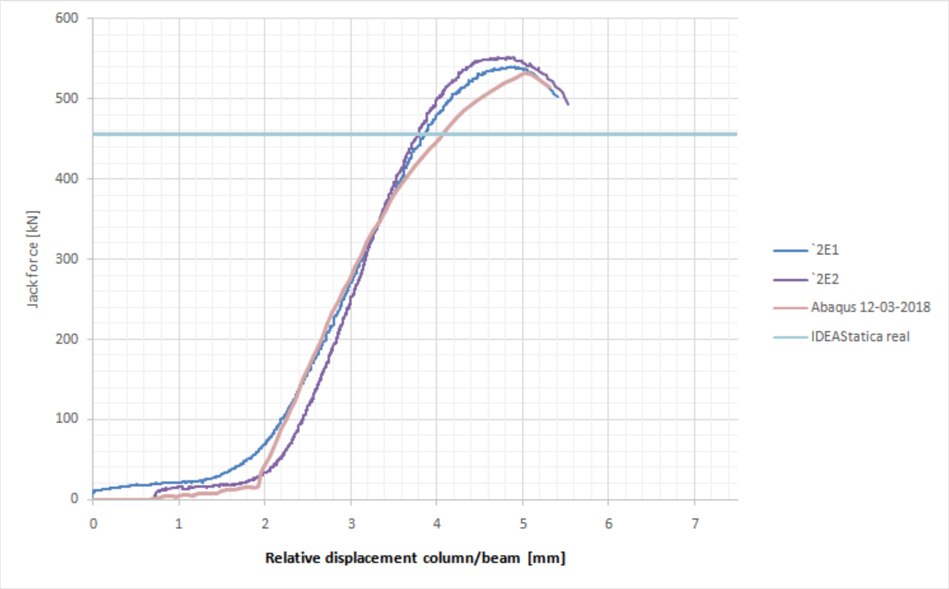

Figure 7.12: Calibration results for 2E series

From figures 7.12, 7.13, 7.14 the followings results are found:

- The abaqus model for the S355 welds in the 2E* series matches the real behaviour closely.

- The abaqus models for the S690 welds in the 3E* and 4E* series matches the real behaviour less closely. The stiffness in the plastic region is less than expected. This can be corrected by either:

- Increasing the yield stress will increase the stiffness slightly, however the failure plane in abaqus follows the border of the HAZ and the base material, which is much more influential. See figure 7.15b for an illustration of the failure plane, in this figure blue equals no plastic strains and gray equals > 0.25 plastic strain. In chapter 5.4.3 the real failure planes from the tests are shown. A big difference is that in the experiments the failure plane changes from being fully in the fin-plate in the tension zone to going through the weld in the compression zone. In Abaqus the plane remains in the fin-plate/HAZ.

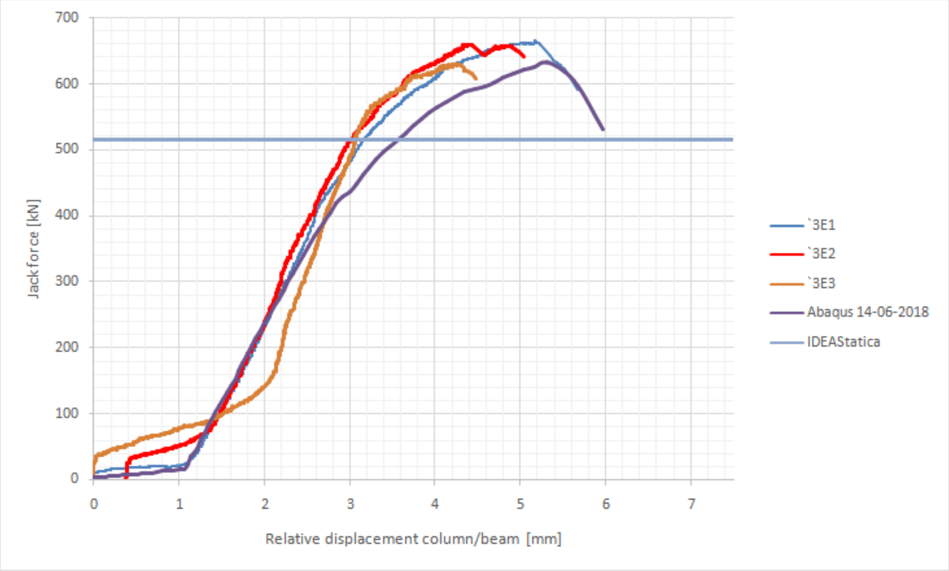

Figure 7.13: Calibration results for 3E series

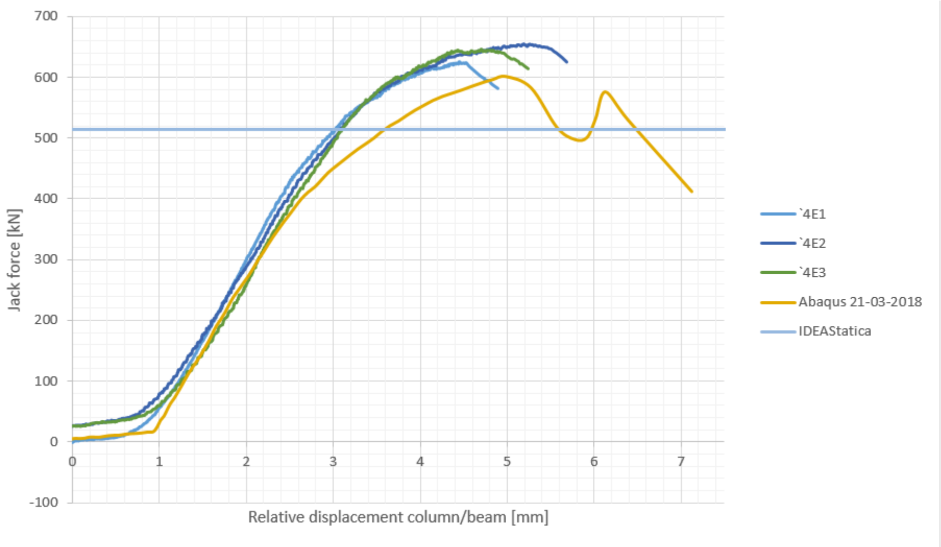

Figure 7.14: Calibration results for 4E series

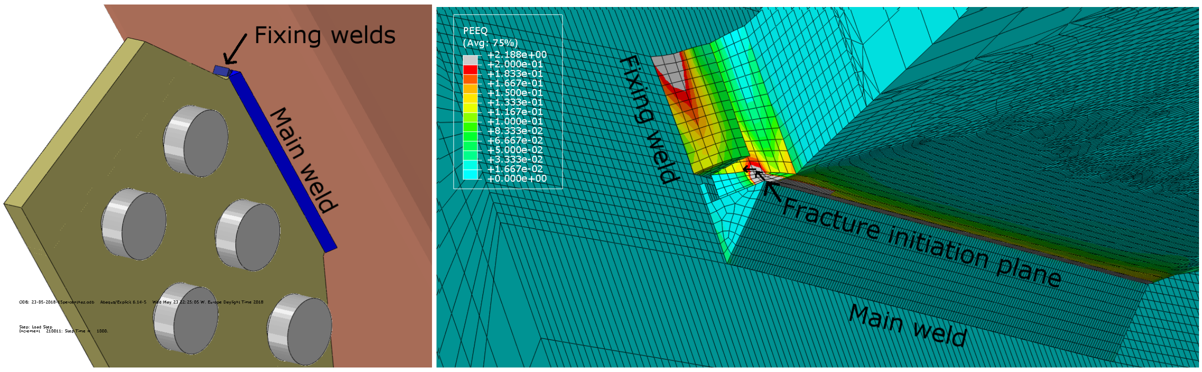
Fixing welds
Main weld
PEEQ
(Avg: 75%)
+2.188e+00
+2.000e-01
+1.833e-01
+1.667e-01
+1.500e-01
+1.333e-01
+1.167e-01
+1.000e-01
+8.333e-02
+6.667e-02
+5.000e-02
+3.333e-02
+1.667e-02
+0.000e+00
Fixing weld
Fracture initiation plane
Main weld

(a) Fixing welds (b) Fracture plane in Abaqus

Figure 7.15: Abaqus weld and fracture plane

- The prediction by IDEAStatica is a bit lower than the experiments. It doesn't take the fixing welds into account, these are illustrated in figure 7.15b. The length of these extra bits of welding are about 24 mm in total, which would add an additional 15% to the IDEA estimate, bringing it closer to reality.

- The failure load does not seem to depend on the base material for the column in both Abaqus and IDEA, this is however based on the definition of the material model, where the yield and ultimate stress used are the same for both S690 weld models. The failure plane is mostly in the fin-plate in this case, for which it would make sense that the column does not have influence. The experiment seems to confirm that in this case there is not a significant difference.

8

Influence of column face stiffness

The key difference between a hollow core column and a H profile is the reduced stiffness of the face. This implicates the force distribution. In this chapter the influence of the stiffness will be quantified by a set of Abaqus models.

8.1. Theory

A major influence on the weld resistance in beam-column joints is the bending moment that needs to be transferred via the weld. In cases with an I profile column, where there is a stiff web preventing rotation of the flange, this moment is described by the shear force exerted onto the fin-plate (by the bolt group) multiplied by the eccentricity. In the case where the fin-plate can rotate freely this shear force still needs to be carried across the eccentricity. Since there is only a small moment possible in the hinged connection of the fin-plate and the column face, the weld will also carry no significant moment. To achieve zero moment here, the bolt group will be loaded with an additional coupled force. The difference in theory is shown in figure 8.1 from the notes on beam-column joints by Stark and Wardenier [9, ch. 2].

When conducting the first set of experiments it became clear that the welds were much stronger than expected, and it seemed that validating any weld properties beyond the elastic phase would become a daunting task. It is an interesting concept that the net resistance of the welds depends on the type of column it is welded on. During a discussion about this problem it was suggested to use this property to increase the stresses in the welds in the next sets. The columns were already prepared for the test set-up so it was not feasible to replace them. The option to be examined was to weld an extra plate onto the face, on which the fin-plate is welded as usual.

The problem to be quantified in this chapter is to determine at what stiffness of the column face, the moment in the weld, and the additional forces in the bolts become influential. This will be tackled by modeling five different column face thicknesses in Abaqus, using the material models validated with experiment data.

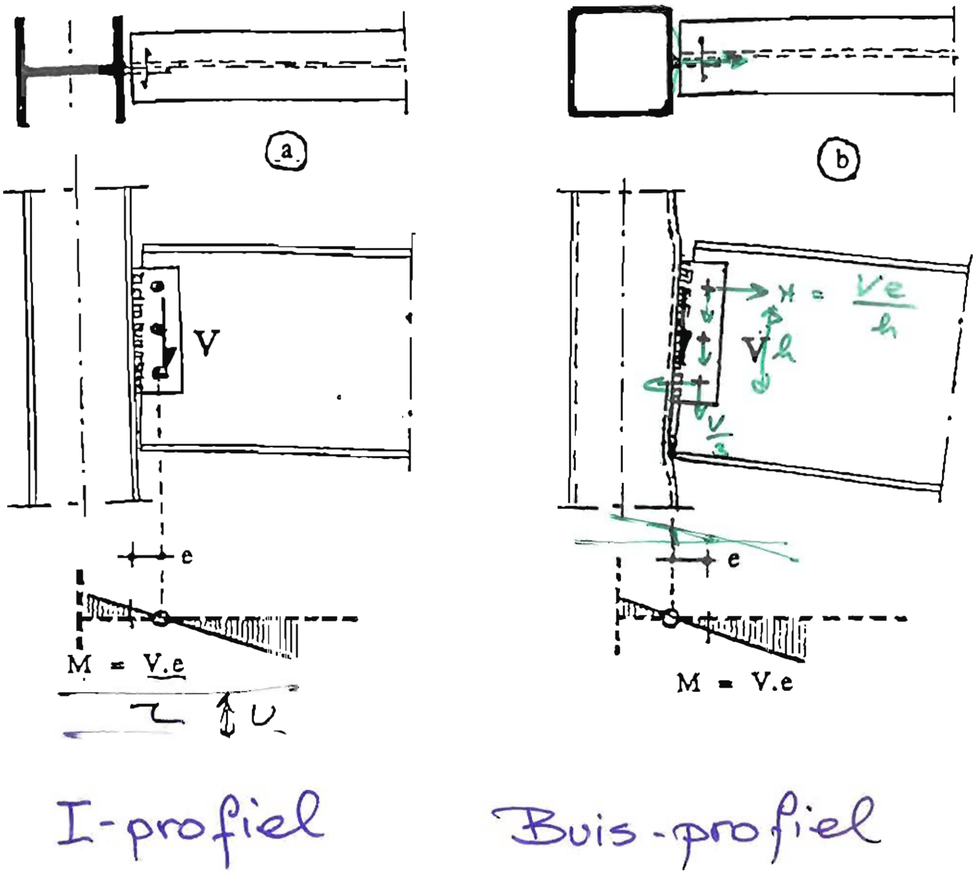
a
b
V
V
H = Ve/h
h
V/2
e
e
M = V.e
M = V.e
I-profiel
Buis-profiel

Figure 8.1: Calculation models for bending moments in stiff and soft columns[9, ch. 2]

8.2. Modeling

For this sensitivity analysis the material model based on the first set of experiments is used. The failure stress of the weld could not be determined from this set, thus an assumption based on the nominal values was made. This model has the nominal yield/fracture values multiplied by 1.2 and the stress/strain relationship is based on hardening from the Eurocode with a slope of E/100. All columns are S690, fin-plates are 10mm S355, the beams are IPE400 S355, and the welds are single sided 220mm. Real stress/strain based on coupon tests is used for these.

To simplify the analysis and to limit the influence of the rotation stiffness from the corners, only the face thickness is varied. An I profile with a similar cross section has been selected to compare the used method for such a profile (SHS200x8, A_s = 6080 mm^2 and HEB200 with A_s = 7810 mm^2). Table 8.1 gives an overview of the chosen objects, figures 8.2 and 8.3b show the geometry of the cross-sections and welds. For this analysis the geometry of the experiment is taken, only the column thickness is varied.

Table 8.1: Abaqus model overview.

Identity	Column	Face thickness [mm]	Weld yield/fracture [N/mm^2]	Weld throat [mm]	Weld length [mm]
M1	SHS 200x8	8	576/708(S355)	5.4	220
M2	SHS 200x8	12	576/708	5.4	220
M3	SHS 200x8	16	576/708	5.4	220
M4	SHS 200x8	24	576/708	5.4	220
M5	SHS 200x8	32	576/708	5.4	220
M6	HEB200	15	576/708	5.4	220

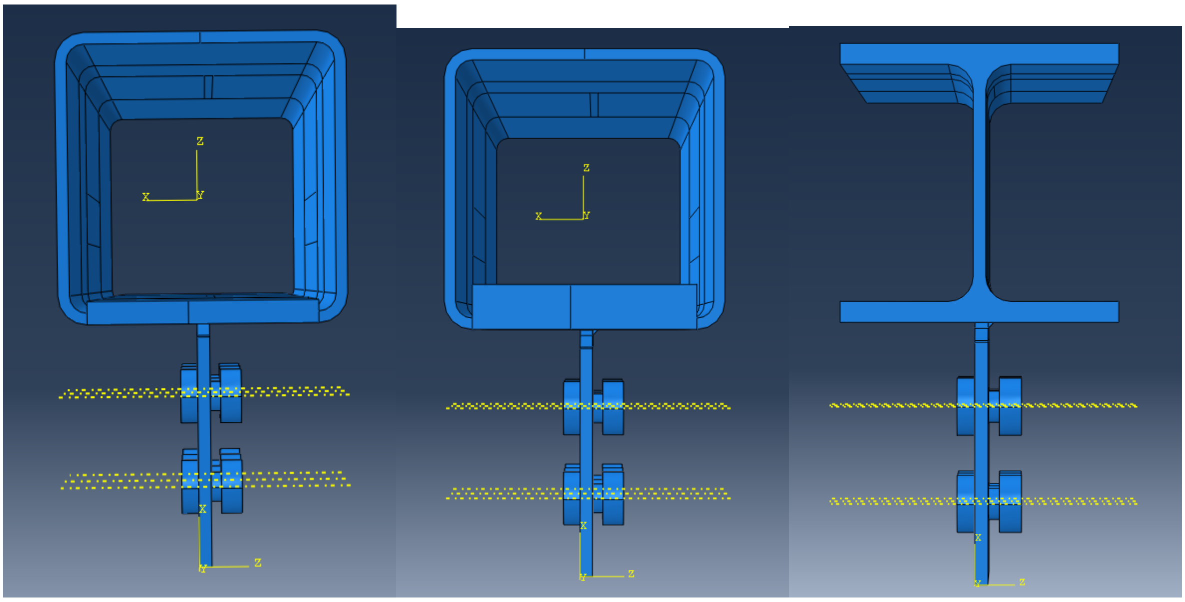

(a) SHS 200x200x8 with 16mm face (b) SHS 200x200x8 with 32mm face (c) HEB200

Figure 8.2: Models in Abaqus

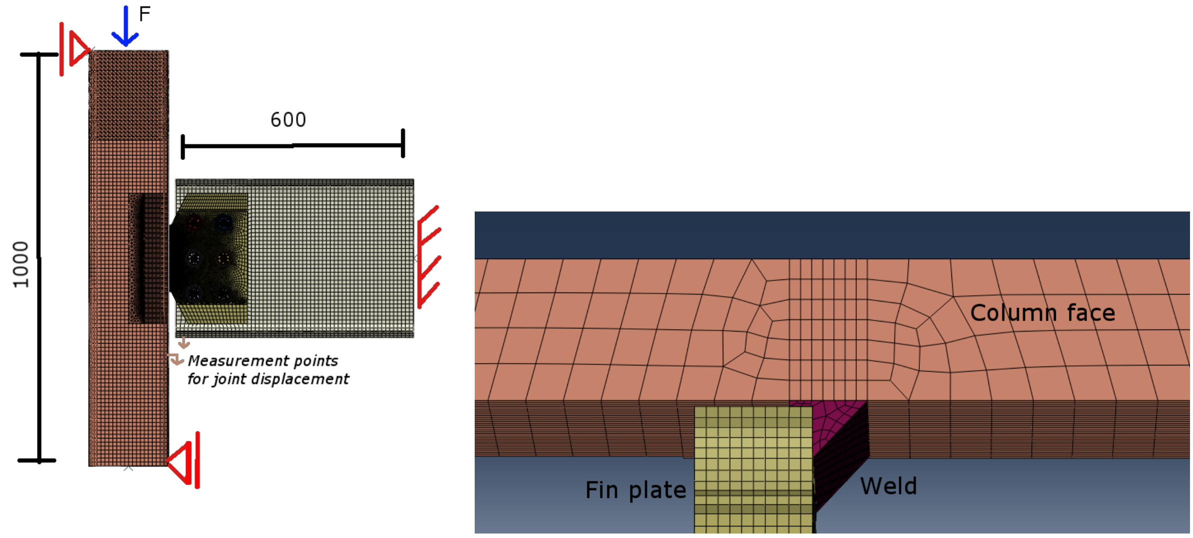

(a) Model size (b) Weld in Abaqus

Figure 8.3: Models in Abaqus (2)

8.3. Results for experiment sizings

The moment distribution is determined for the five models. The center of the bolt group is 100mm from the column face, the first bolt row is 65mm from the column face. The data displayed in table 8.2 is split up into three regions:

1. Elastic phase of all elements at 100 kN loading.

2. End of Elastic phase at 200 kN loading.

3. Plastic phase of the weld at 350 kN loading.

The data specific for this configuration are visualized in two graphs shown side by side: The left graphs (Figure 8.5) show the position of the hinge in the bending moment diagram for these specific cases. The graphs on the right (Figure 8.6) show the distribution of stresses that result in these bending moments, it is displayed in [N/mm2] of average stress in the weld perpendicular to the column face.

In order to make this data compare-able with faces of other dimensions, both the thickness and the width of the column should be considered. A normalization based on the stiffness from elastic beam theory is made. Figure 8.4 and equation 8.1 show how this stiffness is determined, for a SHS200x8 the parameters will be a beam with length L = 200 [mm], width b = 200 [mm] and height = 8 [mm].

Keep in mind that this is a simplification and that the actual stiffness should be determined from the FEM model. The relation between moment and thickness is not solely depended on the bending stiffness, where one could expect a t^3 relation from the second moment of area.

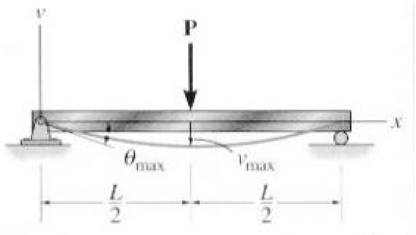

Figure 8.4: Simplified relation between force and displacement on a column face

$$v_{max} = \frac{-PL^3}{48EI}, I = \frac{bt^3}{12}, P = \frac{48 v_{max} EI}{L^3}, P = \frac{48Et^3}{12L^2} \tag{8.1}$$

$$b = L$$
$$v_{max} = 1\ [mm]$$
$$P = Force\ per\ 1mm\ displacement\ [N]$$

Table 8.2: Moments in weld and bolt group for a 10mm fin-plate

			100kN			200kN			350kN		
Identity	t_f	P	M_{weld}	M_{bolts}	Hinge pos	M_{weld}	M_{bolts}	Hinge pos	M_{weld}	M_{bolts}	Hinge pos
	[mm]	[N/mm]	[kNm]	[kNm]	[mm]	[kNm]	[kNm]	[mm]	[kNm]	[kNm]	[mm]
M1	8	$1.1 \cdot 10^4$	2	8	20	3	17	15	4	31	11
M2	12	$3.6 \cdot 10^4$	3	7	30	5	15	25	7	28	20
M3	16	$8.6 \cdot 10^4$	5	5	50	7	13	38	9	26	26
M4	24	$2.9 \cdot 10^5$	6	4	60	9.5	10.5	47	12	23	34
M5	32	$6.9 \cdot 10^5$	6.5	3.5	64	10.5	9.5	52	12.5	22.5	36
M6 (HEB)	15		8	2	80	13	7	65	14.5	20.5	42

8.3.1. Effective hinge location and weld stresses

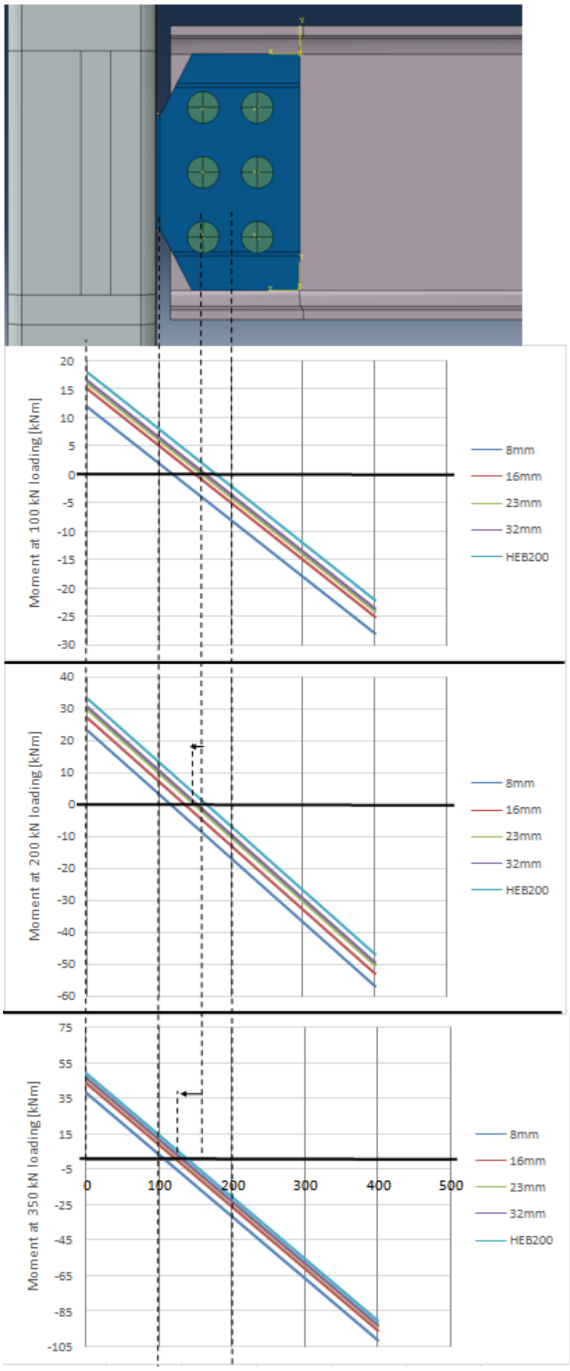

Figure 8.5: Moment distribution and position of hinge

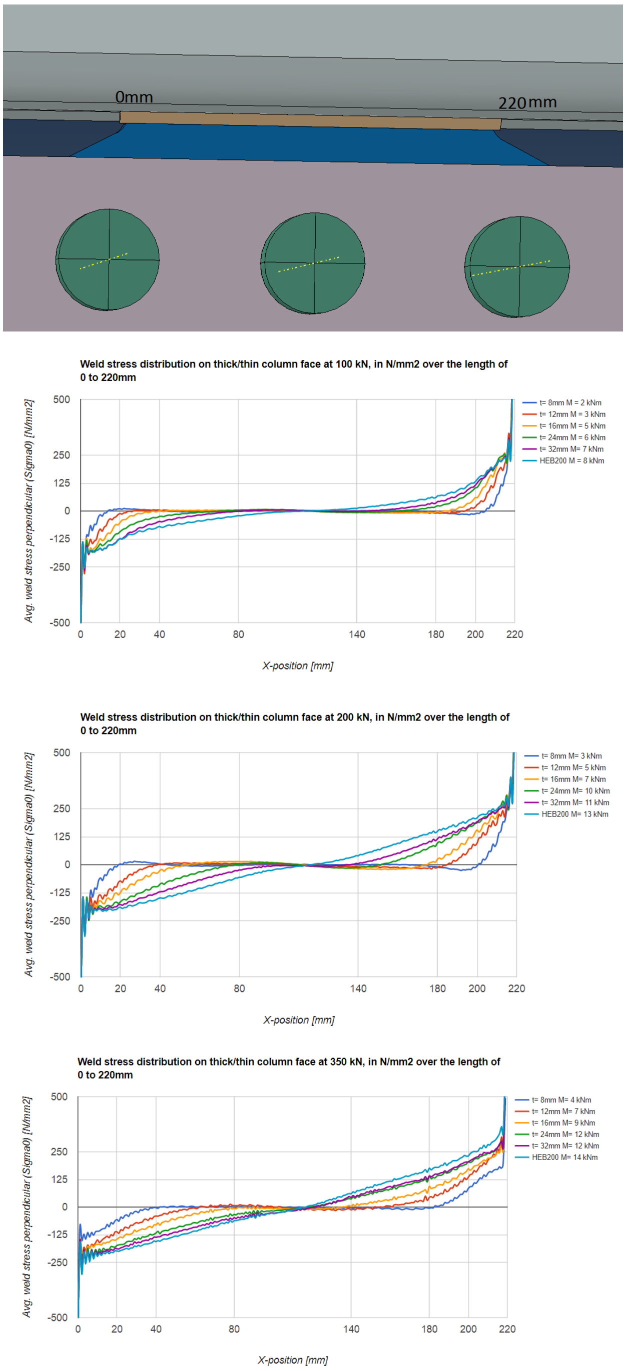

Figure 8.6: Stress distribution across the weld length, perpendicular to the column face

From figure 8.6 the parts of the weld that take this moment are shown:

- For the thin face, the bending stress is almost all taken by the outer 20mm parts of the weld.
- For thicker faces the distribution is much more linear and is taken by a much larger part of the weld.

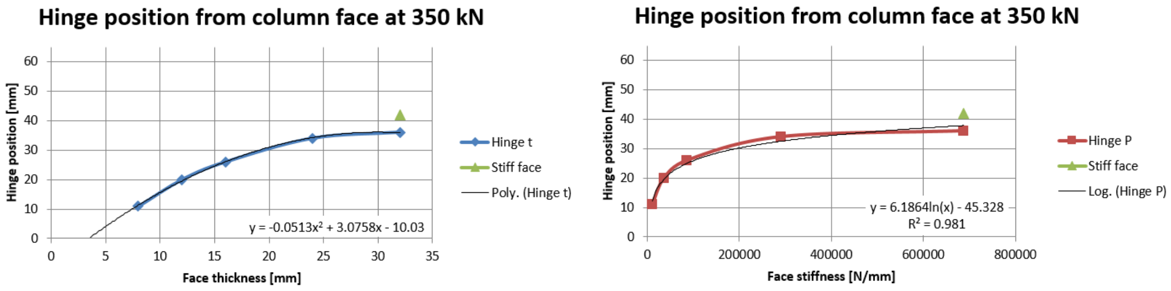

Figure 8.7: Position of hinge with a 10mm fin-plate

From figures 8.5 and 8.7 it can be seen that:

- The thickness of the column face has a big influence in the location of the hinge, a stiffer the face will result in a higher bending moment transferred through the weld.

- From 24mm onward there is little difference and the faces act more closely to the HEB200 model. It is however not realistic to make a SHS200 column face this thick in practice.

- An important thing to be noted on the method used for analysis is that a full-scale practical joint is examined. The stiffest column (HEB200) shows that the position of zero moment is not in line with the first bolt row anymore just before failure. This can be accredited to the fin-plate also showing some yielding, which has influence on the results.

- The expected relation based on t^3 between the thickness and bending moment has not been found, instead the relationship seems to be based on t^2 for this case.

- The 8mm column face provides little stiffness, there is however still a moment transferred through the weld. The equations 8.2 to 8.5 from Eurocode are used to determine the effect of the added moment on the ultimate failure load. With the parameters from table 8.1 the effect is expressed as the influence on the Von-Mises stress, based on an expected shear force before failure of 350 kN. The graphs in 8.8 show the relation between the face stiffness and the weld stress. Again it must be noted that the sensitivity of the fin-plate thickness has not been included yet.

$$\sigma_\perp = \tau_\perp = \frac{2 \cdot 2.12 \cdot M}{a \cdot l^2} \tag{8.2}$$

$$\tau_\parallel = \frac{F}{a * l} \tag{8.3}$$

$$\sigma_{vm} = \sqrt{\sigma_\perp^2 + 3 \cdot (\tau_\perp^2 + \tau_\parallel^2)} \tag{8.4}$$

$$\sigma_{vm0} = \sqrt{3 \cdot \tau_\parallel^2} \tag{8.5}$$

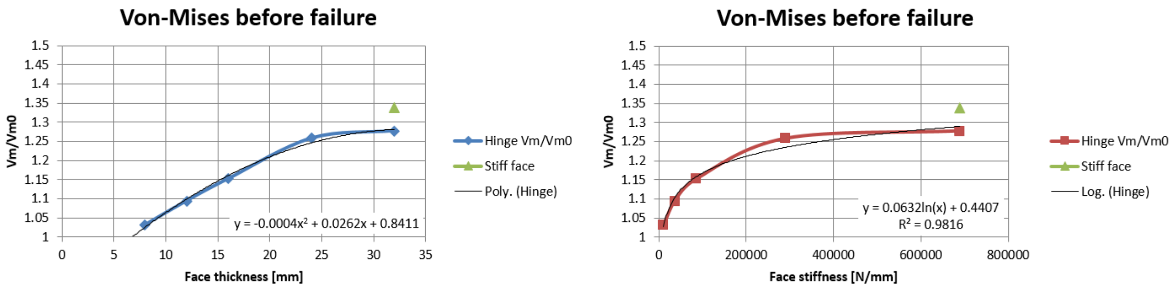

Figure 8.8: Influence of stiffness on the acting VM stress with a 10mm fin-plate

An important conclusion that can be drawn from figure 8.8 with relation to the SHS200x8 joint in the experiment set-up is that the influence of the moment on the VM stress is only 3%. It was also found in the experiment results that the failure load of the specimen could be properly described by examining only the shear force.

8.3.2. Effective bolt forces

The bolt forces are dependent on the stiffness of the column face. The goal of this chapter is to find out if these forces exceed the design loads at any bolt. Two extreme cases are examined, the first with a very flexible face, the second with a stiff face. At loads just before (weld) failure the bolt forces are shown in figure 8.9. Table 8.3 shows how much of the design force of the bolt was used during the experiment. In the first column of the table the design load of the bolt group is listed. The calculation listed in Appendix C is based on the bolts taking an evenly distributed shear force in the vertical direction and and the top and bottom bolts taking horizontal shear due to a moment. The applied load before failure is listed secondly and the acting combination of shear forces in x and y direction is calculated. This is then expressed as a percentage of the design load. It can be seen that even though the applied load was not close to the design load, the utilization was almost 90%. If this is extrapolated to the design load then the individual bolt forces are much greater than they are designed for. Even without taking into the influence of the column stiffness it can already be concluded that for these boundary conditions:

- The first bolt row takes most of the vertical forces, therefor any design with two bolt rows should not evenly distribute these forces.

- With the slim column the first row takes 87% of the vertical forces.

- With the thick column the first row takes 84% of the vertical forces.

- With the slim column the first row takes 66% of the horizontal forces due to bending.

- With the thick column the first row takes 58% of the horizontal forces due to bending.

Table 8.3: Bolt forces

Identity	Group design load [kN]	Applied load [kN]	V_e [kN]	$V_{r,d}$ [kN]	Utility [%]	Utility at design load [%]
8mm	644	350	126	141	89	164
32mm	644	350	121	141	86	158

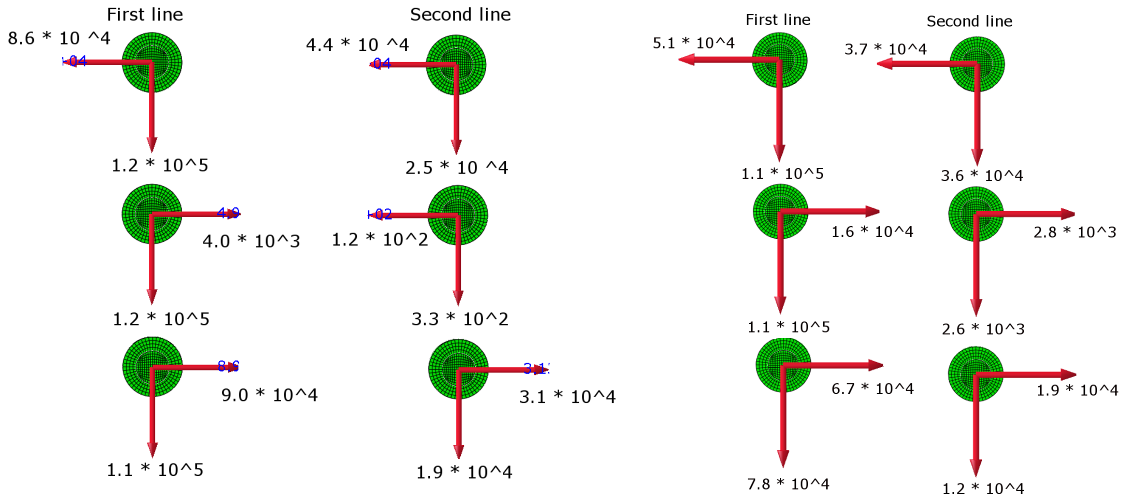

(a) Bolt forces at 400 kN on 8mm column

(b) Bolt forces at 350 kN on 32mm column

Figure 8.9: Comparison of bolt forces before failure

8.3.3. IDEAstatica and a flexible face

CBFEM uses the stiffness of plate elements to determine force distributions in the weld, fin-plate and bolts. This also means that the stresses perpendicular to the column face are based on the stiffness of the column face. This chapter is reviewing to what extend this is influential and what the results are compared to the models from abaqus.

”An ideal plastic model is used and the plasticity state is controlled by the stress in the weld throat section. The weld resistance is reduced in connections to unstiffened flanges or in long joints due to concentrated stress. The plastic strain in a weld is limited to 5% as in the plate. The design resistance of the fillet weld is determined using the Directional method given in section 4.5.3.2 EN1993-1-8:2006.” [1]

IDEA handles welds differently than is done with abaqus;
- The stresses are derived from the parent materials and some plastic redistribution within the weld. For all materials a perfectly plastic material model is used. From the research done on weld materials it was found there is hardly any yield plateau and thus it would be more suitable to apply a hardening curve for the weld material, this means the welds would be stiffer than predicted.

- The forces are converted into three stresses $\sigma_{perpendicular}, \tau_{perpendicular}, \tau_{paralel}$ acting on the throat of the weld.

- This stress state is then checked against the Von-Mises criteria.

The results from IDEA are shown in figure 8.10. It is clear that the software takes into account the stiffer face if the right boundary conditions are applied. The same boundary conditions as in abaqus are applied to get this result. The difference between the shear only stress and the total stress is less pronounced in the software (1.20 vs 1.27 in Abaqus, this is caused by calculating the stresses directly from the stress state. In postprocessing with the abaqus models the bending stress is added by taking the average stress from the bending moment, which is less accurate. The trend from both FEM types are very similar. This leads to the conclusion that CBFem takes into account the stiffness of the column element in a proper manner.

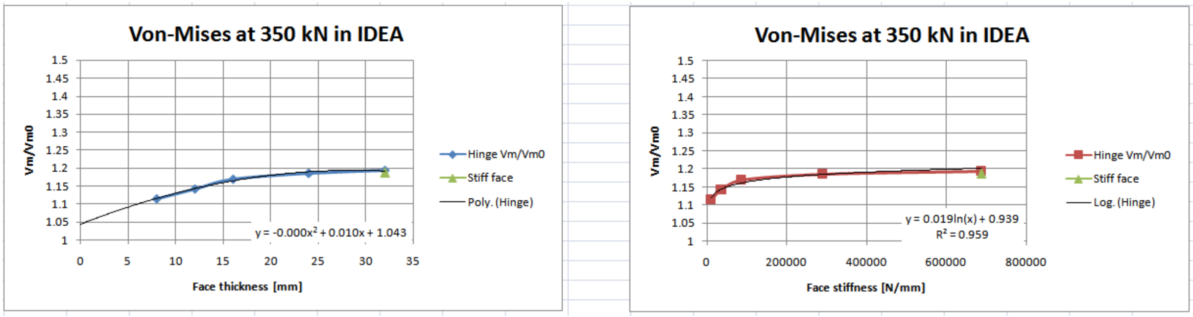

Figure 8.10: IDEAStatica von-mises stress

9

Expanding to full-size

The experiment has allowed for good measurements on the examined joint type. The conclusions for the experiment can however not be directly applicable to the general flexible joint, the deformations of the beam and column do not correspond with a real structure. In order to give conclusions on the joint in general a full-scale model will be made, the material and geometry used has been calibrated with the experiments.

9.1. Modeling properties

A realistic size for the column and beam geometry has been taken from a high-rise office building, a story height of 3m is taken and this is simplified into a 6m column section with moment clamps on the ends.

The moment resistance of the IPE400 in S355 in plastic theory is as follows:

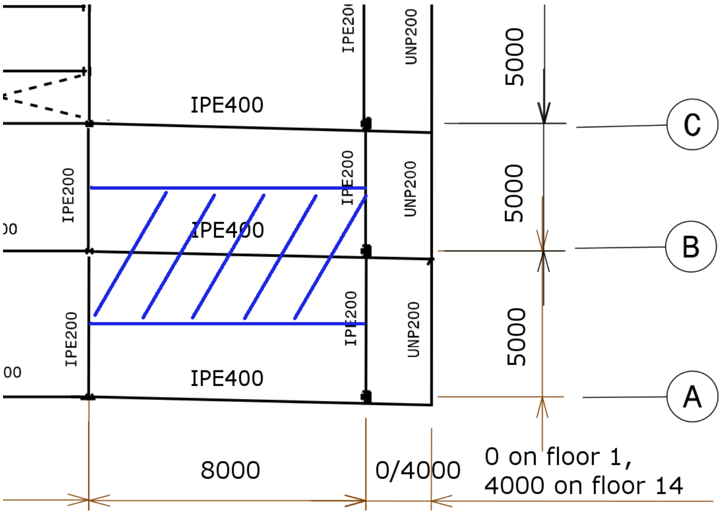
IPE400
IPE400
IPE400
IPE200
IPE200
IPE200
IPE200
IPE20
UNP200
UNP200
UNP200
5000
5000
5000
C
B
A
00
00
8000
0/4000
0 on floor 1,
4000 on floor 14

Figure 9.1: Floor plan for a full scale loaded beam

$$M_{rd} = W_{pl} \cdot f_y = 1.31 \cdot 10^6 \cdot 355 = 4.65 \cdot 10^8 [Nmm] = 465[kNm] \tag{9.1}$$

The design bending moment on an 8m span, with 5m spacing between the beams can be as follows:

$$Loads\ according\ to\ EN - 1991.$$

$$CC2, Y_g = 1.2, Y_q = 1.5$$

$$Permanent\ loads:$$

$$G_k = 4.0\,[\frac{kN}{m^2}]\,for\ a\ steel - concrete\ floor\ with\ finishing$$

$$Variable\ loads:$$

$$Q_{k1} = 2.5\,[\frac{kN}{m^2}]\,for\ an\ office\ building$$

$$Q_{k2} = 0.8\,[\frac{kN}{m^2}]\,for\ walls$$

$$ULS\ design\ load\ per\ beam:$$

$$S = 5\,[m]$$

$$L = 8\,[m]$$

$$Q_d = S \cdot (Y_g \cdot G_k + Y_q \cdot Q_k)$$

$$Q_d = 5 \cdot (1.2 \cdot 4.0 + 1.5 \cdot 3.3) = 49\,[\frac{kN}{m}]$$

$$ULS\ Design\ bending\ moment\ per\ beam:$$

$$M_{ed} = \frac{1}{8} \cdot Q_d \cdot L^2 = \frac{1}{8} \cdot 49 \cdot 8^2 = 392\,[kNm]$$

$$SLS\ design\ load\ per\ beam:$$

$$Q_d = S \cdot (Q_k)$$

$$Q_d = 5 \cdot 3.3 = 16.5\,[\frac{kN}{m}]$$

$$SLS\ design\ variable\ deflection\ per\ beam:$$

$$u_{ed} = \frac{5 \cdot Q_d \cdot L^4}{384 \cdot EI} = \frac{5 \cdot 16.5 \cdot 8000^4}{384 \cdot 4.86 \cdot 10^{13}} = 18\,[mm]$$

$$u_{limit} = \frac{L/333}{=}\frac{8000/333}{=}24\,[mm]$$

$$UC = \frac{392}{465} = 0.84\,for\ ULS$$

$$UC = \frac{18}{24} = 0.75\,for\ SLS$$

The unity check for the plastic capacity is 0.84. It is not too conservative and not too extreme, this means that the design would be applicable in a real world scenario. The design shear force $V_{e,d} = 200\,[kN]$ in the above scenario is lower than the joint resistance found in experiments, it is however larger than the design resistance of the joint.

In figure 9.2 the differences between the small and big model are shown, also the boundary conditions are displayed. The big model has the beam cut in half in order to reduce computation time. For a static distributed load the half-way point of the beam has a negligible rotation, this can be modeled as a moment-clamp which can move up and down. This is also the method of applying the force into the system. In the experiment size the force was introduced via the column, its boundary conditions are shown in the same figure.

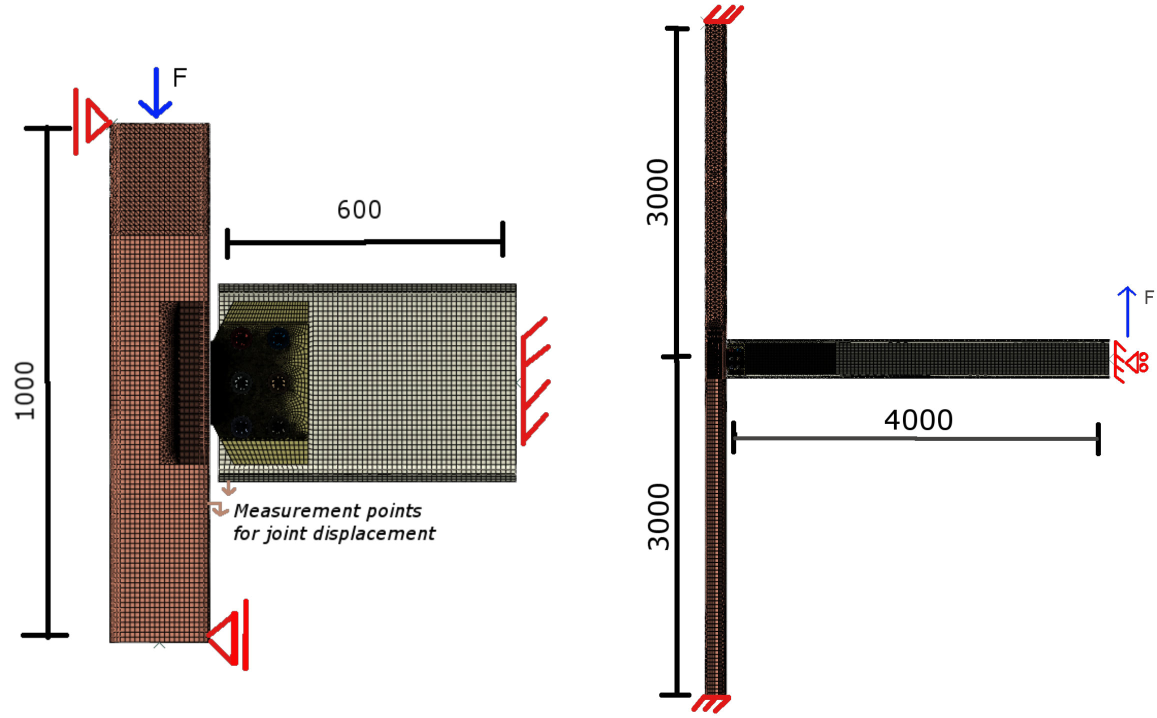

(a) Experiment

(b) Real size

Figure 9.2: Model sizes

9.2. Finite element modelling technique

The modeling technique uses calibrated material and geometry models in Abaqus, it contains all features listed in chapter 7. In order to predict the failure load a limitation of the equivalent strain is defined as function of the tri-axial state in the expected fracture initiation area. This means that the failure is defined differently for each model, ranging from 8 until 25% local plastic deformation in the weld material or in the heat affected zone.

9.3. Weld failure load

To get a first insight of the differences when scaling up, the force-displacement of the joint will be examined. In figure 9.2a the two points that determine the displacement are shown again, the reason for using these points is that they have been measured during the experiment and consequently the experiment Abaqus model matches these. In figure 9.3 the displacement progression in the joint is shown. There is much more deformation occurring and the real sized model shows a significantly (20%) lower failure load for the weld. Secondly when using IDEAStatica to run the same calculation, the difference is even more pronounced (57% lower). To understand the reasons for the lower failure loads the local and global deformations, and the internal forces are examined.

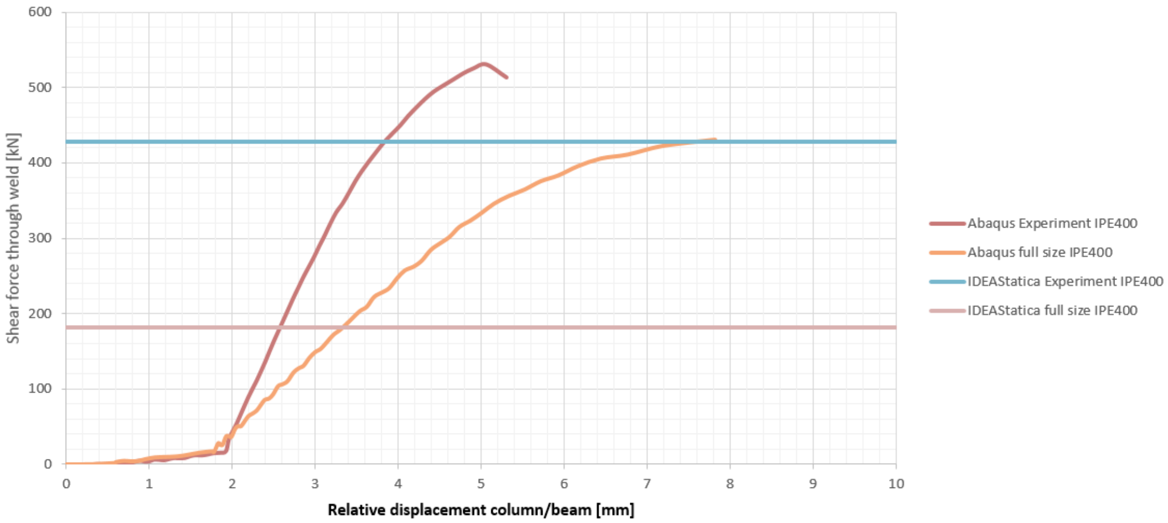

Figure 9.3: Comparison of force displacement between small and big size modelling

9.4. Global deformation

In order to get comparable results for different bending stiffnesses of the beam element there is one problem that needs to be overcome, that is plastic deformation. The method of generating the applied force in abaqus is by applying a displacement. Even though the material model takes into account the post-yielding reserve, in order to reach the weld failure load the applied displacement would be too much for the configuration with the IPE400. The reason for this is the margin that was found for the experiment joint in the weld ultimate stress and throat size between real manufacturing and nominal values. The approach taken is to make the beam, except the bolted region, fully elastic and to find two boundaries:

- At what elastic bending stiffness (EI) the upper bound for the weld resistance is reached. This is to asses the experiment set-up in general, the margin between the set-up and upper bound could provide a recommendation to adjust a similar set-up to achieve a more realistic failure load for future tests.

- At what EI the lower bound for the weld resistance is reached. This resistance could be used to assess the general resistance of the weld for such joints. If a beam starts yielding before failure of the weld, then this lower bound is reached. In general this should be the case, since weld failure is brittle and should be avoided at all cost.

In order to simplify the analysis the same geometry is being used for all models, but the elasticity E is varied to achieve the required EI. Table 9.2 shows the models and their stiffness. figure 9.4 shows the amount of deformation of the beams near failure.

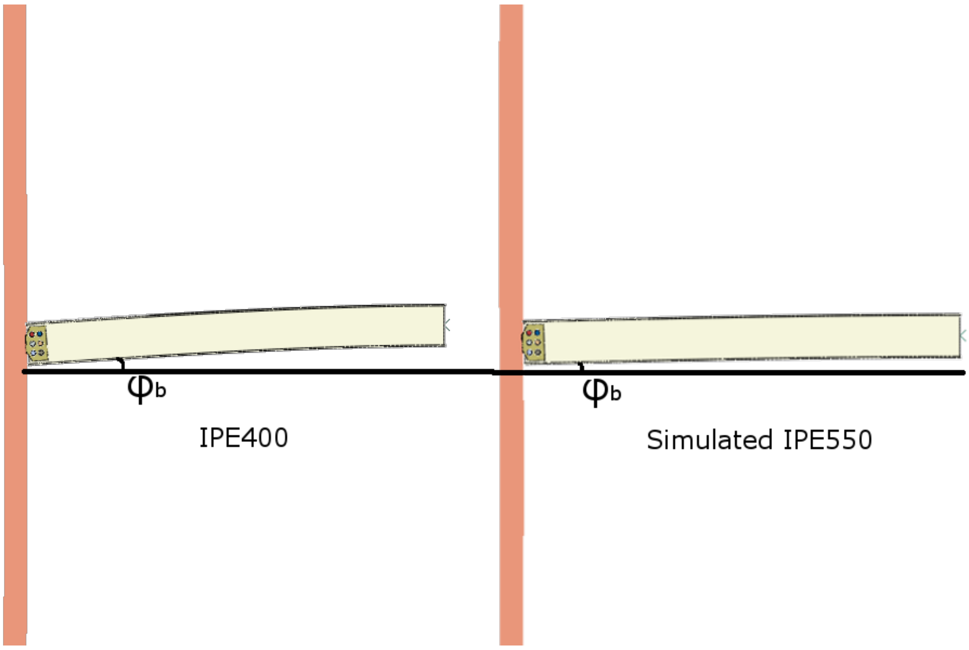

Figure 9.4: deformation at design load

9.5. Local deformation

In order to get more insight on what happens to column face locally the deformation is expressed in two views in figure 9.6. The top is the experiment size model and the bottom is the full-scale one. For the loading case of 400 kN, which is in the plastic phase near failure, the rotation of the beam and fin-plate in real size is much more than in the experiment case. Also the complete column is being pulled to the side of the fin-plate (perpendicular to the column face) by the restrained normal deformation of the beam, the curved beam wants to extend normally since the length of the curved path is longer than a straight beam thus resulting in a pulling force perpendicular to the face of the column. Due to this extra force the column face does not act like strips of a beam in bending anymore, but instead becomes a strip with such an angle ($\alpha = 6/100$ to $\alpha = 6/60$ measured) that the normal forces start contributing to the face resistance. The cut sections from figure 9.6 and 9.7 show the difference in deformation. Figure 9.7 also quantifies the extend of the column face that starts contributing in the bigger model. The left image plots σ_x and σ_y on the outer material of the face combined, showing an almost circular pattern extending 1/3rd of the face width. In the next subchapter the force contribution will be calculated.

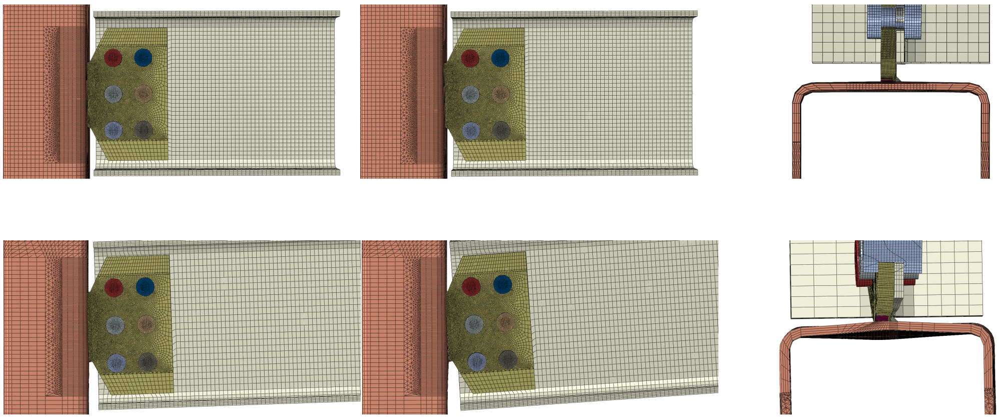
(a) At 100 kN (b) At 400 kN (c) Cut near failure

Figure 9.6: Top: experiment size, Bottom: real size. deformations.

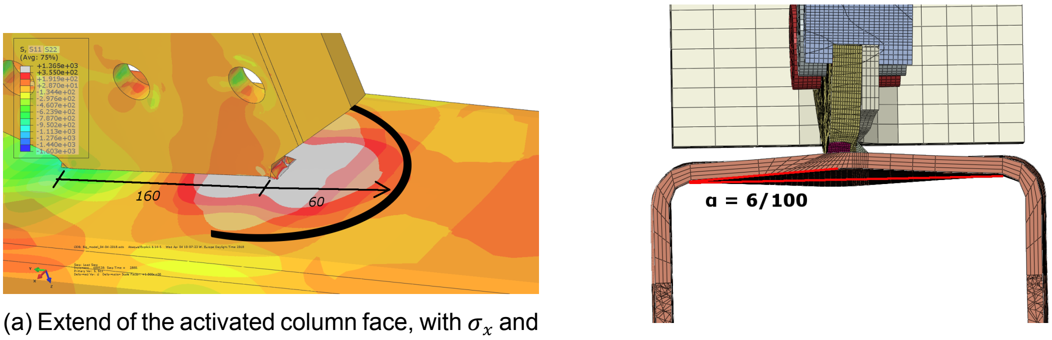

(a) Extend of the activated column face, with σ_x and σ_y plotted

(b) Cut near failure

Figure 9.7: Close up of different deformations

9.6. Internal forces

The difference in internal forces caused by the different path of load transfer reviewed. Most important is the bending moment transferred through the weld, since this greatly determines the failure load. In figure 9.8 the transferred moment is plotted against the applied shear force. The difference is clearly visible, as the moment is roughly three times as high. There is also a normal force perpendicular to the column face that is transferred by the weld, the comparison for this is shown in figure 9.8 right.

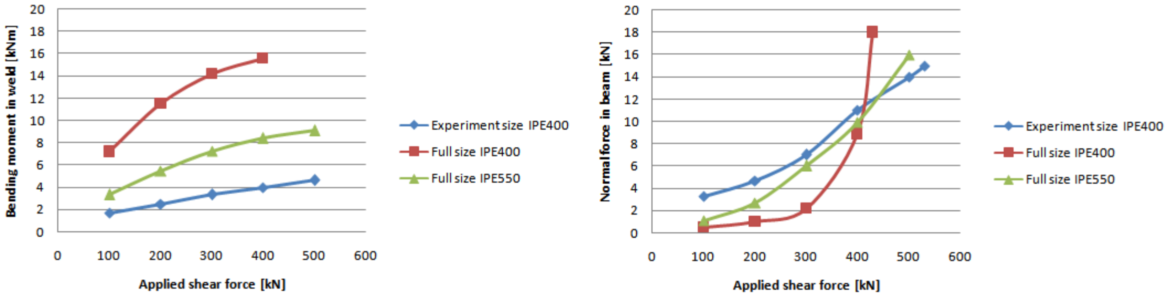

(a) Bending moment

(b) Normal force

Figure 9.8: Bending moment and normal force transferred through the weld

In the experiment set-up the physical requirement that allowed for the low bending in the weld was that the beam hardly rotates and that the bolts were capable of providing the resisting moment. In the full-size joint the bolts can not provide horizontal resistance in the beam web. The beam wants to rotate more than the fin-plate. This has the biggest influence on the failure load of the weld, chapter 9.7 will be dedicated to this.

Secondly there are more forces at work, this is illustrated in figure 9.9 by showing the Von-Mises stress around the bolt holes for both models. The bearing pattern is almost circular around the center of the bolt group in the experiment size joint. There is much more bearing in the web of the full-sized joint, which is caused by: restraining the twist in the beam caused by the asymmetric nature of the fin-plate, in the small size this was not a problem because it was restrained after 600mm.

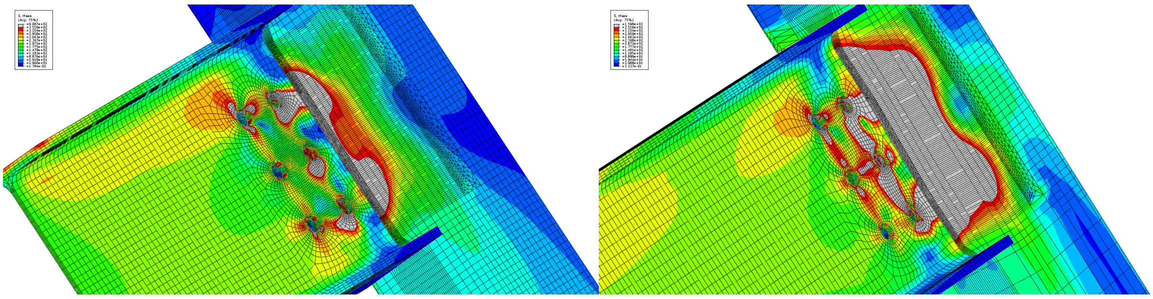
(a) VM stress in experiment size (b) VM stress in full-size

Figure 9.9: Von-mises stress around the bolt holes

The forces in the column face are different when increasing the size, the contributions for this rely mostly on:

- A bigger area being activated at the tip of the weld.

- Normal forces due to significant displacements.

In figure 9.7 the extend of the column face influence was shown. The next step is to quantify the forces that act in this zone of influence. This is done by analyzing the membrane forces in two directions near the weld tip. First the shear and normal force in the column face acting in the direction of the arrows in figure 9.10 is calculated by extracting a strip of material. For a single 10 mm strip of column at the weld tip the internal forces are analysed, this is visualized in figure 9.11. The measurement points are at 75 mm from the edge, or 25mm from the center of the column.

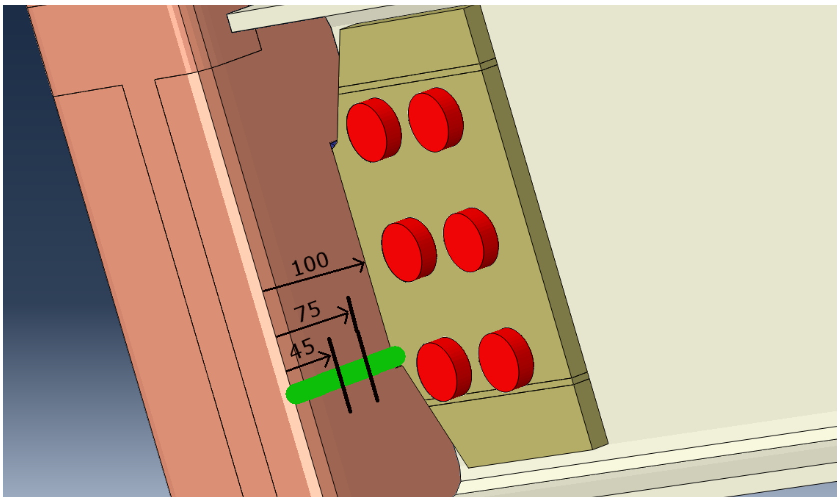

Figure 9.10: Measurement points in the strip near the weld tip

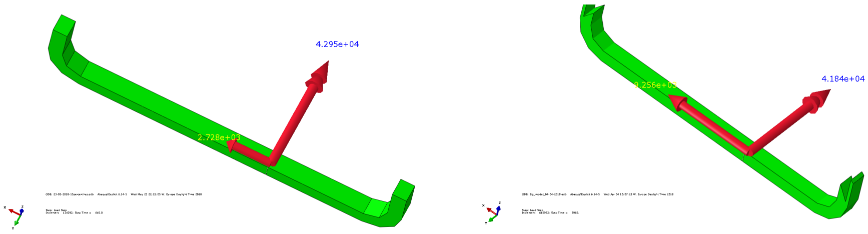

(a) M and N for small size
(b) M and N for full size

Figure 9.11: Bending and normal force in a strip at the weld tip

From abaqus the position of zero bending in the strip is found to be at 45 mm from the edge, equation 9.2 results in a shear force of 139 N/mm due to bending. The contribution from normal forces are calculated with equation 9.3 taking the vertical component 54 N/mm, this is in total $54/(54+139) = 28\%$ of the face resistance aside the weld.

$$q_v = \frac{4.18 \cdot 10^4/10}{75-45} = 139N/mm \tag{9.2}$$

$$q_n = \frac{9.25 \cdot 10^3/10 \cdot 6}{100} = 54N/mm \tag{9.3}$$

As mentioned before, figure 9.7 shows the 60mm radius of influence, the meaning of this line in terms of forces is the line of zero bending. It can be calculated how much this radius contributes to the moment passing through the fin-plate and weld by measuring force distribution as in a strip, then this can be multiplied by the length of the weld to achieve the moment, see equation 9.5. The force on each side of the weld can be estimated by taking the circumference at the distance of 25mm where the forces were measured before in figure 9.8, at the half way point in the circle the measurement is done again and the normal force is found to be much greater with $N = 2700N/mm, q_n = 162N/mm$ being found, the total bending moment is calculated in equations 9.4 and 9.5. This means that $\frac{3.8}{15} \approx 25\%$ of the moment resistance can be attributed to the part extended of the weld length.

$$q_{total} = q_v + n, circle = 139 + 162 = 301N/mm \tag{9.4}$$

$$M = h_w \cdot \pi \cdot r \cdot q_{total} = 160 \cdot \pi \cdot 25 \cdot (301) = 3.8 \cdot 10^6 Nmm = 3.8kNm \tag{9.5}$$

9.7. Rotation stiffness of the structure elements

There are several unknowns in the rotations that can not easily be quantified with FEM models, therefor a mathematical analysis will be performed. For each of the components that rotate in this joint the stiffness is calculated. This is then translated into a prediction model for the real behaviour. To verify these analytical models a group of Abaqus models is created, these are listed in table 9.2.

In the prediction model the ratio between the beam rotation and the fin-plate rotation is calculated. It is then analyzed if this ratio should be used as a discrete joint classification $(if\ R < X\ then\ M_{e,d,weld} = 0)$ or if it can be used as a continuous variable $(M_{e,d,weld} = X \cdot e \cdot V_{e,d})$ or a rotation spring $(K_{fp} = f(t_c, I_c, b_c, h_w))$ for determining stresses in the weld.

This analytical model has the following assumptions:

- On the design load the column face behaves elastically.

- On the design load the beam is also not yielding.

- The spacing in the bolt holes is neglected.

- Deformation due to bearing is neglected.

- The fin-plate is not yielding due to shear or bending.

- The stress state in the weld is defined by the Von-Mises criteria.

- The effective throat of the welds includes the HAZ. (see chapter 5.4.2)

- Secondary rotation in the bolted connection is neglected (But will occur if the eccentricity is too big, see figure 9.12).

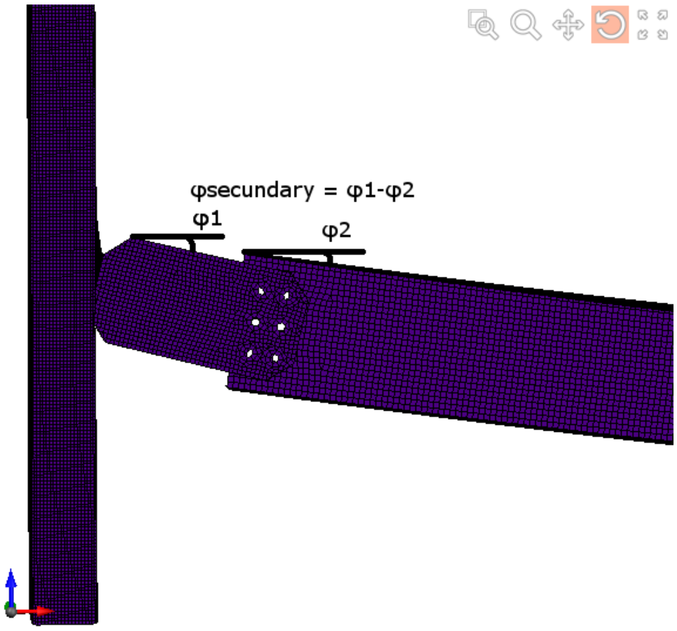

Figure 9.12: Secondary rotations in the bolted connection

Since there are assumptions which are not individually justified, this analytical model will then be verified with models in abaqus, which have many of their elements validated with the experiments and thus rely on less assumptions:

- On the design load the beam is not yielding.

- Deformation due to bearing is taken into account. (see chapter 5.4.4)

- The spacing in the bolt holes is limited $d = 24mm, d_0 = 26mm.$ (see chapter 5.4.4)

- The stress state in the weld is defined by the Von-Mises criteria.

- The geometry of the welds are as measured in the tests. (see chapter 5.1.2)

9.7.1. Beam rotations

The first item is the beam in general, the required rotation for the beam in a pinned joint is given in equation 9.6.

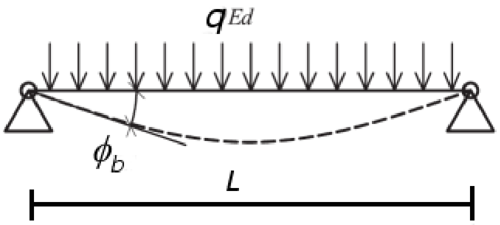

$$\phi_b = \frac{q_{e,d} \cdot L_b^3}{24EI_b} \tag{9.6}$$

$$\phi_b = \frac{F_{e,d} \cdot L_b^2}{16EI_b} \tag{9.7}$$

Where:
ϕ_b = beam rotation at the joint as result of an applied force.
$q_{e,d}$ = Distributed design load on the beam.
$F_{e,d}$ = Point load in the middle of the beam span.
L_b = Length of the beam (distance between two columns).
E = Elasticity modulus of steel.
I_b = Second moment of area of the beam.

9.7.2. Column rotations

The rotation of the column affects the force distribution in the following way: More rotation results in a less stiff behaviour and a lower bending moment through the weld. The method used to calculate this will be limited to a column with a beam on one side only. This can be expanded later on by using the factor B from EN1993-1-8 chapter 6 to include beams on two sides. The equations in 9.8 result in the rotation stiffness against an applied force on the beam.

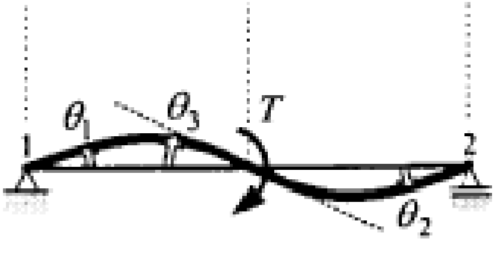

$$\phi_c = \theta_3 = \frac{1 \cdot M_c \cdot 2 \cdot L_c}{12 \cdot E \cdot I_c} \tag{9.8}$$

$$M_c = \frac{q_{e,d} \cdot L_b}{2} \cdot (e + \frac{b}{2}) \tag{9.9}$$

$$\phi_c = \frac{1 \cdot q_{e,d} \cdot (e + \frac{b}{2}) \cdot L_b \cdot 2 \cdot L_c}{24 \cdot E \cdot I_c} \tag{9.10}$$

Where:
ϕ_c = Column rotation as result of an applied distributed force.
L_c = the story height of the examined floor.
I_c = the second moment of area of the column.
b = the gross width of the column face.

e = eccentricity of applied force.

9.7.3. Column face rotations

The column face resistance is modeled as beam elements in equation 9.11. The model depicts the deformation due to a force, per unit length, perpendicular to the column face.

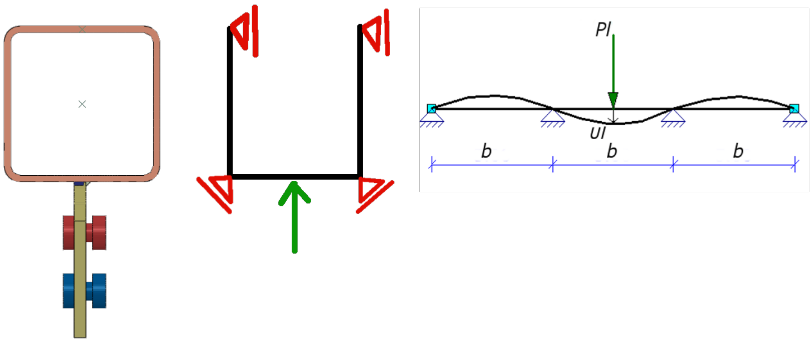

$$I_l = \frac{t^3}{12} \tag{9.11}$$

$$u_l = \frac{12 P_l b^3}{87 E t^3} \tag{9.12}$$

$$P_l = u_l \frac{87 E t^3}{12 b^3} \tag{9.13}$$

Where:
I_l = Second moment of area per column length.
u_l = Displacement perpendicular on the center point of a beam element on the column face.
P_l = Force per unit length to displace perpendicular to the column face.
The column face is then viewed from the side where the rotation due to loading is visible. The equations in 9.14 then turn this rotation into displacements perpendicular to the face, this is then integrated to obtain the moment for a certain rotation.

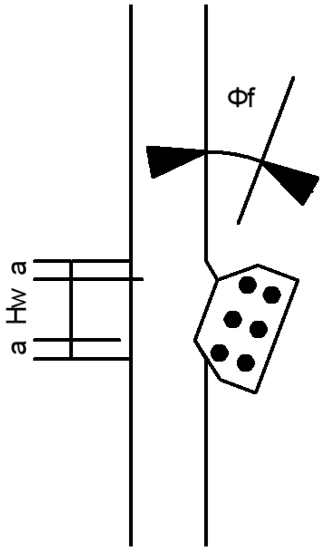

$$h_p = h_w + 2a \approx h_w + 12\pi \frac{\sqrt{b}}{\sqrt{t_c}} \tag{9.14}$$

$$M_{fp} = 2 \cdot \frac{1}{2} \frac{h_p}{2} \frac{h_p}{3} \cdot \frac{\phi_{fp} h_p}{2} \cdot \frac{87 E t_c^3}{12 b^3} \tag{9.15}$$

$$M_{fp} = \frac{\phi_{fp} h_p^3 87 E t_c^3}{144 b^3} \tag{9.16}$$

$$M_{fp} = V \cdot e \tag{9.17}$$

$$V = q_{e,d} \cdot \frac{L}{2} \tag{9.18}$$

$$\phi_{fp} = \frac{M_{fp} 144 b^3}{h_p^3 87 E t^3} \tag{9.19}$$

$$\phi_{fp} = \frac{V \cdot e \cdot 144 b^3}{h_p^3 87 E t^3} \tag{9.20}$$

$$\phi_{fp} = \frac{q_{e,d} \cdot e \cdot 24 b^3 L}{h_p^3 29 E t^3} \tag{9.21}$$

Where:
h_p = Effective column face length against bending out of plane.
t_c = Column face thickness.
h_w = Length of the weld.
M_{fp} = the moment on the column face.
ϕ_{fp} = the rotation of the column face.

Important to note here is that when modeling the stiffness as beam elements, the effective length of the column face (h_p) is bigger than the weld length, figure 9.13 is a good illustration of this. The addition will be *Curve fit* to match the F1 finite element model for the full-size building:

In figure 9.13 it appears that the extra zone of influence has a near circular pattern. In all models the stress contour has been limited to -100   355 MPa, from this the radius of this influence a_0 has been measured. The models vary in t_c and b to fit the dependencies on them. Since only a limited amount of

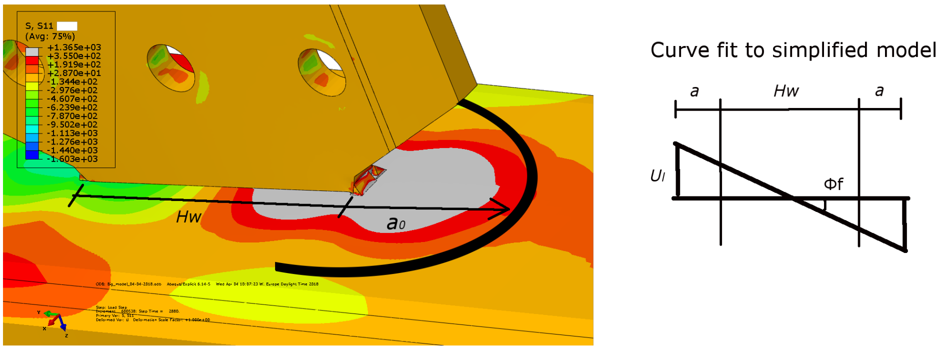

Figure 9.13: Difference between measured a_0 and the effective length $h_w + 2a$ in the calculation model

models have been made, this remains an estimation. Table 9.1 shows the variance that is still present when depending the relationships on $1/\sqrt{t_c}$ and $\sqrt{b}$, more models could increase the accuracy.

Table 9.1: Size of influence zone

Model Identity	b/t [mm/mm]	a_0 [mm]	t [-]	$f(\sqrt{t_0/t})$ [-]	b [-]	$f(\sqrt{b/b_0})$ [-]
F1	200/8	82	-	-	1	1
F9	150/8	75	-	-	0.91	0.87
F10	250/8	95	-	-	1.16	1.12
F4	200/8	75	1	1	-	-
F7	200/12	67	0.89	0.81	-	-
F8	200/16	47	0.63	0.70	-	-

The results are compared to the effective rotation length in Abaqus to calibrate the factor a from a_0. The position of zero bending at the joint design load for model F1 was found to match the analytical formula for R_{full} (explained in the next chapter) by making the effective column face length $h_p = 348mm$. This results in a total addition of $2a = 12\pi\frac{\sqrt{b}}{\sqrt{t}} = 12\pi\frac{\sqrt{200}}{\sqrt{8}} = 188mm$. In the next segments this formula will be verified for the models F2-F10.

9.7.4. Bearing in the bolt holes

As mentioned in the introduction of this chapter, secondary rotations will not be calculated in this chapter. This depends on the bearing deformation in the bolt holes, which in term depends on the initial spacing in the bolts and the distance away from the hinge position, since this introduces many variables the model take it as $\phi_{bearing} = f(e, d_0, t_p, e1, p1) \approx 0$ when the distance to the first bolts is not excessively large. In a short study with IDEAstatica it was found that it does indeed affect the forces in the weld negatively. It was found that the failure load in the weld reduced around 8% for every 100 mm of eccentricity added, e.g. an eccentricity of 500mm lowered the allowed shear force by 40%.

9.7.5. Compatibility

After obtaining the moment due to the rotations the compatibility between beam and fin-plate is created. For the calculations in 9.22 the eccentricity e is taken as the center of the bolt group, the moment is then force times eccentricity. Because the rotations of the beam and the fin-plate both depend on the same force, this force cancels out in the elastic phase. The resulting ratio R is therefore compacted into a formula that only depends on geometry. For this R there will be a simplified version, depending only on the column face and the beam, and a more accurate version, depending also on the column.

$$R_{basic} = \frac{\phi_b}{\phi_{fp}} \tag{9.22}$$

$$R_{basic} = \frac{q_{e,d} \cdot L^3 h_p^3 29Et^3}{q_{e,d} \cdot e \cdot 24b^3 L24EI} \tag{9.23}$$

$$R_{basic} = \frac{29t^3 \cdot L^2 h_p^3}{576 \cdot e \cdot b^3 I} \tag{9.24}$$

$$R_{full} = \frac{\phi_b + \phi_{bearing}}{\phi_{fp} + \phi_c} \tag{9.25}$$

$$R_{full} = \frac{\frac{q_{e,d} \cdot L_b^3}{24EI_b}}{\frac{q_{e,d} \cdot e \cdot 24b^3 L_b}{h_p^3 29Et^3} + \frac{1 \cdot q_{e,d} \cdot (e+b/2) \cdot L_b \cdot 2 \cdot L_c}{24 \cdot E \cdot I_c}} \tag{9.26}$$

(9.27)

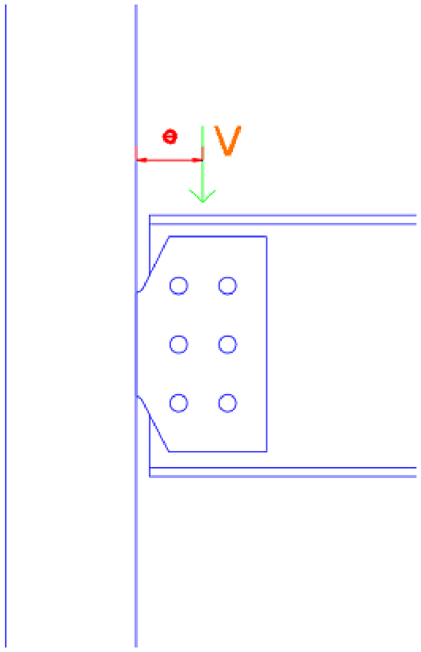

In the Eurocode stiffness factors are supplied for beams and columns, these can be used to reduce the complexity of the fomulas as shown in 9.28. If the force is applied as a point-load, which is the case in the Abaqus and IDEA models, the formule must be adjusted according to equation 9.6, These are given in 9.32.

$$K_b = \frac{I_b}{L_b} \tag{9.28}$$

$$K_c = \frac{I_c}{L_c} \tag{9.29}$$

$$R_{basic} = \frac{L_b}{K_b} \frac{1}{e} \frac{1}{\frac{576b^3}{29t^3 h_p^3}} \tag{9.30}$$

$$R_{full} = \frac{L_b}{K_b} \frac{1}{e(\frac{576b^3}{29t^3 h_p^3} + \frac{2}{K_c}) + \frac{b}{K_c}} \tag{9.31}$$

$$R_{basic} = \frac{24}{16} \frac{L_b}{K_b} \frac{1}{e} \frac{1}{\frac{576b^3}{29t^3 h_p^3}} \tag{9.32}$$

$$R_{full} = \frac{24}{16} \frac{L_b}{K_b} \frac{1}{e(\frac{576b^3}{29t^3 h_p^3} + \frac{2}{K_c}) + \frac{b}{K_c}} \tag{9.33}$$

In summary this theoretical formula for R has three states;

- If $R < 1$ then the column face provides a low stiffness compared to the rest of the system. The force transfer through the weld will be reduced and the bolts carry extra horizontal forces due to a coupling moment.

- If $R \approx 1$ then the system will move in sync, the force transfer through the weld is based on a shear force and a bending moment caused by the eccentricity. The bolts only carry vertical forces.

- If $R > 1$ then the beam generates extra horizontal forces in the bolts, which are limited by the bearing capacity near the holes. These extra forces should also be taken by the weld and the column face.

9.8. Validation of the proposed formula

The proposed formulas for R will be validated with a set of abaqus models. In total 10 models are created with varying beam and column stiffness. Table 9.2 shows the model identities and their beam/column profiles. All models use the same material geometry and properties in the weld and fin-plate, which have been defined for the S355 welds in the chapter on material calibration. The unity checks and design shear loads are calculated in the same way as in chapter 9.1. The required beam rotation is according to the point load formula 9.6.

First the position of zero bending moment will be validated at the **design load**. Secondly analytical formulas used with the directional method will be verified at the **failure load**.

Table 9.2: Stiffness overview

Model Identity	Beam	Column	Length	UC_{uls}	UC_{sls}	$V_{e,d}$	ϕ_b	R_{full}
			[m]	[-]	[-]	[kN]	[rad]	-
X1	IPE400	SHS200x8	1.2					
F1	IPE400	SHS200x8	8	0.84	0.75	200	0.033	0.54
F2	IPE550	SHS200x8	8	0.39	0.25	200	0.011	0.18
F3	IPE330	SHS200x8	8	1.37	1.51	200	0.066	1.08
F4	IPE400	SHS200x8	6	0.47	0.31	150	0.014	0.31
F5	IPE550	SHS200x8	6	0.84	0.75	150	0.005	0.10
F6	IPE330	SHS200x8	6	0.78	0.63	150	0.028	0.61
F7	IPE400	SHS200x12	6	0.47	0.31	150	0.014	0.74
F8	IPE400	SHS200x16	6	0.47	0.31	150	0.014	1.31
F9	IPE400	SHS150x8	8	0.84	0.75	200	0.033	0.94
F10	IPE400	SHS250x8	8	0.84	0.75	200	0.033	0.34

9.8.1. Position of zero bending

The abaqus models show a clear movement of the hinge location (or e_{real} or position of zero bending moment) e, dependent on the stiffness of the elements. The location of the zero bending moment as measured from the column face is displayed in figure 9.14. Here the x-axis shows the predicted ($e = e_{boltgroup} \cdot R_{full}$), and the y-axis the modelled hinge position at the **Design load**. It can be seen that there is a clear correlation between the two, the formulas underestimate the position of the hinge slightly, this could be corrected by shifting it upward ($e = e_{boltgroup} \cdot (R + 0.10)$) for designing purposes.

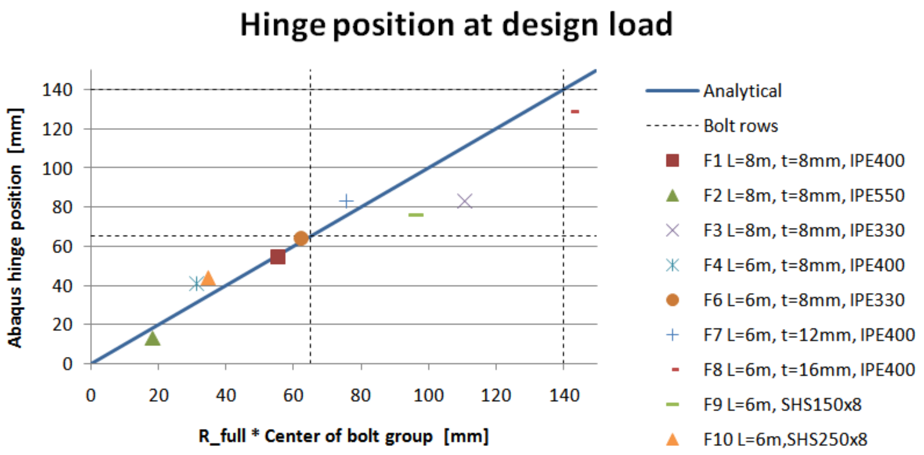

Figure 9.14: Abaqus results for the hinge position and analytical results based on R

9.8.2. Estimated failure load

The ratio R will be used to find a relationship between the analytical formulas combining shear and moment (9.34 - 9.37) in a weld, and the results from FEM.

Each of the models are calculated with these formulas with the moment taken as in equation 9.38. Here e is the distance to the center of the bolt group.

$$\sigma_\perp = \tau_\perp = \frac{2 \cdot 2.12 \cdot M}{a \cdot h_w^2} \tag{9.34}$$

$$\tau_\parallel = \frac{F}{a \cdot l} \tag{9.35}$$

$$\sigma_{vm} = \sqrt{\sigma_\perp^2 + 3 \cdot (\tau_\perp^2 + \tau_\parallel^2)} \tag{9.36}$$

$$\sigma_{vm0} = \sqrt{3 \cdot \tau_\parallel^2} \; (shear\ only) \tag{9.37}$$

$$M_{e,d} = V_{e,d} \cdot e \cdot R \tag{9.38}$$

The material models used in abaqus are primarily based on the shear tests. Since damage modeling is not applied they could be too generous in their failure criteria. In order to predict failure more accurately the failure strain in the fracture strain will be limited according to the tri-axial stress state in each model. In chapter 4.5 this is explained more in detail. In chapter 7.3 the strain formula $\epsilon_f = 0.25e^{-1.54\sigma_m/\sigma_e}$ has been estimated. Table 9.3 shows the estimated strains. These points are based on the following:

- Measured in Abaqus, in the integration point at the end of the weld in the tension zone, in the infused weld zone on the edge with the base material. This is the same point as the observed fracture initiation point in figure 7.15.

- Measured at around 0.1 plastic deformation in this point.

Table 9.3: Estimation of fracture strains

Model	σ_H $[N/mm^2]$	σ_e $[N/mm^2]$	State [-]	ϵ_f [-]
F1	302	904	0.33	0.14
F2	40	900	0.04	0.23
F3	552	906	0.60	0.09
F4	297	906	0.32	0.15
F6	238	903	0.26	0.16
F7	400	906	0.44	0.12
F8	660	906	0.72	0.08
F9	300	906	0.33	0.15
F10	220	900	0.24	0.17

In figure 9.15 the failure load is calculated as the maximum applied force divided by the maximum applied force with only shear transfer. This is then compared to the force found in the FEM models. The reason for using the ratio maximum force over the maximum shear only force is that it is much more practical to use in an engineering perspective, and it can be compared to the results from IDEAStatica.

In figure 9.15 the data points from abaqus and the analytical curve are compared. The analytical curve is not perfectly smooth, this is caused by manually entering data points. From the graph it can be seen that the analytical prediction using equations 9.34 to 9.38 provide a good estimate for the failure load. Even though this model does not take into account bearing or plastic deformation in the column face or near the weld, the results coincide accurately. It is important to note that the maximum shear shear force is greater than the design force, 540 kN compared to 200 kN. As was investigated in chapter 8.3.1, figure 8.5, the position of the zero bending moment moves closer to the column face as the force increases and more elements deform elastically. In this case this has a positive effect on the forces acting on the weld as $M = V \cdot e$ decreases.

The limitations are however very important:

- Only the column thickness of 8,12,16mm with 200mm width, and 8mm with 150mm, 250mm has been modelled. The formulas are only valid for very similar ranges.

- Only 6 and 8 m beams are modelled. These models take a day to run on available hardware, thus limitations are made.

- In Abaqus the beams are set to not yield to provide artificial rotation, if yielding occurs at the design load this model is not valid, only the rotational stiffness of the column face should be used in a component based calculation.

- The experiment could not prove that using Von-Mises criteria for combining bending and shear in a weld was accurate. Damage modelling should be used to more accurately predict failure in abaqus.

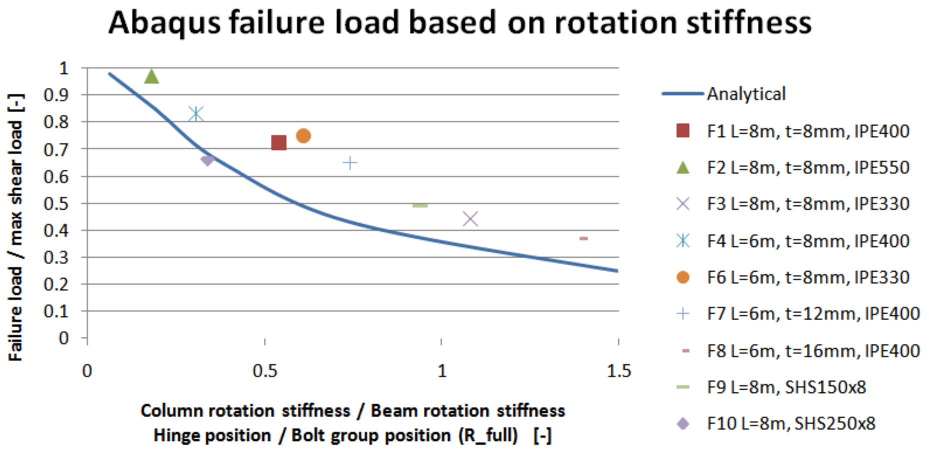

Figure 9.15: Abaqus results and analytical results based on R

9.9. Possible simplifications of the calculation model

The difference between the simplified version and the full version is shown in table 9.4. For the examined models the maximum difference is only 6%. This is interesting as it indicates the influence of the column length is not significant and could be neglected for certain boundary conditions. Secondly the moment in the plate and weld is calculated by equation 9.38, if R is taken as R_{basic} then e cancels out and the moment only depends on the stiffness of the beam and column face. This means it is not heavily dependent on the eccentricity of the bolt holes.

Table 9.4: Difference between Simplified and non simplified ratio

Model identity	R_{simple}	R_{full}	Difference [%]
F1 L=8m,t=8mm, IPE400	0.203	0.201	-1.0
F2 L=8m, t=8mm, IPE550	0.0678	0.067	-1.2
F3 L=8m,t=8mm, IPE330	0.407	0.402	-1.2
F4 L=6m,t=8mm, IPE400	0.114	0.113	-0.9
F5 L=6m, t=8mm, IPE550	0.0382	0.0377	-1.3
F6 L=6m,t=8mm, IPE330	0.229	0.226	-1.3
F7 L=6m, t=12mm, IPE400	0.3	0.293	-2.4
F8 L=6m, t=16mm, IPE400	0.605	0.581	-4.1
F9 L=6m,SHS150x8	0.402	0.378	-6.3

9.10. Effect of cross-section yielding

The moment in the weld depends on the rotation of the beam at the position of the joint. When yielding of the cross-section of the beam occurs, this rotation increases significantly. The extend of the negative influence on the weld will be quantified by comparing two variants of the model F4, a 6 m IPE400 beam with the experiment joint dimensions. One variant stays elastic and the other yields at $f_y = 435MPa$. The beams are loaded by a *point load* with the free body diagram from figure 9.2.

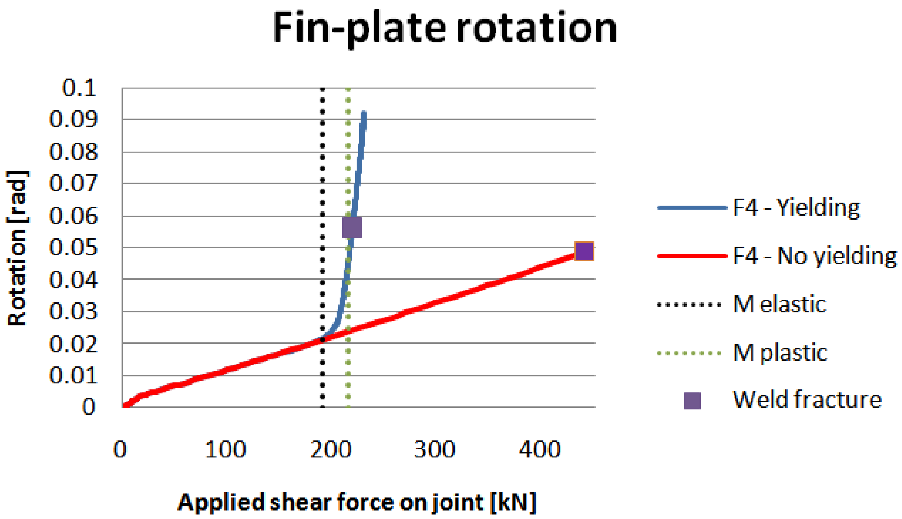

Figure 9.16: Rotation of the fin-pate when the beam yields in global analysis

Figure 9.16 shows the rotation of the fin-plate plotted against the applied vertical shear force. The model with yielding of the beam cross section clearly shows a steep increase of rotation after reaching the elastic capacity. The estimated failure load of the weld is half of what it would be if it was a fully elastic beam. The moment transfer through the weld is quantified in figure 9.17.

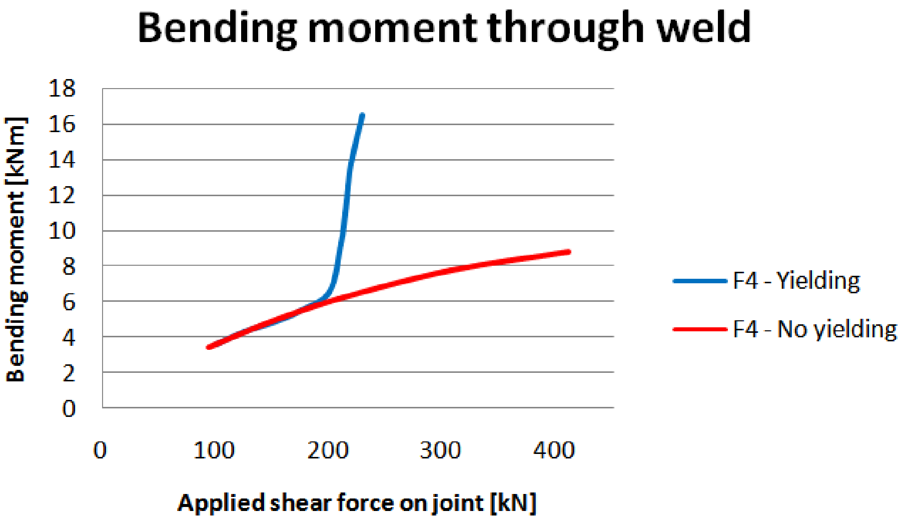

Figure 9.17: Moment in the weld when the beam yields in global analysis

9.11. Component based stiffness of the column face

In the previous sections the stiffness ratio's have been validated against FE Models, Since there was a good correlation it is possible to obtain a stiffness coefficient for the column face. It is specifically important to include a component stiffness because the beams have been modelled as elastic beams which do not yield. As shown inthe previous chapter, yielding increases the joint rotation, which increases the eccentricity that should be taken. The components that will be discussed in this chapter are shown in figure 9.18.

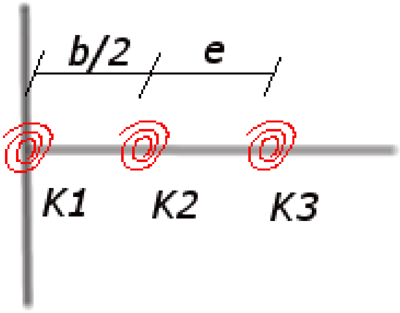

Figure 9.18: Component based calculation model

Where:
b = Width of the column.
e = Eccentricity to the center of the bolt group.
$K1$ = Column stiffness. [Nmm/rad]
$K2$ = Column face stiffness. [Nmm/rad]
$K3$ = Bearing stiffness.[Nmm/rad]

As mentioned before, the bearing stiffness $k3$ will not be calculated. The column stiffness was found to have only a 6% influence, still it can be described by equation 9.39. In figure 9.19 this stiffness is compared to the values found with the finite element model boundary conditions and load application. The difference is caused by the assumption that forces transfer through the centroid of the column. The column boundaries allow for a reaction force that could be on the edge of the column cross section.

$$K1 = \frac{12 \cdot E \cdot I_c}{2 \cdot L_c} \tag{9.39}$$

Where:
L_c = the story height of the examined floor.
I_c = the second moment of area of the column.
E = the modulus of elasticity of steel.

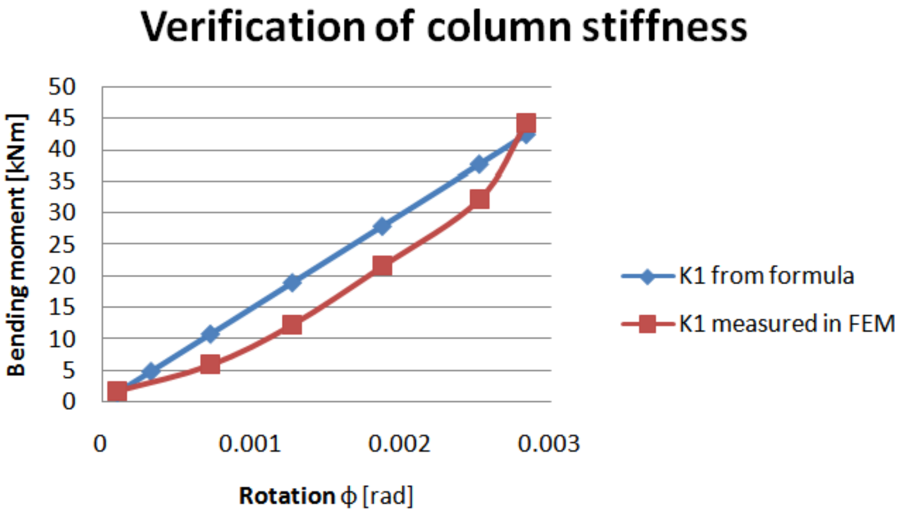

Figure 9.19: Moment-rotation diagram of the column at the joint

For the column face the effective length of the face should be calculated with equation 9.40. The stiffness of the column face then follows from equation 9.41. The verification of this formula with the results from FEM are shown in figure 9.20. There is a clear correlation between analytical and FEM. When the elastic bending capacity of the face elements is reached then the formula over-estimates the stiffness.

$$h_p = h_w + 12\pi \frac{\sqrt{b}}{\sqrt{t_c}} \tag{9.40}$$

Where:
h_p = Effective column face length against bending out of plane.
t_c = Column face thickness.
h_w = Length of the weld.
b = the gross width of the column face.

$$K2 = \frac{h_p^3 87 E t_c^3}{144 b^3} \tag{9.41}$$

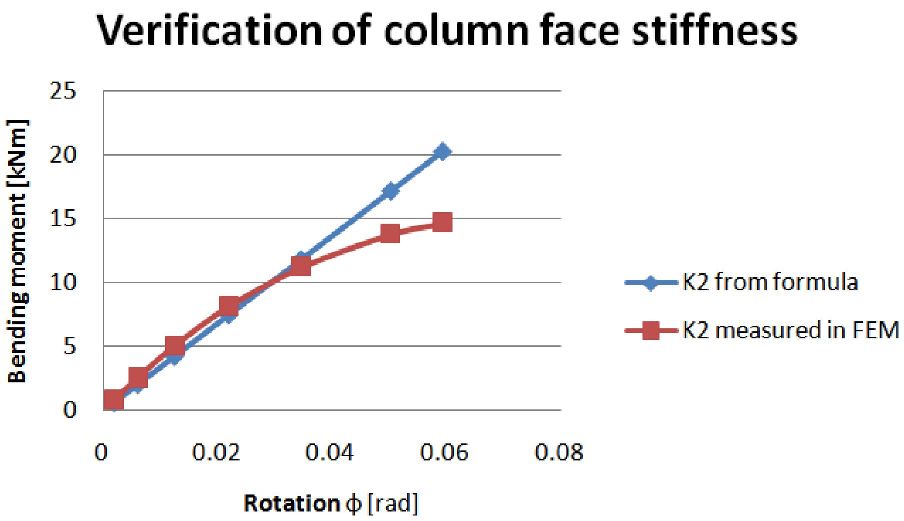

Figure 9.20: Moment-rotation diagram of the column face

9.12. IDEAStatica modelling of full-size beams

In order to take full advantage of having both the column and beam stiffness in IDEA, the same boundary conditions as set in abaqus should be used, generating a model such as 9.21. The weld failure loads that are found are displayed in figure 9.22. A quick glance will show that all the calculated values are slightly below the analytical line. This is different to what results from Abaqus, where most results are just above the line. The main reason for this difference is that the plastic redistribution in the weld is limited to 5% in IDEA with no hardening, whilst in the abaqus models this is varied between 8 and 25% with hardening. Since IDEA is a program for designing this is a slightly conservative method of redistributing forces plastically.

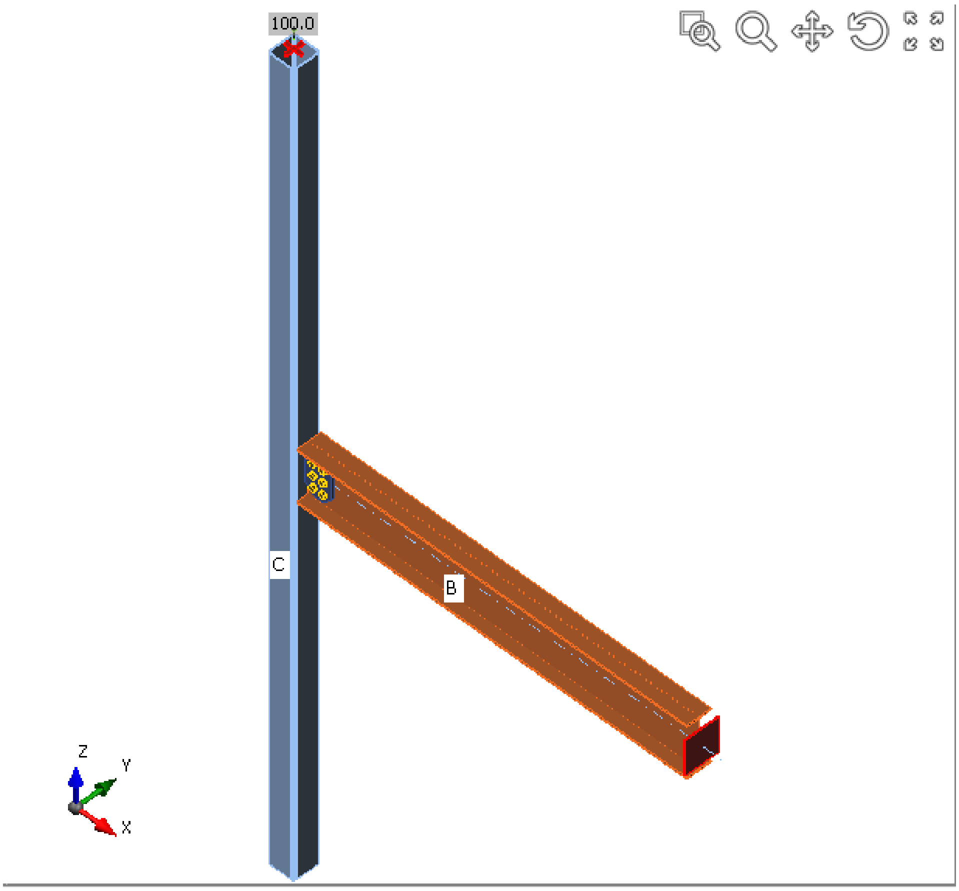

Figure 9.21: IDEAStatica force application

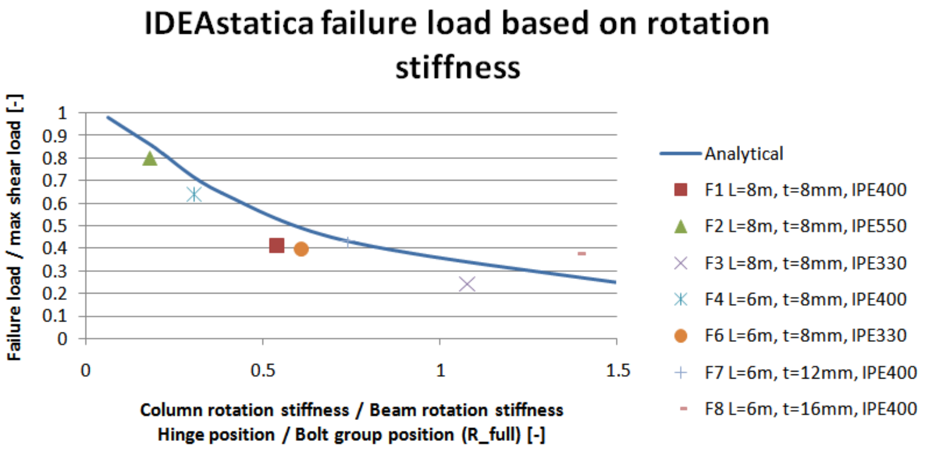

Figure 9.22: IDEAStatica results and analytical results based on R

9.13. Conclusions on designing a weld for fin-plate joints

It is important to consider the stiffness of all the elements in the joint, the bending moment and normal force transferred through the weld are influenced by:

- The stiffness of the column face, a stiffer face is more likely to transfer more bending stresses. See chapter 8 for the sensitivity analysis.

- The bending stiffness of the beam. If the beam element deforms plastically then the deformations are such that:

- The bolts will not provide a resisting bending moment anymore.

- The face of the column will deform significantly more, such that normal forces in the column face will contribute to the perpendicular resistance, these forces will be transferred through the weld.

- If the beam member will be designed such that it is allowed to yield in the ultimate limit state in the global structure analysis, it will not be stiff enough in ULS to provide a lower rotation at the connection location than the fin-plate wants to rotate, the moment that transfers the shear force over the bolt eccentricity is provided by the weld, not the bolts. Coming back to the two calculation models from figure 9.23 this means that the weld should generally be designed by the left moment distribution, meaning $M_{e,d} = V \cdot e$.

- If the beam member is calculated according to elastic theory in ultimate limit state in the global structure analysis, then it is possible to reduce the bending moment in the weld to $M_{e,d} = V \cdot e \cdot R$, where R is the ratio of the beam/column face rotation stiffness. The limitations of this function should still be defined.

- One way to use the shear only calculation from the right moment distribution would be in an analysis were the weld is weaker than the beam resistance. In this case a calculation should be made to prove that the beam provides enough stiffness to allow the bolts to provide the bending resistance at the weld's shear resistance.

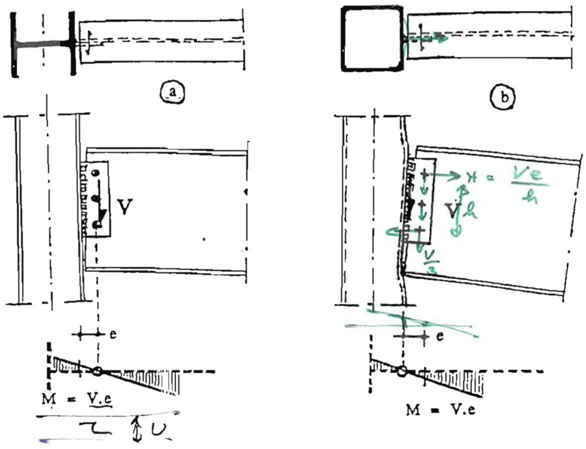

Shear + bending through weld

Shear only through weld

Figure 9.23: Calculation models for bending moments in stiff and soft columns[9, ch. 2]

10

Conclusions and recommendations

10.1. On the design of the welds

With the performed experiments the following two research questions can now be answered:

- *What is the resistance of a single pass weld and what factors influence this resistance?*

- *What is the resistance of an overmatched single pass weld and what factors influence this resistance?*

The resistance of the single pass welds was found to be much greater than suggested by the nominal values from the Eurocode. In chapter 6 it was examined where the overstrength of the welds originated from. The conclusion was that for this specific single sided 3mm weld; The utilization of the *design resistance* compared to the *failure load in experiments* was 19% with EN1993-1-8:2005 and 25% with EN1993-1-8:2020. Two main factors influence this resistance. The main reason was that When welding a 3mm weld according to standard procedure the high penetration depth increased the effective weld throat, accounting for a 100% increase in resistance. The second reason was that the failure stress was 50% higher for both the matching (Class 46 on S355) and overmatching (Class 89 on S355) infused weld material.

Welding on one side did not result in a significantly lower failure load with the eccentricities occuring in the experiment. In the finite element models there were some eccentric stresses but the influence did also not significantly affect the failure load. Both cases were loaded symmetrically and a sensitivity study has not been performed so the effect can not be quantified.

As for the resistance of overmatched welds, the results from the experiments showed that the failure started in the border between the infused zone and the fin-plate base material. The failure stress was much closer to that expected from the weld material and not the base material. The failure path was not through the column and the influence of the column material on the failure stress was negligible.

This results in the following conclusion: The proposed allowed use of 75% weld material with 25% base material for determining fu of the weld is acceptable for the examined joint under the condition that the 25% will be taken from the weakest base material. The stronger base material will not effect the weld strength if the failure path is only through the weakest. It was however not possible to determine the actual ratio from the tests, but the failure stress was *consistently* 50% higher than nominal when taking 25% influence.

The low utilization rate of the design load leads to the following recommendations in application:

– Allow for the welding company to use not full-strength welds for 15mm fin-plate.

- Allow for taking into account part of the infused zone for small (3-5mm) welds. For all specimens the depth of the infused zone was consistently $>= 2.0mm$. This resulted in the utility of the nominal calculation throat compared to the actual failure throat to be only 54%. Allowing the addition of 0.5mm brings this to 63% and 1mm to 72% for the 3mm weld.

10.2. On the use for fin-plate connections on SHS columns

With the help of the finite element models the following four research questions can now be answered:

- *What is the design load acting on the weld and bolts and what factors influence this load?*

- *What is the column face stiffness influence?*

- *What is the influence of the beam stiffness?*

- *How to set up an engineering approach to calculate such flexible joints?*

At the start of this thesis there was a discussion on what force distribution to use for calculating the design loads transferred through the weld and the bolts. The two models are again shown in figure 10.1. For a SHS column it would mean a significant reduction of weld material if the calculation is done via the shear transfer only model, the model combining shear and bending will in turn have larger weld forces. To achieve equilibrium in the shear only model the bolts in the top and bottom row will have a shear force increase of 50% resulting from horizontal forces.

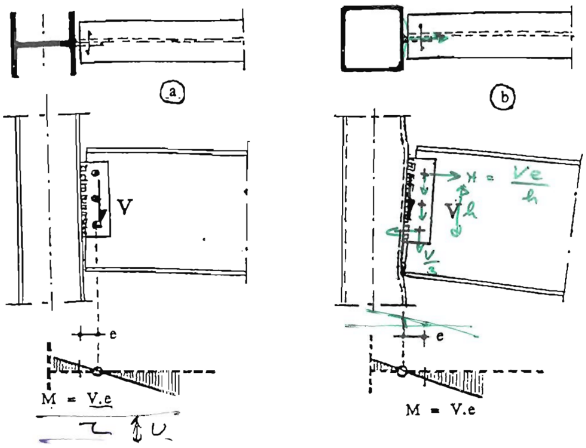

Shear + bending
through weld

Shear only
through weld

Figure 10.1: Calculation models for bending moments in stiff and soft columns[9, ch. 2]

It was proven that for certain boundary conditions it is possible to only account for shear transfer through the weld. However it was found that when expanding the Abaqus model to a full building size the boundary conditions change such that also a moment needs to be transferred through the weld and the bolts. The ratio between the stiffness of the beam and the column face determines the magnitude of these moments.

The variables that affect this distribution have been mechanically defined and verified via sensitivity analysis with Abaqus. The result is that the moment transfer through the weld from bridging the force eccentricity can be reduced according to the stiffness ratio of the beam and the column face. There are four stiffness factors which influence the force distribution; The column stiffness K_c, the column face stiffness K_cf, the plate bearing stiffness K_p and the beam rotation stiffness K_b.

The column face stiffness depends on the effective area that can be activated by the fin-plate. For the effective column face length against bending the relation 10.1 was calculated. This is then applied in the equation for the stiffness of the column face 10.2.

$$h_p = h_w + 12\pi\frac{\sqrt{b}}{\sqrt{t_c}} \tag{10.1}$$

$$K2 = \frac{87h_p^3Et_c^3}{144b^3} \tag{10.2}$$

Where:
h_p = Effective column face length against bending out of plane.
t_c = Column face thickness.
h_w = Length of the weld.
b = the gross width of the column face.
$K2$ = rotational stiffness of the column face.

The stiffness of the beam has a big influence on the rotation of the beam at the joint. This in turn determines the bending moment in the weld. If the beam yields in its cross-section then this rotation increases significantly. Also increasing the bending moment significantly, up to the plastic capacity of the column face. This is also the reason why there should be a clear distinction between calculating the beam with M_{el} or M_{pl}.

The engineering approach follows from the two governing influences: The face stiffness and the beam stiffness. If the beam is calculated elastically the problem can be simplified and welds could be calculated with taking into account the shear force V_{ed} and the bending moment $M_{ed} = V_{ed} \cdot e \cdot R$. Here R is defined by either of the two formulas from 10.3 or 10.4. The benefit of using R_{basic} is that the resulting moment does not rely on the distance to the bolt holes. R_{full} has the benefit of providing a more favourable ratio. In other cases, for example with a very short beam, it may be proven that the beam will not be close to yielding and the weld may be calculated with only V_{rd}.

$$R_{basic} = \frac{L_b}{K_b}\frac{1}{e}\frac{1}{\frac{576b^3}{29t_c^3h_p^3}} \tag{10.3}$$

$$R_{full} = \frac{L_b}{K_b}\frac{1}{e(\frac{576b^3}{29t_c^3h_p^3} + \frac{2}{K_c}) + \frac{b}{K_c}} \tag{10.4}$$

Where:
L_c = the story height of the examined floor.
I_c = the second moment of area of the column.
L_b = the distance between the columns.
I_b = the second moment of area of the beam.
K_b = $\frac{I_b}{L_b}$
K_c = $\frac{I_c}{L_c}$
e = Distance to the bolt group center.

10.3. On the usage of IDEAStatica

The commercial software IDEAStatica can provide a close estimate to the results found in experiments. When applying the same boundary conditions as in the experiment with the ultimate strength and dimensions of the weld material as measured a utility of 84% is found. Because the software uses a lower amount of plastic redistribution (5%) and no hardening than reality the outcome is on the safe side.

In order to achieve the correct stiffness ratio in the software, the full length of the beam and column has to be modelled. This is not desireable and to avoid this a hand calculation of the stiffness is required. In order to model only the column face and fin-plate, the point of force application should be taken based on the ratio R. The eccentricity should be taken as $e_{effective} = e_{boltgroup} \cdot R$.

10.4. Recommendations for further research

10.4.1. Stress distribution in the weld

The formula commonly used for calculating stresses in a weld following from a bending moment [eq 10.5] are based on a stiff base and the hollow section does not provide this stiff base. It is recommended to use a different calculation method such as CBFEM or FEM software, or a different analytical approach. The difference in peak stresses in the outer parts of the weld are shown in figure 10.2. Due to the stiffness being concentrated near the ends of the weld, the stresses are much greater than estimated.

$$\sigma_{\perp} = \tau_{\perp} = \frac{2 \cdot 2.12 \cdot M}{a \cdot h_w^2} \tag{10.5}$$

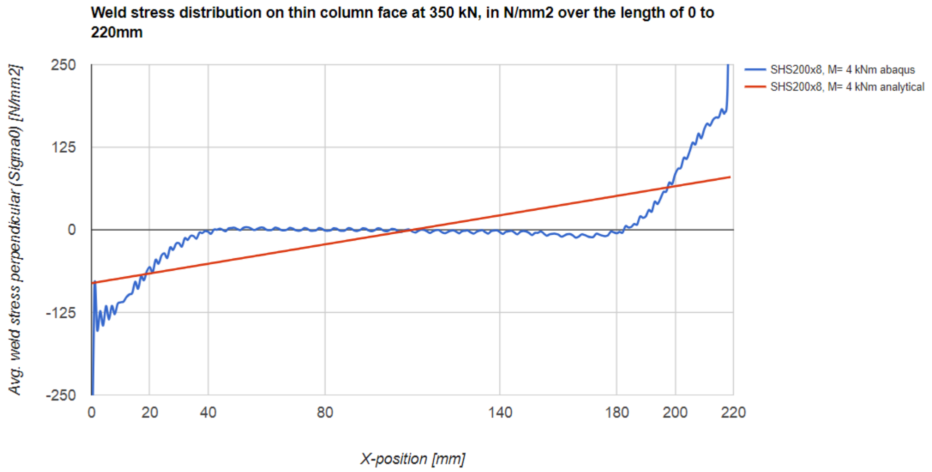

Figure 10.2: Stress distribution in the weld, FEM and analytical

During the validation of the analytical formula for R the difference in failure load was not as great as the difference in peak stresses. This could be because the shear stress is taken as an average value, while theory for a rectangular section suggests it is lowest near the ends. The added stiffness could however still have an influence and increase the shear flow near the ends, for this reason this can not simply be held as the explanation. More post processing should be done to map all the stress components in the failure plane.

10.4.2. Single side welding

The effect of welding on a single side should be investigated further. In the modelling of the full size building the geometry from experiments was used. These include the fixing welds and large infused weld zone, both can act positively on the resistance. A sensitivity analysis should be performed on:

- The effect of fixing welds at the tips on preventing peak stresses in the main weld due to the eccentricity
- The effect of fin-plate thickness on a single sided weld without fixing welds
- The effect of applying asymmetric loading on the beam
- The effect of mounting the beam on the wrong side of the fin-plate with a single sided weld

10.4.3. Effective column length

The effective column face length depends on $\sqrt{b}$ and $\sqrt{t}$. This dependency is the result of curve-fitting with only 6 datapoints from table 9.1. A more accurate relationship is needed in order to apply this formula to all column sizes. Currently it is only valid from $b = 150mm$ to $b = 250mm$

10.4.4. The effect of the bolt thread and bearing

The effect of the bolt thread has not been taken into account. It was observed during the experiment that the rotation of the fin-plate was significantly affected by the sharp threads penetrating the fin-plate material. The difference found from experiments is shown in figure 7.10. The effect of the threads will be a reduction of bending moment capacity in the bolt group. More specifically it means that the horizontal force capacity for both a positive and negative bending moment is reduced. This could have the following effect:

- If the position of zero bending moment is found to be between the column face and the first bolt row, then this position could move towards the bolt row and result in a higher moment transfer through the weld.
- In the case of a stiff column face, the position of zero bending moment could be greater than the first bolt row. The position could then shift back towards the bolts, resulting in a positive effect for the bolts.
- In any case the horizontal shear force in the bolts would be reduced, this has a positive effect on the bolt failure load.

Since the study on yielding of the beam cross section gave more insight on the effect of rotation on the weld failure load, see figure 9.16. It is important that the effect of increased or descreased rotation caused by different bolt types will be quantified.

A

New specimens

This appendix includes the manufacturing drawings of the specimens ordered in January of 2018. The square section columns are re-used from the experimental specimens from Sebastian Navarro.

Table A.1: Bill of materials

Part code	Name	Profile	Length [mm]	Material	Amount	Amount newly manufactured
E1.1	Column	SHS 200x8	1050	S690	5	**0**
E1.2	Column	SHS 200x8	1050	S355	3	**0**
E2	Beam	IPE400	600	S355	8	**2**
E3	Fin plate	PL200x15	330	S355	8	**8**
E6	End plate	PL300x30	600	S355	8	**2**

Table A.2: Specimen overview - Nominal values

Identity	Column	Fin-plate	Weld yield [N/mm^2]	Weld throat [mm]	Weld length [mm]
2E1	S690/E1.1	S355/E3	>355	3	160
2E2	S690/E1.1	S355/E3	>355	3	160
3E1	S690/E1.1	S355/E3	>690	3	160
3E2	S690/E1.1	S355/E3	>690	3	160
3E2	S690/E1.1	S355/E3	>690	3	160
4E1	S355/E1.2	S355/E3	>690	3	160
4E2	S355/E1.2	S355/E3	>690	3	160
4E2	S355/E1.2	S355/E3	>690	3	160
					All single side weld

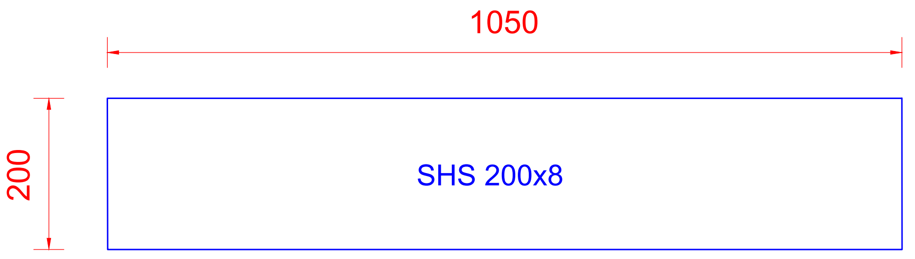
1050
200
SHS 200x8

E1.1/E1.2

Table B.1: Bill of materials

Part code	Name	Profile	Length [mm]	Material	Amount	Amount newly man-ufactured
E1.1	Column	SHS 200x8	1050	S690	5	**0**
E1.2	Column	SHS 200x8	1050	S355	3	**0**
E2	Beam	IPE400	600	S355	8	**2**
E3	Fin plate	PL200x15	330	S355	8	**8**
E6	End plate	PL300x30	600	S355	8	**2**

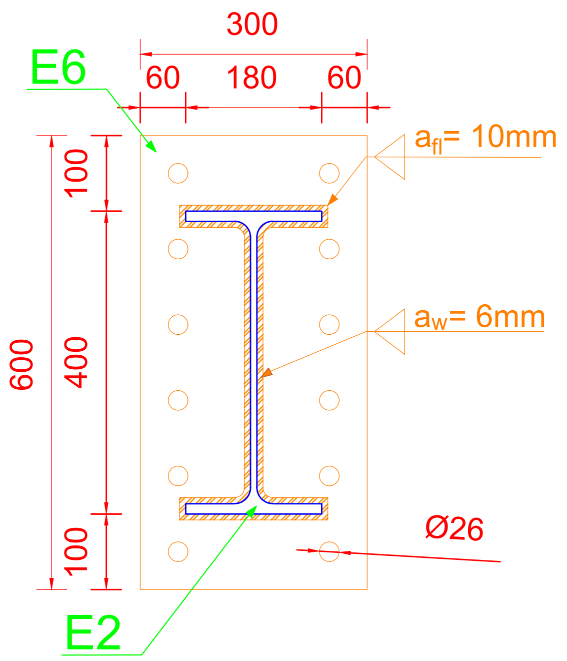
300
60
180
60
E6
a_{fl}= 10mm
a_w= 6mm
600
100
400
100
Ø26
E2

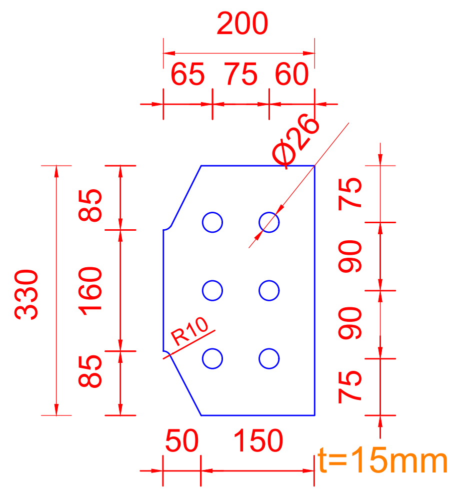
200
65
75
60
Ø26
330
85
160
85
R10
75
90
90
75
50
150
t=15mm

E3

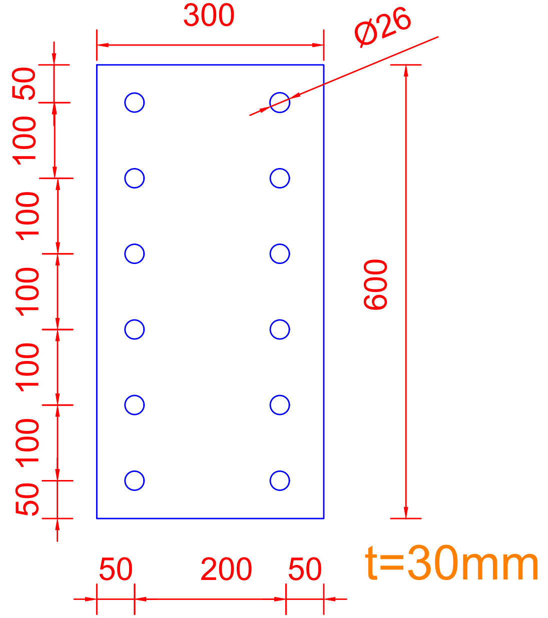
300
Ø26
50
100
100
100
100
100
50
600
50
200
50
t=30mm

E6

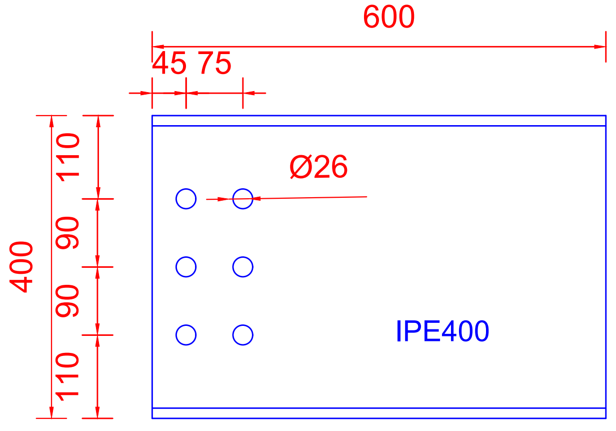
600
45
75
400
110
90
90
110
Ø26
IPE400

E2

ASK ROMEIN **TUDelft** Delft University of Technology

Thesis	Optimization of Steel Joint Design in Daily Engineering Practice		
Author	M. van Arragon	Date	12/12/2017
Content	Specimen elements page1	Code	SPEC1

Table B.2: Specimen overview - Nominal values

Identity	Column	Fin-plate	Weld yield [N/mm^2]	Weld throat [mm]	Weld length [mm]
2E1	S690/E1.1	S355/E3	>355	3	160
2E2	S690/E1.1	S355/E3	>355	3	160
3E1	S690/E1.1	S355/E3	>690	3	160
3E2	S690/E1.1	S355/E3	>690	3	160
3E2	S690/E1.1	S355/E3	>690	3	160
4E1	S355/E1.2	S355/E3	>690	3	160
4E2	S355/E1.2	S355/E3	>690	3	160
4E2	S355/E1.2	S355/E3	>690	3	160
					All single side weld

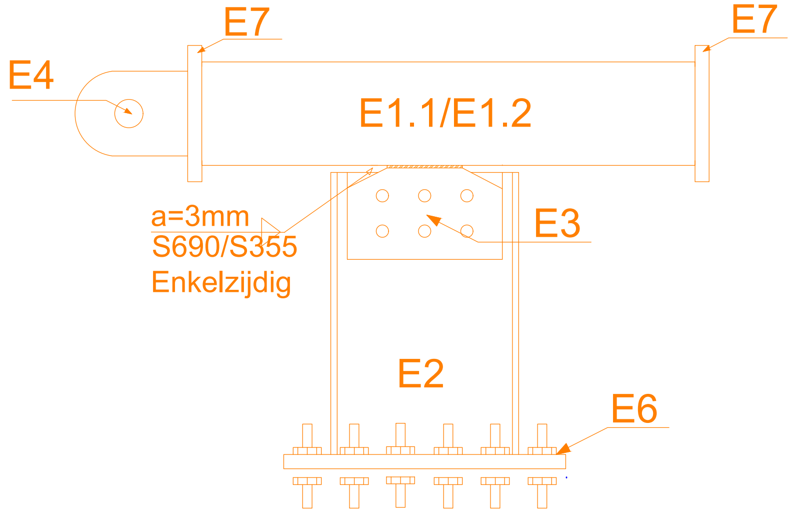
E7
E7
E4
E1.1/E1.2
a=3mm
S690/S355
Enkelzijdig
E3
E2
E6

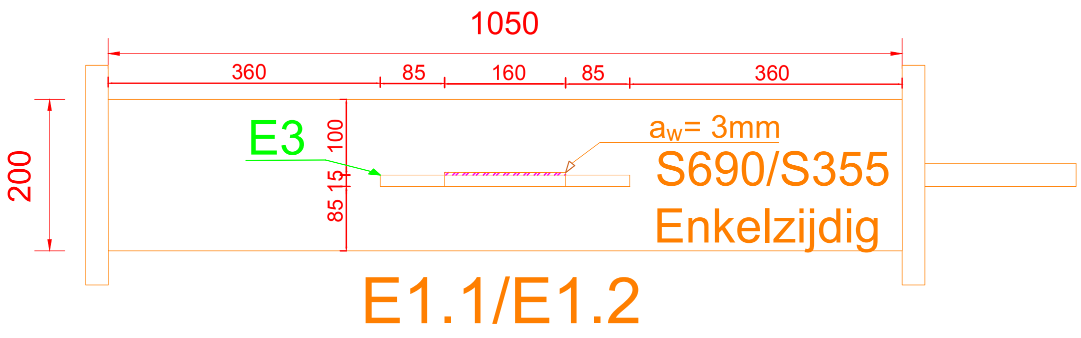
1050
360
85
160
85
360
200
E3
100
15
85
a_W= 3mm
S690/S355
Enkelzijdig
E1.1/E1.2

Nieuwe FIN platen bevestigen aan de zijde tegenover de bestaande platen
Er zijn 3 sets, waarvan set 2E* met een S355 las en sets 3E*, 4E* met een S690 las

ASK ROMEIN TU Delft Delft University of Technology

Thesis	Optimization of Steel Joint Design in Daily Engineering Practice		
Author	M. van Arragon	Date	14/12/2017
Content	Specimen elements page2	Code	SPEC2

B

Welding procedures

No. :	6
Rev. :	0
Page :	1 of 1
Date :	26-May-

WELDING PROCEDURE SPECIFICATION

Client : GENERAL	**Project :** GENERAL	**Project N**ENERA

Ref. Specificatio :	EN-15609	Joint types qualified :	Single / Multi pass fillet welds
Proposed by :	W.Tak	Thickness qualified :	5- unl.
Checked by :	A, de Bruin	Diam. range qualifie :	150 mm and over.
Site / Shop :	Shop	Mat. types qualified :	group 1.1 & 1.2 acc. EN 15608

Weld preparation

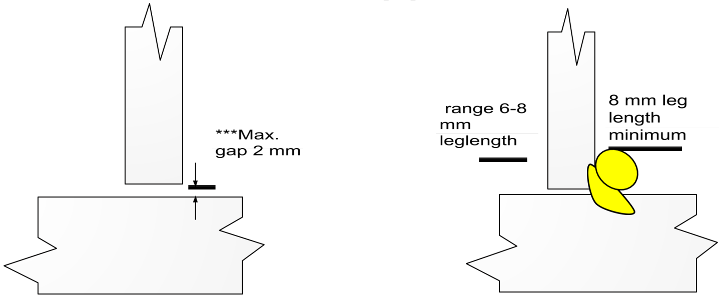

Prep method Grind	**Gouging method** Arc-Air	**Gouge dre** Grind	**Gouge check meth** N.A.

Side	Pass No.	Welding Process	Weld Pos.	ELECTRODE Size ø mm	 Code EN	 Name Lincoln	DC Polarity	Amps Min - Max	Volts Min - Ma	Welding Speed Cm / Min Min - Max	Welding Energy Kj / mm Min - Max
SP / MP	1	138	A/PE	1.2	42 3 MM	IC 710H	Pos.	280 - 320	29 - 33	35.0 - 45.0	1.1 - 1.8
MP	N+1	138	A/PE	1.2	42 3 MM	IC 710H	Pos.	280 - 320	29 - 33	50.0 - 70.0	0.7 - 1.3

Welding consumable con :	Max. 5ml H²/100gr weld meta	Tack welding procedure:	N A
Consumable handling & :	I-06-22	Pre-heat method & instr:	Propane burner
Weaving technique :	No	Minimum pre-heat temp:	See table below
Maximum bead width :	String Bead	Maximum interpass tem:	250° C
Remarks :		Heat treatment (soakir:	N.A.

* Covered by WPQR S 10-015 & S10-020

S10-015 S10-020

** Gascomp : 80%ar / 20 % CO2 / 16-20ltr. /min.
(Acc. En ISO 14175 M21)

*** If the gap exceeds 1.6 mm the leg length shall be increased by the size of the gap.

Preheat Requirements
T ≤ 60 mm ambient
T > 60 mm 50° C

ASK-Romein	**Approved by Client**	**Approved by Cert. Authority**
Name : W.Tak	Name :	Name :
Signature :	Signature :	Signature :
Date : 26-May-	Date :	Date :

Preheat sheet

HILLEBRAND

Removable Spudcan Shoe

160081

Base material	Thickness	Ceq	Preheat temperature	Remarks
S355J2+N	≤40 mm	≤0,40	20°C	
S355J2+N	50 mm	≤0,43	75°C	
S355J2+N	80 mm	≤0,43	75°C	
S355J2+N	130 mm	≤0,43	75°C	
S690	≤20 mm	≤0,43	20°C	
S690	25 mm	≤0,45	50°C	
S690	35 mm	≤0,49	75°C	
S690	45 mm	≤0,50	100°C	
S690	60 mm	≤0,51	125°C	

Preheat temperature measured 75 mm from center of weld

Interpass temperature measured at center of weld

Manufacturer

HILLEBRAND
J. Sinke
IWI C683
21 JUN 2016

checked

DNV GL 1864
☐ Witnessed ☑ Reviewed
And found to comply with:
Date 22 JUNI 2016
Sign: L. Knops

Outershield® MC715-H

B.1. S355 weld material

CLASSIFICATION

AWS A5.18	E70C-6M H4	**A-Nr**	1
EN ISO 17632-A	T 46 4 M M 2 H5	**F-Nr**	6
		9606 FM	1

GENERAL DESCRIPTION

Metal cored gas shielded wire for all positions
Few silicates and virtually no spatter, fast travel speed, excellent wire feeding
Excellent arc characteristics give outstanding operator appeal
Excellent mechanical properties (CNV >47J at -40°C)
Superior product consistency with optimal alloy control
Depending on application good alternative for basic flux cored wires

WELDING POSITIONS (ISO/ASME)

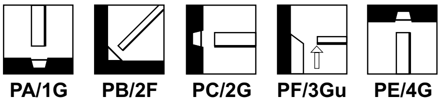

CURRENT TYPE / SHIELDING GAS (ISO 14175)

DC +
M21 : Mixed gas Ar+ (>15-25%) CO_2
Flow rate : 15-25 l/min

APPROVALS

Shielding gas	BV	DB	DNV	GL	RINA
M21	SA3,3YMHH	+	IV Y40H5	4Y40H5S	4YSH5

CHEMICAL COMPOSITION (W%), TYPICAL, ALL WELD METAL

Shielding gas	C	Mn	Si	P	S	HDM
M21	0.04	1.5	0.4	0.012	0.020	3 **ml/100 g**

MECHANICAL PROPERTIES, TYPICAL, ALL WELD METAL

	Shielding gas	Condition	Yield strength (N/mm²)	Tensile strength (N/mm²)	Elongation (%)	Impact ISO-V(J)		
						-30°C	-40°C	-50°C
Required: AWS A5.18			min. 400	min. 480	min. 22			
EN ISO 17632-A			min. 460	530-680	min. 20		min. 47	
Typical values	M21	AW	480	580	27	120	110	80
	M21	SR	430	485	30		120	90

SR : 2h/640°C

PACKAGING AND AVAILABLE SIZES

Diameter (mm)	1.0	1.2	1.4	1.6
5 kg plastic spool S200	X	X		
16 kg spool B300	X	X	X	X
200 kg Accutrak® Drum	X	X	X	X

All information in this data sheet is accurate to the best of our knowledge at the time of printing. Please refer to www.lincolnelectric.eu for any updated information.
Download Safety datasheets (SDS)

Megafil 742M

CATEGORIE	FCAW Flux-Cored
TYPE	Seamless high strength metal-cored wire for M21 without slag.
APPLICATIONS	Crane-, plant-, craft-, lifting and steel construction, pipe work, foundries.
PROPERTIES	Remarkable crack resistant weld metal in combination with very low (<3ml/100gr) hydrogen content. Therefore, suitable for the economic processing of high-strength and low temperature fine grained structural steels. Excellent welding properties in short and spray arc. High deposition rate and no intermediate cleaning required with very low spatter loss. Excellent wetting properties compare to solid wires that results in a bigger parameter range and improved duty cycle for the welder.
CLASSIFICATION	AWS A5.28: E110C-K4 H4 A5.36: E111T15-M21A8-K4-H4 EN ISO 18276-A: T 69 6 Mn2NiCrMo M M21 1 H5
SUITABLE FOR	Naxtra 70, Weldox 700, S690, S620, EStE 690, 690V, XABO 620, S620Ql1, S690QL1, S600MC, S700MC, Naxtra 63, Naxtra 70, Optim 700 mc plus, TStE620, TStE690, Weldox 500, Hardox, L480 - L550, X65, X80, X90, X100, Hardox 400, XAR 400, Dilidur 400, Domex 600MC, Domex 650 MC, 20MnCr65, 28CrMn43, ASTM: A 517, A 537, A 625, HY100, (16NiCrMo12-6), Oceanfit 100, Oceanfit 690
APPROVALS	LRS (5Y69), ABS (5Y69), DNV, DB, TÜV, GL, BWB-WIWEB, CE approved

WELDING POSITIONS:

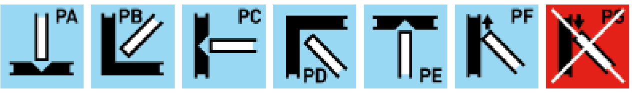

WELD METAL ANALYSIS % (TYPICAL VALUES FOR M21)

C	Mn	Si	Cr	Ni	Mo	P	S
0.05	1.6	0.4	0,5	2,2	0,5	<0.015	<0.015

MECHANICAL PROPERTIES

Heat Treatment	$R_{P0,2}$ (N/mm^2)	Rm (N/mm^2)	A5 (%)	Impact Energy (J) ISO-V			Hardness HRc / HV
				-20°C	-40°C	-60°C	
AW	>690	780-960	>17		>69	>69	
SR	>670	760-850	>17		>60	>47	

AW: as welded, SR: stress relieved 580ºC / 2hr

WELDING PARAMETERS / PACKING

Welding Parameters			Packing		
D (mm)	Voltage (V)	Current (A) DC+	spool type	kg / spool /drum	kg / pallet
1,0	14-26	70-230	D-200 / K-300 / Drum	5 / 16 / 300	1000 / 1024 / 600
1,2	14-31	90-310	D-200 / K-300 / Drum	5 / 16 / 300	1000 / 1024 / 600
1.6	17-36	120-380	D-200 / K-300 / Drum	5 / 16 / 300	1000 / 1024 / 600

REDRYING TEMPERATURE	Not required
GAS ACC. EN ISO 14175:	M21

C

Estimation of joint resistance

C.1. Nominal eurocode calculation procedure

C.1.1. Joint geometry

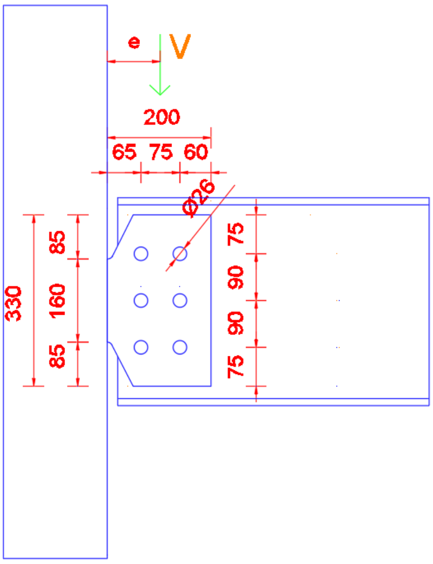

Material factors

$y_{m0} = 1.0, y_{m1} = 1.0, y_{m2} = 1.25$

Column SHS200x8

$t_w = 8\,[mm]$

$Grade = S690\ for\ 1Ex, 2Ex, 3Ex$

$Grade = S355\ for\ 4Ex$

Beam IPE400

$t_w = 8.65\,[mm]$

$h = 400\,[mm]$

$Grade = S355\ for\ all$

Fin-plate

$t_w = 10\,[mm]\ for\ 1Ex$

$t_w = 15\,[mm]\ for\ 2Ex, 3Ex, 4Ex$

$Grade = S355\ for\ all$

Bolts M24 10.9

$d = 24\,[mm]$

$d_0 = 26\,[mm]$

$A_s = 353\,[mm]\ in\ thread$

Eccentricities and spacing

$$z_d = \frac{65 + (65 + 75)}{2} = 102.5\,[mm]\ Bolts\ rotation\ center\ from\ weld$$

$e_1 = 75\,[mm]$

$e_2 = 60 = 50\,[mm]\ for\ 1Ex$

$e_2 = 65 - 10 = 55\,[mm]\ for\ 2Ex, 3Ex, 4Ex$

$p_1 = 90\,[mm]$

$p_2 = 75\,[mm]$

C.1.2. fin-plate resistance

Bending due to bolt eccentricity

$h_p > 2.73z_d \, design\, rule\, not\, satisfied$

$$W_{el} = \frac{t_p \cdot h_p^2}{6}$$

$$F_{rd} = \frac{W_{el} \cdot f_y}{z_d}$$

Bearing resistance

$$F_{b,ver} = k_1 \cdot \alpha_b \cdot d \cdot t_p \cdot f_{up}/y_{m2}$$

$$\alpha_b = min(\frac{e_1}{3d_0}, \frac{p_1}{3d_0} - \frac{1}{4}, \frac{f_{ub}}{f_u p})$$

$$k_1 = min(\frac{2.8e_2}{d_0} - 1.7; 2.5)$$

$$F_{b,hor} = k_1 \cdot \alpha_b \cdot d \cdot t_p \cdot f_{up}/y_{m2}$$

$$\alpha_b = min(\frac{e_1}{3d_0}, \frac{f_{ub}}{f_u p})$$

$$k_1 = min(\frac{2.8e_1}{d_0} - 1.7; \frac{1.4p_1}{d_0} - 1.7; 2.5)$$

$$\beta = \frac{6z}{p_1 n(n+1)}$$

$$V_{rd} = \frac{1}{\sqrt{(\frac{\frac{1}{6}}{F_{b,ver}})^2 + (\frac{\beta}{F_{b,hor}})^2}}$$

Shear

$$V_{rd,gross} = \frac{h_p t_p f_y}{\sqrt{3} y_{m0}}$$

C.1.3. weld resistance

Acting forces

$M = V_{rd} \cdot z_d\, for\, general\, joint$

$M = 0\, for\, experiment\, boundary\, conditions$

$\sigma_{\perp} = \tau_{\perp} = \frac{2 \cdot 2.12 \cdot M}{a \cdot l^2}\, Single\, side\, weld$

$\sigma_{\perp} = \tau_{\perp} = \frac{2.12 \cdot M}{a \cdot l^2}\, Double\, side\, weld$

$\tau_{\parallel} = \frac{F}{a \cdot l}\, Single\, side\, weld$

$\tau_{\parallel} = \frac{F}{a \cdot 2l}\, Double\, side\, weld$

$\sigma_{vm} = \sqrt{\sigma_{\perp}^2 + 3 \cdot (\tau_{\perp}^2 + \tau_{\parallel}^2)}$

Resistance according to 1993-1-8:2005

$\sigma_{vm} < \frac{f_u}{\beta_w y_{m2}}$

$\sigma_{\perp} < \frac{0.9 f_u}{y_{m2}}$

$f_u = f_u\, from\, weakest\, part\, joined$

$a_d esign = \frac{t_{pl} \cdot f_{y,pl} \cdot y_{m2} \cdot \beta_w}{\sqrt{2} \cdot f_{u,weld} \cdot y_{m0}}$

Resistance according to 1993-1-8:2020

$\sigma_{vm} < \frac{f_u}{\beta_{w,mod} y_{m2}}$

$\sigma_{\perp} < \frac{0.9 f_u}{y_{m2}}$

$f_u = 0.25 f_{u,PM} + 0.75 f_{u,FM}$

$f_{u,PM} = f_u\, from\, weakest\, part\, joined$

$f_{u,FM} = f_u\, from\, filler\, material$

$Values\, from\, table\; 6.2\; 1993 - 1 - 8 : 2020\; draft\; 4$

C.1.4. Bolt resistance

$$V_{rd} = \frac{n1 n2 F_{vrd}}{\sqrt{1 + (\frac{6z}{n1(n2+1)p_1})^2}}$$

$n1 = 2\, bolt\, columns$

$n2 = 3\, bolt\, rows$

$F_{vrd} = \alpha_v A_s f_{ub} / y_{m2}$

$\alpha_v = 0.5$

C.2. Set 1 - C690-W355-F355-B355-3mm

C.2.1. Estimated joint resistance 1E1 1E2

Bolts

$V_{rd,bolts} = 644\ [kN]$

Fin-plate resistance

$h_p = 300\ [mm]$

$t_p = 10\ [mm]$

$V_{rd,bending} = 520\ [kN]$

$V_{rd,bearing} = 901\ [kN]$

$V_{rd,shear} = 614\ [kN]$

Weld resistance

$l = 300\ [mm]$

$a = 3\ [mm]$

Resistance according to 1993-1-8:2005

$f_u = 470\ [N/mm^2]$

$\beta_w = 0.9$

$V_{rd} = 223\ [kN]\, for\ general\ joint$

$V_{rd} = 430\ [kN]\, for\ experiment\ boundary\ conditions$

$a_d esign = 6\ [mm]$

Resistance according to 1993-1-8:2020

$f_u = 0.25 f_{u,PM} + 0.75 f_{u,FM}$

$f_{u,PM} = 470\ [N/mm^2]$

$f_{u,FM} = 530\ [N/mm^2]\, class\ 46$

$\beta_{w,mod} = 0.9$

$V_{rd} = 260\ [kN]\, for\ general\ joint$

$V_{rd} = 505\ [kN]\, for\ experiment\ boundary\ conditions$

$a_d esign = 5.2\ [mm]$

$Values\ from\ table\ 6.2\ 1993 - 1 - 8 : 2020\ draft\ 4$

C.3. Set 2 - C690-W355-F355-B355-3mm-single

Bolts

$V_{rd,bolts} = 644\ [kN]$

Fin-plate resistance

$h_p = 160\ [mm]$

$t_p = 15\ [mm]$

$V_{rd,bending} = 220\ [kN]$

$V_{rd,bearing} = 1300\ [kN]$

$V_{rd,shear} = 491\ [kN]$

Weld resistance

$l = 160\ [mm]$

$a = 3\ [mm]$

Resistance according to 1993-1-8:2005

$f_u = 470\ [N/mm^2]$

$\beta_w = 0.9$

$V_{rd} = 35\ [kN]\ for\ general\ joint$

$V_{rd} = 115\ [kN]\ for\ experiment\ boundary\ conditions$

$a_d esign = 18\ [mm]$

Resistance according to 1993-1-8:2020

$f_u = 0.25 f_{u,PM} + 0.75 f_{u,FM}$

$f_{u,PM} = 470\ [N/mm^2]$

$f_{u,FM} = 530\ [N/mm^2]\ class\ 46$

$\beta_{w,mod} = 0.9$

$V_{rd} = 41\ [kN]\ for\ general\ joint$

$V_{rd} = 135\ [kN]\ for\ experiment\ boundary\ conditions$

$a_d esign = 15.4\ [mm]$

$Values\ from\ table\ 6.2\ 1993-1-8 : 2020\ draft\ 4$

C.4. Set 3 - C690-W690-F355-B355-3mm-single

Used values

$l = 160\ [mm]$

$a = 3\ [mm]$

Resistance according to 1993-1-8:2005

$f_u = 470\ [N/mm^2]$

$\beta_w = 0.9$

$V_{rd} = 35\ [kN]\ for\ general\ joint$

$V_{rd} = 115\ [kN]\ for\ experiment\ boundary\ conditions$

$a_d esign = 16\ [mm]$

Resistance according to 1993-1-8:2020

$f_u = 0.25 f_{u,PM} + 0.75 f_{u,FM}$

$f_{u,PM} = 470\ [N/mm^2]$

$f_{u,FM} = 940\ [N/mm^2]\ class\ 89$

$\beta_{w,mod} = 1.19$

$V_{rd} = 47\ [kN]\ for\ general\ joint$

$V_{rd} = 153\ [kN]\ for\ experiment\ boundary\ conditions$

$a_d esign = 13.6\ [mm]$

$Values\ from\ table\ 6.2\ 1993 - 1 - 8 : 2020\ draft\ 4$

C.5. Set 4 - C355-W690-F355-B355-3mm-single

Used values

$l = 160\ [mm]$

$a = 3\ [mm]$

Resistance according to 1993-1-8:2005

$f_u = 470\ [N/mm^2]$

$\beta_w = 0.9$

$V_{rd} = 35\ [kN]\ for\ general\ joint$

$V_{rd} = 115\ [kN]\ for\ experiment\ boundary\ conditions$

$a_d esign = 18\ [mm]$

Resistance according to 1993-1-8:2020

$f_u = 0.25 f_{u,PM} + 0.75 f_{u,FM}$

$f_{u,PM} = 470\ [N/mm^2]$

$f_{u,FM} = 940\ [N/mm^2]\ class\ 89$

$\beta_{w,mod} = 1.19$

$V_{rd} = 47\ [kN]\ for\ general\ joint$

$V_{rd} = 153\ [kN]\ for\ experiment\ boundary\ conditions$

$a_d esign = 13.6\ [mm]$

$Values\ from\ table\ 6.2\ 1993 - 1 - 8 : 2020\ draft\ 4$

Bibliography

[1] How are welds modeled in idea statica. `https://www.ideastatica.com/resource/Content/02_Steel/FAQ/Design/How_are_welds_modeled.htm`. Accessed: 20-04-2018.

[2] Tuominen N Björk T, Ahola A. On the design of fillet welds made of uhss - internal - lappeenranta university of technology - 2017.

[3] Chang-Sik Oh et al. *A finite element ductile failure simulation method using stress-modified fracture strain model*. Engineering Fracture Mechanics 78 (2011) 124-137.

[4] J. Carrier et al. Thermal effect of the welding process on the dynamic behavior of the hss constitutive materials of a fillet welded joint, ch 3.1 - université de valenciennes - 2017, .

[5] J.P. Jaspart et al. *European recommendations for the design of simple joints in steel structures - 2009*. ECCS Technical Committee 10 - steelconstruct.com, .

[6] M. Pavlović et al. *Calibration of the Ductile Damage Material Model Parameters for a High Strength Steel. In The 13th Nordic Steel Construction Conference: NSCC-2015 (pp. 231–232). Tampere: Tampere University of Technology, Department of Civil Engineering.* .

[7] A.M. Gresnigt. *Design rules for fillet welds in eurocode 3 and AISC*. EUROSTEEL 2014, September 10-12, Naples, Italy.

[8] J.P. Jaspart. *Recent advances in the field of steel joints, Column bases and further configurations for beam-to-column joints and beam splices*. Universite de Liege - 1997.

[9] J. Wardenier J.W.B. Stark. *Knopen. Berekenen van geboute en gelaste verbindingen in raamwerken en in buisconstructies volgens Eurocode 3*. Bouwen met Staal.

[10] D. Kozak. Finite element model of welded joint with crack-tip in the heat affected zone - university of osijek. `https://bib.irb.hr/datoteka/83867.cim_999.doc`. Accessed: 20-03-2018.

[11] G. Maheninggalih. *A demountable structural system of multi-storey building - 2017*.

[12] S. Navarro. *Validation of the calculation models and design tools for steel beam-column joints by experiments and FEA - 2017*.

[13] NEN. *Eurocode 3: design of steel structures - part-1-8 Design of joints (includes C1:2006)*. Nederlands normalisatie-instituut, .

[14] NEN. *Eurocode 3: design of steel structures - part-1-8 Design of joints - Draft v4.0 2018*. Internal, .

[15] M. Pavlovic. Workshop ductile damage material models for modelling of cracking of the steel material in abaqus - 2017 - internal.

[16] ASK Romein. Internal interviews with welders (2018).

[17] C. Schmidt-Rasche. Load bearing capacity of fillet welded connections of high strength steel. 81: 71–78, 01 2010.

[18] DSS Simula. Abaqus analysis user's guide v6.14.

[19] H. van Egeraat. *Calculation methods for steel joints - 2017*.

[20] L. L. Yaw. Nonlinear static - explicit and implicit analysis example. `https://gab.wallawalla.edu/~louie.yaw/nonlinear/ExIm_analysis.pdf`. Accessed: 30-12-2017.